

**LOADS ON TIE-DOWN SYSTEMS FOR FLOATING DRILLING RIGS  
DURING HURRICANE CONDITIONS**

A Thesis

by

YOON HYEOK BAE

Submitted to the Office of Graduate Studies of  
Texas A&M University  
in partial fulfillment of the requirements for the degree of

MASTER OF SCIENCE

May 2009

Major Subject: Ocean Engineering

**LOADS ON TIE-DOWN SYSTEMS FOR FLOATING DRILLING RIGS  
DURING HURRICANE CONDITIONS**

A Thesis

by

YOON HYEOK BAE

Submitted to the Office of Graduate Studies of  
Texas A&M University  
in partial fulfillment of the requirements for the degree of

MASTER OF SCIENCE

Approved by:

Chair of Committee,	Moo-Hyun Kim
Committee Members,	Richard Mercier
	David Brooks
Head of Department,	David V. Rosowsky

May 2009

Major Subject: Ocean Engineering

**ABSTRACT**

Loads on Tie-down Systems for Floating Drilling Rigs during Hurricane Conditions.

(May 2009)

Yoon Hyeok Bae, B.S., Seoul National University

Chair of Advisory Committee: Dr. Moo-Hyun Kim

Tie-down systems are used to fasten drilling rigs to the deck of offshore structures during harsh environmental conditions such as hurricanes. During Hurricane Ivan (2004) and Katrina (2005), a number of offshore structures were moved and several tie-down systems were damaged. In the present study, the reaction force and connection capacity of tie-down systems for a TLP and SPAR are investigated. The environmental conditions are taken from the API Bulletin 2INT-MET which has been updated after several major storms during 2004-2005. The hydrodynamic coefficients of the TLP and SPAR are obtained using a 3D diffraction/radiation panel method. The motions of the TLP and SPAR are then simulated in the time domain by using the hull-mooring-riser coupled dynamic analysis tool CHARM3D. Based on the simulated motion and acceleration time series, the inertial and gravity loads on derrick and skid base footing are calculated. In addition to the inertial-gravity loads, wind forces exerted on the derrick are also calculated. All the external forces and resultant hull motions are simulated for 100-year, 200-year and 1000-year storms to observe the derrick structural integrity with increasing environmental intensity. Various environmental headings are also considered

to find the maximum reaction forces. In the present method, the phase differences between gravity-inertia forces and wind forces are taken into consideration to obtain more realistic loads on derrick and skid base footings. This research shows that the maximum and minimum load values are appreciably higher for the SPAR. In addition, the direction of external forces is also important to determine maximum reaction forces on footings. The capacities of the clamps in slip, bolt tension, and bolt shear can be also analyzed using the resultant data to provide guidance on appropriate design values.

## **DEDICATION**

This thesis is dedicated to my parents, with love and thanks for all they have done for me throughout my life.

## ACKNOWLEDGEMENTS

I would like to thank my committee chair, Dr. Moo-Hyun Kim, for his guidance and encouragement throughout this study. His knowledge and insight were essential in helping me through many problems. I also would like to thank my committee members, Dr. Richard Mercier and Dr. David Brooks, for their guidance and support throughout the course of this research.

I also want to extend my gratitude to Dr. E.G. Ward for his technical advice and to Dr. C.K. Yang for sharing his knowledge and numerical data for this study. Thanks to API (American Petroleum Institute) for their financial support throughout the duration of this study.

Finally, thanks to my parents for their love and to my younger sister and her husband for their encouragement.

## TABLE OF CONTENTS

	Page
ABSTRACT .....	iii
DEDICATION .....	v
ACKNOWLEDGEMENTS .....	vi
TABLE OF CONTENTS .....	vii
LIST OF FIGURES .....	x
LIST OF TABLES .....	xviii
<b>1 INTRODUCTION</b> .....	<b>1</b>
1.1 General .....	1
1.2 Revised Wind Force Calculation Method .....	2
1.3 Characteristics of TLP and SPAR Motion .....	3
1.4 Objectives and Literature Review .....	3
<b>2 DYNAMIC LOAD ANALYSIS ON TIE-DOWN SYSTEMS</b> .....	<b>5</b>
2.1 Problem Description.....	5
2.1.1 Numerical Modeling of TLP .....	6
2.1.2 Numerical Modeling of SPAR .....	6
2.1.3 Configurations of Derrick and Skid Base .....	9
2.1.4 Environmental Condition .....	14
2.2 Coupled Dynamic Analysis in Time Domain Using CHARM3D .....	20
2.2.1 Added Mass and Damping Coefficient .....	20
2.2.2 Forces on Derrick and Skid Base .....	22
2.2.3 Reaction Forces on the Footings .....	23
<b>3 TLP CASE STUDY</b> .....	<b>28</b>
3.1 TLP Motion Analysis .....	28
3.2 External Forces and Moments .....	28
3.3 Reaction Forces .....	28
<b>4 CASE 1. SPAR (3000FT) WITH DERRICK AA – 0 DEGREE CASE</b> .....	<b>31</b>

	Page
4.1	SPAR Motion Time History..... 31
4.2	Inertia Force ..... 32
4.3	Wind Force..... 34
4.4	Gravity Force..... 36
4.5	Total Force ..... 37
4.6	Reaction Force..... 39
4.6.1	Derrick Reaction Force ..... 39
4.6.2	Skid Base Reaction Force ..... 42
4.7	200-year and 1000-year Hurricane Conditions ..... 45
4.7.1	200-year Hurricane Condition..... 45
4.7.2	1000-year Hurricane Condition..... 47
5	CASE 2. SPAR (3000FT) WITH DERRICK AA – 21.25 DEGREE CASE.... 51
5.1	SPAR Motion Time History..... 51
5.2	Inertia Force ..... 54
5.3	Wind Force..... 55
5.4	Gravity Force..... 58
5.5	Total Force ..... 59
5.6	Reaction Force..... 61
5.6.1	Derrick Reaction Force ..... 61
5.6.2	Skid Base Reaction Force ..... 64
5.7	200-year and 1000-year Hurricane Conditions ..... 65
5.7.1	200-year Hurricane Condition..... 66
5.7.2	1000-year Hurricane Condition..... 68
6	CASE 3. SPAR (3000FT) WITH DERRICK AA – 45 DEGREE CASE..... 72
6.1	SPAR Motion Time History..... 72
6.2	Inertia Force ..... 73
6.3	Wind Force..... 75
6.4	Gravity Force..... 76
6.5	Total Force ..... 78
6.6	Reaction Force..... 79
6.6.1	Derrick Reaction Force ..... 80
6.6.2	Skid Base Reaction Force ..... 82
6.7	200-year and 1000-year Hurricane Conditions ..... 85
6.7.1	200-year Hurricane Condition..... 85
6.7.2	1000-year Hurricane Condition..... 87
7	CASE 4. SPAR (3000FT) WITH DERRICK AA – 90 DEGREE CASE..... 91



	Page
7.1 SPAR Motion Time History.....	91
7.2 Inertia Force .....	91
7.3 Wind Force.....	92
7.4 Gravity Force.....	94
7.5 Total Force .....	96
7.6 Reaction Force.....	97
7.6.1 Derrick Reaction Force .....	97
7.6.2 Skid Base Reaction Force .....	99
7.7 200-year and 1000-year Hurricane Conditions .....	101
7.7.1 200-year Hurricane Condition.....	101
7.7.2 1000-year Hurricane Condition.....	104
8 SUMMARY .....	107
8.1 TLP vs SPAR Analysis .....	107
8.2 Incident Angle Analysis .....	110
8.3 External Force Contribution Analysis.....	115
8.4 Reaction Force Contribution Analysis .....	117
9 CONCLUSION .....	120
REFERENCES.....	121
APPENDIX.....	123
VITA .....	128

## LIST OF FIGURES

	Page
Fig 1-1 Side View of Medusa Platform after Hurricane Ivan (Murphy Exploration & Production Company, 2006).....	1
Fig 2-1 Configuration of SPAR Hull and Mooring/Riser .....	7
Fig 2-2 Mesh Generation of the SPAR.....	9
Fig 2-3 Derrick Structure General Arrangement.....	10
Fig 2-4 Derrick and Skid Base Footings .....	12
Fig 2-5 Simplified Model for Radius of Gyration Calculation .....	13
Fig 2-6 Wave Elevation and Spectrum.....	16
Fig 2-7 Wind Speed Time Series and Spectrum .....	18
Fig 2-8 Current Profile in Hurricane Conditions.....	19
Fig 2-9 Added Mass Coefficient of (a) TLP and (b) SPAR .....	20
Fig 2-10 Damping Coefficient of (a) TLP and (b) SPAR .....	21
Fig 2-11 Horizontal Reaction Forces .....	24
Fig 2-12 Vertical Reaction Forces.....	26
Fig 3-1 TLP Mean Surge Reaction Force (0 Degrees).....	29
Fig 3-2 TLP Mean Heave Reaction Force (0 Degrees).....	30
Fig 4-1 SPAR Surge Motion and Spectrum (0 Degrees) .....	31
Fig 4-2 SPAR Heave Motion and Spectrum (0 Degrees).....	32
Fig 4-3 SPAR Pitch Motion and Spectrum (0 Degrees).....	32
Fig 4-4 Surge Inertia Force of (a) Derrick and (b) Derrick + Skid Base (0 Degrees) .....	33

	Page
Fig 4-5 Heave Inertia Force of (a) Derrick and (b) Derrick + Skid Base (0 Degrees) .....	33
Fig 4-6 Surge Wind Force of (a) Derrick and (b) Derrick + Skid Base (0 Degrees) .....	35
Fig 4-7 Heave Wind Force of (a) Derrick and (b) Derrick + Skid Base (0 Degrees) .....	35
Fig 4-8 Surge Gravity Force of (a) Derrick and (b) Derrick + Skid Base (0 Degrees) .....	36
Fig 4-9 Heave Gravity Force of (a) Derrick and (b) Derrick + Skid Base (0 Degrees) .....	37
Fig 4-10 Surge Total Force of (a) Derrick and (b) Derrick + Skid Base (0 Degrees) .....	38
Fig 4-11 Heave Total Force of (a) Derrick and (b) Derrick + Skid Base (0 Degrees) .....	38
Fig 4-12 Direction of Force and Node Location of Derrick (0 Degrees) .....	39
Fig 4-13 (a) Surge Reaction (b) Heave Reaction on Footing 1 (0 Degrees) .....	40
Fig 4-14 (a) Surge Reaction (b) Heave Reaction on Footing 2 (0 Degrees) .....	40
Fig 4-15 (a) Surge Reaction (b) Heave Reaction on Footing 3 (0 Degrees) .....	41
Fig 4-16 (a) Surge Reaction (b) Heave Reaction on Footing 4 (0 Degrees) .....	41
Fig 4-17 Direction of Force and Node Location of Skid Base (0 Degrees) .....	42
Fig 4-18 (a) Surge Reaction (b) Heave Reaction on Footing 5 (0 Degrees) .....	43
Fig 4-19 (a) Surge Reaction (b) Heave Reaction on Footing 6 (0 Degrees) .....	43
Fig 4-20 (a) Surge Reaction (b) Heave Reaction on Footing 7 (0 Degrees) .....	44
Fig 4-21 (a) Surge Reaction (b) Heave Reaction on Footing 8 (0 Degrees) .....	44
Fig 4-22 SPAR Mean Surge Reaction Force (0 Degrees) .....	50

	Page
Fig 4-23 SPAR Mean Heave Reaction Force (0 Degrees) .....	50
Fig 5-1 SPAR Surge Motion and Spectrum (21.25 Degrees) .....	51
Fig 5-2 SPAR Sway Motion and Spectrum (21.25 Degrees).....	52
Fig 5-3 SPAR Heave Motion and Spectrum (21.25 Degrees).....	52
Fig 5-4 SPAR Roll Motion and Spectrum (21.25 Degrees).....	52
Fig 5-5 SPAR Pitch Motion and Spectrum (21.25 Degrees).....	53
Fig 5-6 SPAR Yaw Motion and Spectrum (21.25 Degrees) .....	53
Fig 5-7 Surge Inertia Force of (a) Derrick and (b) Derrick + Skid Base (21.25 Degrees) .....	54
Fig 5-8 Sway Inertia Force of (a) Derrick and (b) Derrick + Skid Base (21.25 Degrees) .....	54
Fig 5-9 Heave Inertia Force of (a) Derrick and (b) Derrick + Skid Base (21.25 Degrees) .....	55
Fig 5-10 Surge Wind Force for (a) Derrick and (b) Derrick + Skid Base (21.25 Degrees) .....	56
Fig 5-11 Sway Wind Force for (a) Derrick and (b) Derrick + Skid Base (21.25 Degrees) .....	57
Fig 5-12 Heave Wind Force for (a) Derrick and (b) Derrick + Skid Base (21.25 Degrees) .....	57
Fig 5-13 Surge Gravity Force for (a) Derrick and (b) Derrick + Skid Base (21.25 Degrees) .....	58
Fig 5-14 Sway Gravity Force for (a) Derrick and (b) Derrick + Skid Base (21.25 Degrees) .....	58
Fig 5-15 Heave Gravity Force for (a) Derrick and (b) Derrick + Skid Base (21.25 Degrees) .....	59

	Page
Fig 5-16 Surge Total Force for (a) Derrick and (b) Derrick + Skid Base (21.25 Degrees) .....	60
Fig 5-17 Sway Total Force for (a) Derrick and (b) Derrick + Skid Base (21.25 Degrees) .....	60
Fig 5-18 Heave Total Force for (a) Derrick and (b) Derrick + Skid Base (21.25 Degrees) .....	60
Fig 5-19 (a) Surge Reaction (b) Sway Reaction (c) Heave Reaction on Footing 1 (21.25 Degrees) .....	62
Fig 5-20 (a) Surge Reaction (b) Sway Reaction (c) Heave Reaction on Footing 2 (21.25 Degrees) .....	62
Fig 5-21 (a) Surge Reaction (b) Sway Reaction (c) Heave Reaction on Footing 3 (21.25 Degrees) .....	62
Fig 5-22 (a) Surge Reaction (b) Sway Reaction (c) Heave Reaction on Footing 4 (21.25 Degrees) .....	63
Fig 5-23 (a) Surge Reaction (b) Sway Reaction (c) Heave Reaction on Footing 5 (21.25 Degrees) .....	64
Fig 5-24 (a) Surge Reaction (b) Sway Reaction (c) Heave Reaction on Footing 6 (21.25 Degrees) .....	64
Fig 5-25 (a) Surge Reaction (b) Sway Reaction (c) Heave Reaction on Footing 7 (21.25 Degrees) .....	64
Fig 5-26 (a) Surge Reaction (b) Sway Reaction (c) Heave Reaction on Footing 8 (21.25 Degrees) .....	65
Fig 5-27 SPAR Mean Surge Reaction Force (21.25 Degrees) .....	70
Fig 5-28 SPAR Mean Sway Reaction Force (21.25 Degrees) .....	70
Fig 5-29 SPAR Mean Heave Reaction Force (21.25 Degrees) .....	71
Fig 6-1 SPAR Surge Motion and Spectrum (45 Degrees) .....	72
Fig 6-2 SPAR Heave Motion and Spectrum (45 Degrees) .....	73

	Page
Fig 6-3 SPAR Pitch Motion and Spectrum (45 Degrees).....	73
Fig 6-4 Surge Inertia Force of (a) Derrick and (b) Derrick + Skid Base (45 Degrees) .....	74
Fig 6-5 Heave Inertia Force of (a) Derrick and (b) Derrick + Skid Base (45 Degrees) .....	74
Fig 6-6 Surge Wind Force of (a) Derrick and (b) Derrick + Skid Base (45 Degrees) .....	75
Fig 6-7 Heave Wind Force of (a) Derrick and (b) Derrick + Skid Base (45 Degrees) .....	76
Fig 6-8 Surge Gravity Force of (a) Derrick and (b) Derrick + Skid Base (45 Degrees) .....	77
Fig 6-9 Heave Gravity Force of (a) Derrick and (b) Derrick + Skid Base (45 Degrees) .....	77
Fig 6-10 Surge Total Force of (a) Derrick and (b) Derrick + Skid Base (45 Degrees) .....	78
Fig 6-11 Heave Total Force of (a) Derrick and (b) Derrick + Skid Base (45 Degrees) .....	78
Fig 6-12 Direction of Force and Node Location of Derrick (45 Degrees).....	79
Fig 6-13 (a) Surge Reaction (b) Heave Reaction on Footing 1 (45 Degrees) .....	80
Fig 6-14 (a) Surge Reaction (b) Heave Reaction on Footing 2 (45 Degrees) .....	80
Fig 6-15 (a) Surge Reaction (b) Heave Reaction on Footing 3 (45 Degrees) .....	81
Fig 6-16 (a) Surge Reaction (b) Heave Reaction on Footing 4 (45 Degrees) .....	81
Fig 6-17 Direction of Force and Node Location of Skid Base (45 Degrees) .....	82
Fig 6-18 (a) Surge Reaction (b) Heave Reaction on Footing 5 (45 Degrees) .....	83
Fig 6-19 (a) Surge Reaction (b) Heave Reaction on Footing 6 (45 Degrees) .....	83

	Page
Fig 6-20 (a) Surge Reaction (b) Heave Reaction on Footing 7 (45 Degrees) .....	83
Fig 6-21 (a) Surge Reaction (b) Heave Reaction on Footing 8 (45 Degrees) .....	84
Fig 6-22 SPAR Mean Surge Reaction Force (45 Degrees) .....	89
Fig 6-23 SPAR Mean Heave Reaction Force (45 Degrees) .....	89
Fig 7-1 Sway Inertia Force of (a) Derrick and (b) Derrick + Skid Base (90 Degrees) .....	91
Fig 7-2 Heave Inertia Force of (a) Derrick and (b) Derrick + Skid Base (90 Degrees) .....	92
Fig 7-3 Sway Wind Force of (a) Derrick and (b) Derrick + Skid Base (90 Degrees) .....	93
Fig 7-4 Heave Wind Force of (a) Derrick and (b) Derrick + Skid Base (90 Degrees) .....	94
Fig 7-5 Sway Gravity Force of (a) Derrick and (b) Derrick + Skid Base (90 Degrees) .....	95
Fig 7-6 Heave Gravity Force of (a) Derrick and (b) Derrick + Skid Base (90 Degrees) .....	95
Fig 7-7 Sway Total Force of (a) Derrick and (b) Derrick + Skid Base (90 Degrees) .....	96
Fig 7-8 Heave Total Force of (a) Derrick and (b) Derrick + Skid Base (90 Degrees) .....	96
Fig 7-9 (a) Surge Reaction (b) Heave Reaction on Footing 1 (90 Degrees) .....	97
Fig 7-10 (a) Surge Reaction (b) Heave Reaction on Footing 2 (90 Degrees) .....	98
Fig 7-11 (a) Surge Reaction (b) Heave Reaction on Footing 3 (90 Degrees) .....	98
Fig 7-12 (a) Surge Reaction (b) Heave Reaction on Footing 4 (90 Degrees) .....	98
Fig 7-13 (a) Surge Reaction (b) Heave Reaction on Footing 5 (90 Degrees) .....	100

	Page
Fig 7-14 (a) Surge Reaction (b) Heave Reaction on Footing 6 (90 Degrees) .....	100
Fig 7-15 (a) Surge Reaction (b) Heave Reaction on Footing 7 (90 Degrees) .....	100
Fig 7-16 (a) Surge Reaction (b) Heave Reaction on Footing 8 (90 Degrees) .....	101
Fig 7-17 SPAR Mean Sway Reaction Force (90 Degrees) .....	106
Fig 7-18 SPAR Mean Heave Reaction Force (90 Degrees) .....	106
Fig 8-1 (a) Surge and (b) Heave Inertia Force .....	107
Fig 8-2 (a) Surge and (b) Heave Wind Force .....	107
Fig 8-3 (a) Surge and (b) Heave Gravity Force.....	108
Fig 8-4 (a) Surge and (b) Heave Total Force .....	108
Fig 8-5 (a) Surge and (b) Heave Reaction Force at Node 1 .....	109
Fig 8-6 (a) Surge and (b) Heave Reaction Force at Node 2 .....	109
Fig 8-7 (a) Surge and (b) Heave Reaction Force at Node 3 .....	109
Fig 8-8 (a) Surge and (b) Heave Reaction Force at Node 4 .....	110
Fig 8-9 SPAR Derrick Uplift Force.....	110
Fig 8-10 External Force Components of SPAR (a) 21.25 Degree and (b) 45 Degree .....	112
Fig 8-11 SPAR Skid Base Uplift Force.....	112
Fig 8-12 Derrick and Skid Base Slip Conditions .....	113
Fig 8-13 SPAR Derrick Slip Reaction.....	114
Fig 8-14 SPAR Skid Base Slip Reaction.....	114
Fig 8-15 TLP Skid Base Surge Reaction Component .....	115
Fig 8-16 SPAR Skid Base Surge Reaction Component .....	116



	Page
Fig 8-17 TLP Skid Base Sway Reaction Component .....	116
Fig 8-18 SPAR Skid Base Sway Reaction Component.....	117
Fig 8-19 (a) TLP Surge Reaction and (b) Spectral Density .....	118
Fig 8-20 (a) TLP Heave Reaction and (b) Spectral Density .....	118
Fig 8-21 (a) SPAR Surge Reaction and (b) Spectral Density .....	119
Fig 8-22 (a) SPAR Heave Reaction and (b) Spectral Density.....	119

## LIST OF TABLES

		Page
Table 2-1	Principal Particulars of the SPAR Platform .....	7
Table 2-2	Mooring and Riser System Characteristics .....	8
Table 2-3	Center of Pressure and Center of Gravity .....	11
Table 2-4	Projected Area in Different Projected Angles .....	11
Table 2-5	Environmental Conditions.....	15
Table 4-1	Inertia Force Statistics for (a) Derrick and (b) Derrick + Skid Base (0 Degrees).....	33
Table 4-2	Wind Force of Derrick and Skid Base (0 Degrees).....	34
Table 4-3	Wind Force Statistics for (a) Derrick and (b) Derrick + Skid Base (0 Degrees).....	36
Table 4-4	Gravity Force Statistics for (a) Derrick and (b) Derrick + Skid Base (0 Degrees).....	37
Table 4-5	Total Force Statistics for (a) Derrick and (b) Derrick + Skid Base (0 Degrees).....	39
Table 4-6	Derrick Reaction Force Statistics (0 Degrees) .....	41
Table 4-7	Skid Base Reaction Force Statistics (0 Degrees) .....	44
Table 4-8	Force Statistics for (a) Derrick and (b) Derrick + Skid Base (0 Degrees, 200-year Hurricane Condition).....	46
Table 4-9	Reaction Force Statistics (0 Degrees, 200-year Hurricane Condition) .....	47
Table 4-10	Force Statistics for (a) Derrick and (b) Derrick + Skid Base (0 Degrees, 1000-year Hurricane Condition).....	48
Table 4-11	Reaction Force Statistics (0 Degrees, 1000-year Hurricane Condition) .....	49

	Page
Table 5-1 Inertia Force Statistics for (a) Derrick and (b) Derrick + Skid Base (21.25 Degrees).....	55
Table 5-2 Wind Force of Derrick and Skid Base (21.25 Degrees).....	56
Table 5-3 Wind Force Statistics for (a) Derrick and (b) Derrick + Skid Base (21.25 Degrees).....	57
Table 5-4 Gravity Force Statistics for (a) Derrick and (b) Derrick + Skid Base (21.25 Degrees).....	59
Table 5-5 Total Force Statistics for (a) Derrick and (b) Derrick + Skid Base (21.25 Degrees).....	61
Table 5-6 Derrick Reaction Force Statistics (21.25 Degrees) .....	63
Table 5-7 Skid Base Reaction Force Statistics (21.25 Degrees) .....	65
Table 5-8 Force Statistics for (a) Derrick and (b) Derrick + Skid Base (21.25 Degrees, 200-year Hurricane Condition) .....	66
Table 5-9 Reaction Force Statistics (21.25 Degrees, 200-year Hurricane Condition) .....	67
Table 5-10 Force Statistics for (a) Derrick and (b) Derrick + Skid Base (21.25 Degrees, 1000-year Hurricane Condition) .....	68
Table 5-11 Reaction Force Statistics (21.25 Degrees, 1000-year Hurricane Condition) .....	69
Table 6-1 Inertia Force Statistics for (a) Derrick and (b) Derrick + Skid Base (45 Degrees).....	74
Table 6-2 Wind Force of Derrick and Skid Base (45 Degrees).....	75
Table 6-3 Wind Force Statistics for (a) Derrick and (b) Derrick + Skid Base (45 Degrees).....	76
Table 6-4 Gravity Force Statistics for (a) Derrick and (b) Derrick + Skid Base (45 Degrees).....	77

	Page
Table 6-5 Total Force Statistics for (a) Derrick and (b) Derrick + Skid Base (45 Degrees).....	79
Table 6-6 Derrick Reaction Force Statistics (45 Degrees).....	81
Table 6-7 Skid Base Reaction Force Statistics (45 Degrees).....	84
Table 6-8 Force Statistics for (a) Derrick and (b) Derrick + Skid Base (45 Degrees, 200-year Hurricane Condition).....	85
Table 6-9 Reaction Force Statistics (45 Degrees, 200-year Hurricane Condition).....	86
Table 6-10 Force Statistics for (a) Derrick and (b) Derrick + Skid Base (45 Degrees, 1000-year Hurricane Condition).....	87
Table 6-11 Reaction Force Statistics (45 Degrees, 1000-year Hurricane Condition).....	88
Table 7-1 Inertia Force Statistics for (a) Derrick and (b) Derrick + Skid Base (90 Degrees).....	92
Table 7-2 Wind Force of Derrick and Skid Base (90 Degrees).....	93
Table 7-3 Wind Force Statistics for (a) Derrick and (b) Derrick + Skid Base (90 Degrees).....	94
Table 7-4 Gravity Force Statistics for (a) Derrick and (b) Derrick + Skid Base (90 Degrees).....	95
Table 7-5 Total Force Statistics for (a) Derrick and (b) Derrick + Skid Base (90 Degrees).....	97
Table 7-6 Derrick Reaction Force Statistics (90 Degrees).....	99
Table 7-7 Skid Base Reaction Force Statistics (90 Degrees).....	101
Table 7-8 Force Statistics for (a) Derrick and (b) Derrick + Skid Base (90 Degrees, 200-year Hurricane Condition).....	102
Table 7-9 Reaction Force Statistics (90 Degrees, 200-year Hurricane Condition).....	103

	Page
Table 7-10 Force Statistics for (a) Derrick and (b) Derrick + Skid Base (90 Degrees, 1000-year Hurricane Condition).....	104
Table 7-11 Reaction Force Statistics (90 Degrees, 1000-year Hurricane Condition).....	105

## 1 INTRODUCTION

### 1.1 General

For many years, research about the hurricane survival condition of offshore structures has been conducted. Current offshore structural design is based on the standard that reflects the hurricane environmental condition. However, lots of drilling rigs in the Gulf of Mexico were damaged during both Hurricane Ivan (2004) and Katrina (2005), as shown in Figure 1-1, so the demand for more reliable and accurate dynamic analysis is greatly increased.



**Fig 1-1 Side View of Medusa Platform after Hurricane Ivan  
(Murphy Exploration & Production Company, 2006)**

The research in this thesis presents the calculation of dynamic loading on derrick and skid base footings due to dynamic behavior of floating structures. Two different

---

This thesis follows the style of the Journal of Ocean Engineering.

types of drilling rigs are selected for this research, 3000ft depth TLP and SPAR. Hydrodynamic coefficients such as added mass and radiation/diffraction damping are simulated using WAMIT (Lee, 1995), and fully coupled time domain analysis is carried out using CHARM3D (Kim, 1997) with the hydro coefficient which is derived from WAMIT. These two analysis tools have been proved and tested through real offshore projects and laboratory experiments for all kinds of offshore structures, so we can take advantage of the simulated result to design offshore structures (Kim et al., 2005).

## 1.2 Revised Wind Force Calculation Method

Previous study has utilized API Specification 4F 2<sup>nd</sup> Edition (1995) to calculate wind force exerted on the structures. The wind force on a structure with projected area  $A$  would be :

$$F = P \times A \quad (1.1)$$

where  $P$  and  $F$  represent the pressure and total force exerted on the structure respectively.

The pressure can be calculated as

$$P = \frac{1}{2} \rho_{air} V_{10}^2 C_h C_s \quad (1.2)$$

where  $V_{10}$  stands for 1-hour mean velocity 10m above mean water level.  $C_h$  and  $C_s$  represent height coefficient and shape coefficient. The resultant wind force, however, is relatively less than the actual wind force because (1.2) does not fully consider the effect of appurtenances. Donnes (2007) studied the difference between previous API standard

and proposed standard. In this study, proposed API Specification 4F 3<sup>rd</sup> Edition (2008) will be explained and used to get total wind force exerted on the derrick and skid base.

### 1.3 Characteristics of TLP and SPAR Motion

The motion characteristics of TLP and SPAR in the ocean are quite different due to the geometric shape of each structure and mooring configurations. These differences cause the different loading on tie-down systems. To some extent, the rotational motion of TLP is restricted because the vertical tendon of each column is strongly connected to the bottom to have TLP rotate along 3 axes. Thus, horizontal inertial force due to the horizontal motion of TLP and wind force are dominant external forces for the dynamic loading of derrick and skid base. However, rotational and heel acceleration inertial forces, as well as wind force, should be taken into account as important external forces to calculate dynamic loading on footings of SPAR. Each characteristic of TLP and SPAR motion will be presented with time domain analysis.

### 1.4 Objectives and Literature Review

The main objective of this study is to extend previous research for the purpose of developing more accurate and reliable guidelines for structural design of drilling rigs on various types of Floating Production Systems (FPSs). A number of research studies have been done for years, and structural design guidance of tie-down systems is suggested. Ward and Gebara (2006a) collected information on FPSs that had drilling rig movements during Hurricane Ivan, and carried out preliminary analysis to compare resultant



movements and design codes and rules (Ward and Gebara, 2006b). Kim and Yang (2006) studied the load at the connection of derrick and substructure on TLP platform. Fully coupled time domain analysis tool CHARM3D is employed to simulate time domain response. Similar research on the performance of tie-down systems of SPAR platform has been done by Gebara and Ghoneim (2007) using STRUCAD3D, a finite element software. In the present study, updated wind force calculation method and new environmental conditions are employed and analyzed. The target derrick and substructure are also replaced by bigger ones to understand the variation and sensitivity of tie-down loads.

To determine the design requirement for various tie-down systems, maximum forces and moments on the footings will be presented in this study. The results will also be compared with the simpler approach adopted by current offshore industry.

## 2 DYNAMIC LOAD ANALYSIS ON TIE-DOWN SYSTEMS

### 2.1 Problem Description

The problem being analyzed is the reaction force on derrick and skid base footings. Firstly, hydrodynamic coefficient is determined either by integrating the boundary element of submerged structures of interest or by the geometry itself in frequency domain. The external stiffness due to tendon and riser should be also considered to ensure a more reliable result. All of these procedures are carried out by the second-order diffraction/radiation program WAMIT. For simplicity, wave excitation forces in the present study are calculated up to first order and mean drift force is employed using Newman's approximation method.

The corresponding forces calculated by WAMIT are converted to the time domain using two-term Volterra series expansion (Ran and Kim, 1997). Translational and rotational motions of each structure can be analyzed using 3 hour time domain simulation. The analysis tool of coupled hull, mooring and riser system, CHARM3D is employed to find time history of structures. By utilizing hydrodynamic coefficient which is previously calculated by WAMIT, CHARM3D carries out time domain analysis to obtain the dynamic responses of the coupled system.

Subsequently, the reaction force calculation on the footings is done by dynamic and static force equilibrium relation under the assumption that the derrick and skid base are rigid body. The reaction force at each footing can be separately considered as longitudinal, lateral, and uplift reaction forces in order to provide design engineers with information about various possibilities of failure mode. In this study, simulations of

loads on a tie-down system on two types of platforms, a TLP and a SPAR, are conducted for hurricane environmental conditions by using a newly developed dynamic analysis tool in the time domain (Yang, 2009).

#### 2.1.1 Numerical Modeling of TLP

The TLP has eight vertical tendons (two tendons for each column), one drilling riser, and seven production risers. Risers are connected to the hull by hydraulic pneumatic tensioners and modeled as they should be. The particulars of the TLP used for this study is given in Kim et al, (2001) and Yang (2009). The present hulls, risers, and mooring lines are for 3000-ft water depth. The numerical simulations of the platform motions by using the present hull-mooring-riser coupled dynamic analysis tool were verified against various model tests (e.g. Steen et al, (2004); Kim et al, (2005)).

#### 2.1.2 Numerical Modeling of SPAR

The SPAR analyzed in this study is a classic SPAR which has a length of 705ft and diameter of 122 ft, as shown in Figure 2-1. This SPAR platform consists of 14 mooring lines and 23 risers. Each of the mooring line and riser connections is modeled as a spring with large stiffness. The connection node between riser and hull is modeled as a horizontal spring so as to make vertical motion of SPAR free. The details of SPAR and principal dimensions are tabulated in Tables 2-1 and 2-2.

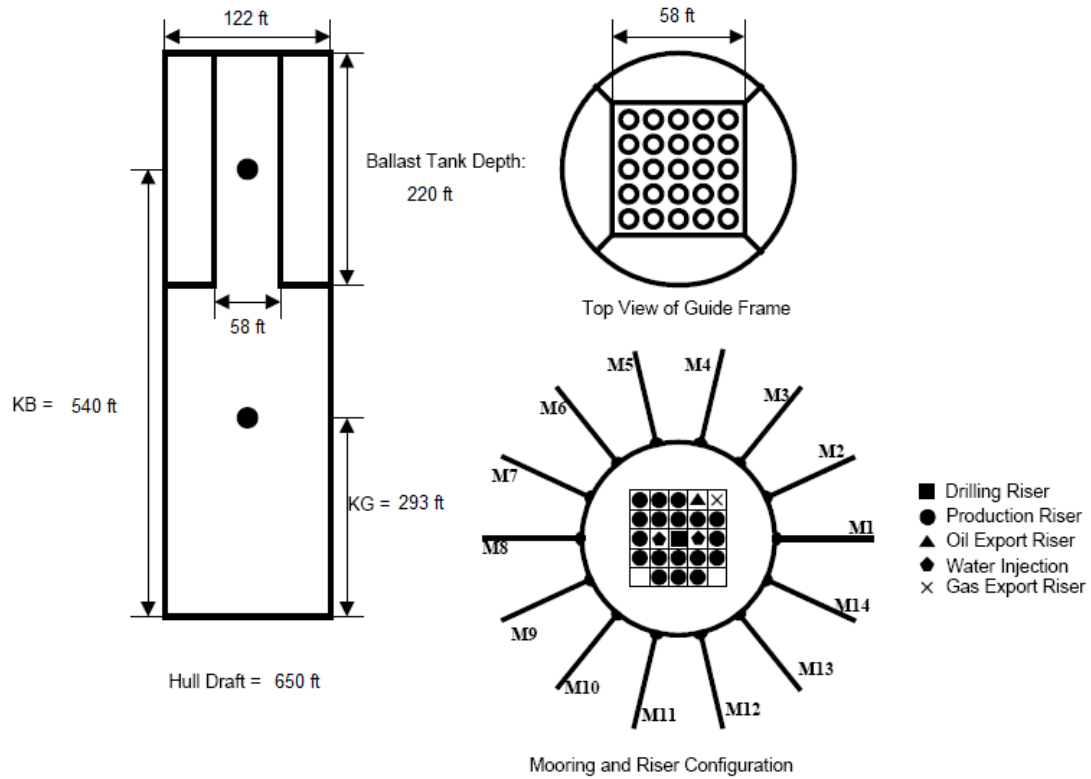


**Fig 2-1 Configuration of SPAR Hull and Mooring/Riser**

**Table 2-1 Principal Particulars of the SPAR Platform**

Description	Magnitude
Displacement (m.ton)	53,600
Total Displacement (m.ton)	220,740
Diameter (ft)	122
Length (ft)	705
Draft (ft)	650
Hard Tank Depth (ft)	220
Well Bay Dimensions (25 slots) (ft)	58 × 58

**Table 2-1 Continued**

Description	Magnitude
KB (ft)	540
KG (ft)	412
KG (Based on Total Displacement) (ft)	293
Radius of Gyration (Based on Total Displacement) (ft)	Pitch = 221, Yaw = 28.5
Drag Force Coefficient	1.15
Wind Force Coefficient (kips/(ft/sec) <sup>2</sup> )	0.0848
Center of Pressure (ft)	722

**Table 2-2 Mooring and Riser System Characteristics**

Line	No.	Top Tension (kips)	Axial Stiffness (kips)
Chain	14	680	2.98E+05
Wire			3.66E+05
Drilling Riser	1	735	2.70E+06
Production Riser	18	473	6.73E+05
Water Injection	2	306	4.13E+05
Oil Export	1	400	1.04E+06
Gas Export	1	200	1.04E+06

Submerged hull is discretized into 1504 rectangular panels so that WAMIT can calculate hydrodynamic coefficients. Figure 2-2 shows the panel model of submerged SPAR hull.

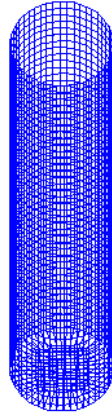


**Fig 2-2 Mesh Generation of the SPAR**

### 2.1.3 Configurations of Derrick and Skid Base

In this study, medium size derrick and skid base are mounted at the center of the deck and they are designed to move in longitudinal and lateral directions. The size of the derrick is greatly increased compared with the derrick adopted by previous research therefore, the wind force exerted on the derrick will be increased. Center of gravity of the derrick is located at 105 ft from the deck, and center of gravity of skid base is located at 5 ft from the deck. The location of CG from the MWL plays an important role in calculating the overturning moment of derrick, so it should be calculated with care. Details of its dimension and weight are presented in Figure 2-3.

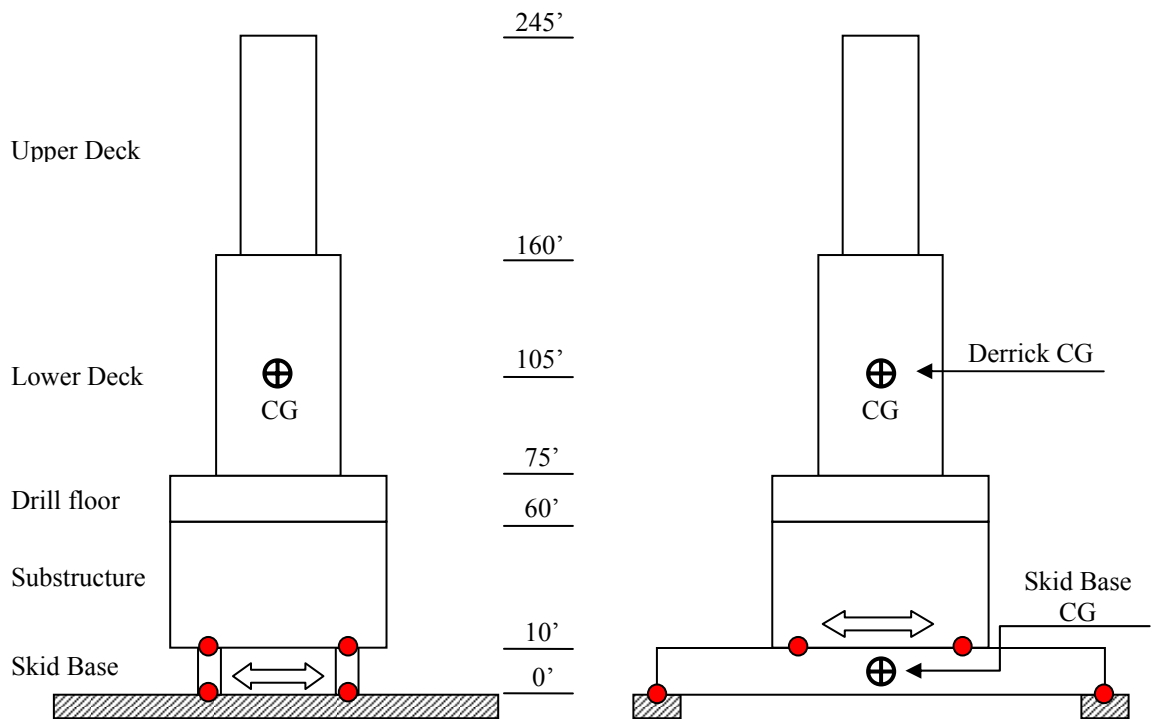


**Fig 2-3 Derrick Structure General Arrangement**

The center of gravity and center of pressure should be calculated individually from derrick and derrick with skid base, because the derrick itself will only contribute to the reaction of derrick footing and total weight will affect the reaction of skid base. The detail of CG and CP is tabulated in Table 2-3. The vertical location of derrick is different from each floating structure due to the structural difference between TLP and SPAR. For TLP, the derrick is located 200ft from MWL and 140ft for SPAR. For this reason, external wind force on TLP derrick is stronger than that on SPAR derrick. The projected area should be also carefully calculated in order to get proper wind force of various wind directions. Table 2-4 shows the maximum projected area.

**Table 2-3 Center of Pressure and Center of Gravity**

Description	TLP		SPAR	
	Derrick	Derrick + Skid Base	Derrick	Derrick + Skid Base
Weight (kips)	1777	2347	1777	2347
COP from MWL (ft)	313	306	254	247
COP from each footings (ft)	103	106	104	107
CG from MWL (ft)	305	280.7	245	220.7
CG from each footings (ft)	95	80.7	95	80.7
Deck level from MWL (ft)	200		140	

**Table 2-4 Projected Area in Different Projected Angles**

	Angle	0 deg	21.25 deg	45 deg	90 deg
	Upper derrick (ft <sup>2</sup> )	2805	3631	3995	2805
	Lower derrick (ft <sup>2</sup> )	2975	3851	4165	2975
	Drill floor (ft <sup>2</sup> )	750	971	1065	750
	Substructure (ft <sup>2</sup> )	2500	3236	3550	2500
	<b>Derrick Total (ft<sup>2</sup>)</b>	<b>9030</b>	<b>11689</b>	<b>12775</b>	<b>9030</b>
	Skid Base (ft <sup>2</sup> )	1000	1077	990	400
	<b>Derrick + Skid Base Total (ft<sup>2</sup>)</b>	<b>10030</b>	<b>12766</b>	<b>13765</b>	<b>9030</b>

Maximum projected area of derrick is 12,775 ft<sup>2</sup> and maximum projected area of total structure is 13,765 ft<sup>2</sup> with incident angle of 45 degree. The projected area of skid base is considered maximum at 21.25 degree of incident angle, but the total area is still less than that of 45 degree incident angle case.



The derrick is supported by 4 footings, and the skid base is also supported by 4 footings. The node location and reference numbers are shown in Figure 2-4. The upper structures are able to move along the y-direction and the distance between footings is 35ft. Skid base, which has rectangular positioned footings of 35ft by 90ft, can move along the x-direction. In this study, the derrick is assumed to be located at the center of floating structures for simplicity.

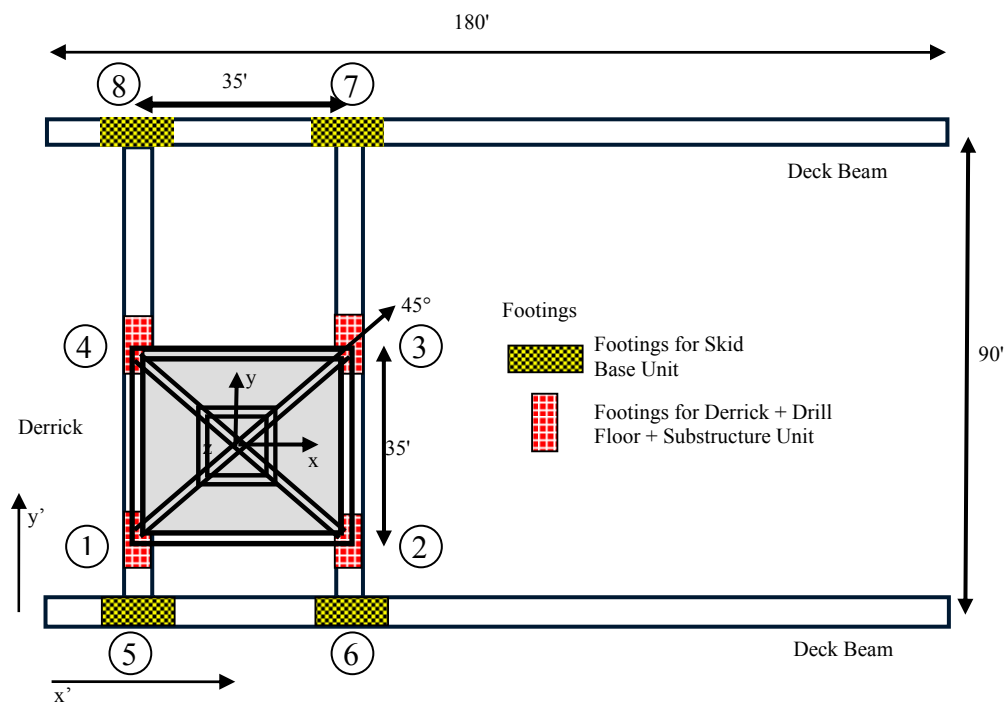


**Fig 2-4 Derrick and Skid Base Footings**

The radius of gyration of derrick and skid base should be approximated to get a rotational moment of inertia. Simplified model for derrick which consists of rectangular cubic is used to calculate rotational moment of inertia as shown in Figure 2-5. The derrick and skid base are assumed to be homogeneous material for calculation.

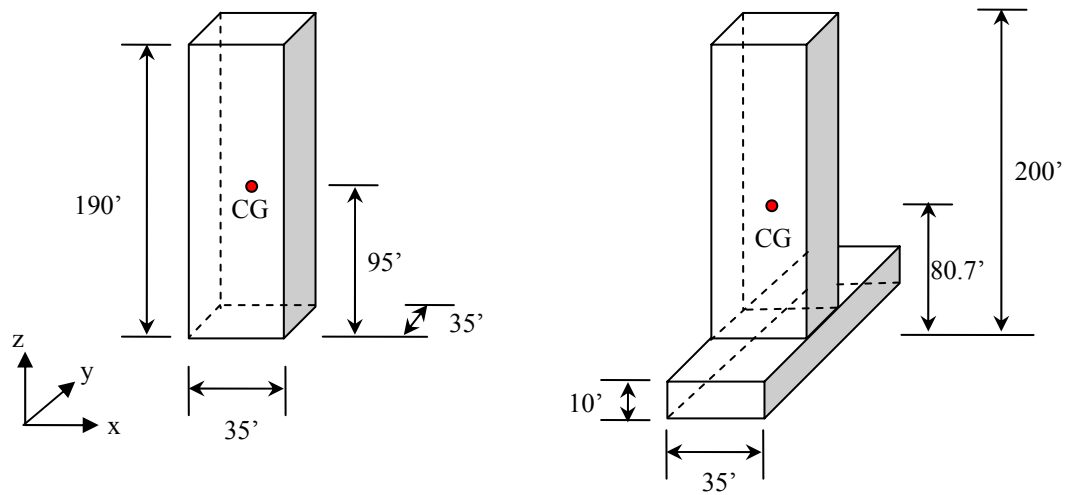


**Fig 2-5 Simplified Model for Radius of Gyration Calculation**

- Radius of Gyration of Derrick

Locate the origin of coordinate axis on the bottom center of derrick, and let the mass of derrick be  $M$ , and radius of gyration of each axis be  $R_x$ ,  $R_y$  and  $R_z$ . Then, rotational moment of inertia with respect to center of gravity would be:

$$X - \text{axis} : I_x = \frac{1}{12} M (35^2 + 190^2) = MR_x^2$$

$$Y - \text{axis} : I_y = \frac{1}{12} M (35^2 + 190^2) = MR_y^2$$

$$Z - \text{axis} : I_z = \frac{1}{12} M (35^2 + 35^2) = MR_z^2$$

$$\text{Thus, } [R_x, R_y, R_z] = [55, 55, 14]$$

Due to the derrick's tall-rectangular shape, the radius of gyration of x and y components are much greater than their z component.

### - Radius of Gyration of Derrick + Skid Base

The center of gravity of derrick + skid base is located at 80.7ft high above bottom of skid base. The moment of inertia of total structure is calculated by taking the moment of inertia of each cubic and applying parallel axis theorem to get the total moment of inertia for derrick and skid base. The offset distance from center of gravity to derrick is 24.3ft and to skid base is 75.7ft. The mass of skid base  $M_1$  is 570 kips and derrick  $M_2$  is 1777 kips.

X – axis :

$$I_x = \frac{1}{12}M_1(90^2 + 10^2) + M_1(75.7^2) + \frac{1}{12}M_2(35^2 + 190^2) + M_2(24.3^2) = (M_1 + M_2)R_x^2$$

Y – axis :

$$I_y = \frac{1}{12}M_1(35^2 + 10^2) + M_1(75.7^2) + \frac{1}{12}M_2(35^2 + 190^2) + M_2(24.3^2) = (M_1 + M_2)R_y^2$$

$$Z – axis : I_z = \frac{1}{12}M_1(35^2 + 90^2) + \frac{1}{12}M_2(35^2 + 35^2) = (M_1 + M_2)R_z^2$$

Thus,  $[R_x, R_y, R_z] = [66, 65, 18]$

The radius of gyration of y component is slightly less than x component, because the longer length of skid base has a negative effect on the rotation of total structures, especially for the rotation along the x axis.

#### 2.1.4 Environmental Condition

The environmental condition, which is one of the input parameters of this study, is provided by API Bulletin 2INT-MET (2007). To generate long crested irregular

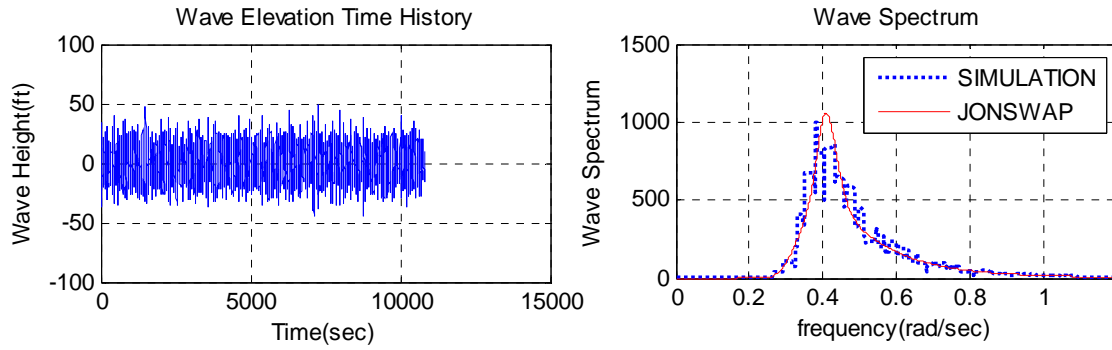
random waves, the JONSWAP spectrum is employed in this analysis with stiffness parameter of 2.4. Time-varying wind speed series is generated for 3 hours using API wind spectrum. Wind, wave and current are propagating to the same direction, so only collinear case is considered for simplicity. Four incident angles, 0 degree, 21.25 degrees, 45 degrees and 90 degrees are used for analysis. Table 2-5 shows the environmental conditions for 100, 200 and 1000-year return period hurricane events at central area of Gulf of Mexico.

**Table 2-5 Environmental Conditions**

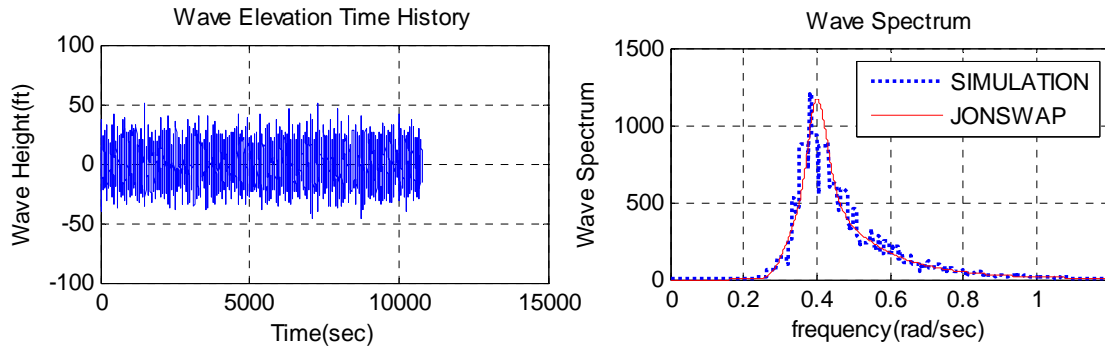
<b>Return Period</b>	<b>100 year</b>		<b>200 year</b>		<b>1000 year</b>	
Hs (ft)	51.8		54.1		65	
Tp (sec)	15.4		15.7		17.2	
$\gamma$	2.4		2.4		2.4	
1-hour Mean Wind Speed (ft/sec)	157.5		167.3		196.9	
Current Profile	Depth (ft)	Speed (ft/sec)	Depth (ft)	Speed (ft/sec)	Depth (ft)	Speed (ft/sec)
	0.0	7.9	0.0	8.4	0.0	9.8
	-165.5	5.9	-175.5	6.3	-206.5	7.4
	-331.0	0	-351.0	0	-413.0	0
	-3000	0	-3000	0	-3000	0

Figure 2-6 shows the time history of wave elevation for each return period. 3-hour random wave is generated by CHARM3D and wave spectrum of the generated wave is compared with JONSWAP wave spectrum. The spectral density of random wave

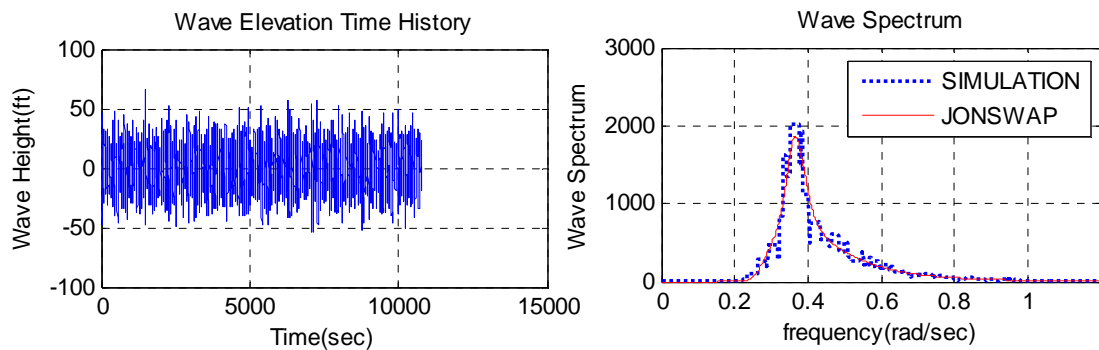
for hurricane conditions shows a good agreement between simulated data and target wave spectrum.



(a) Wave elevation for 100-year hurricane case



(b) Wave elevation for 200-year hurricane case



(c) Wave elevation for 1000-year hurricane case

**Fig 2-6 Wave Elevation and Spectrum**

The wind force coefficients  $C_{eff} = F_w / V_{10}^2 = 0.0665 \text{kips} / (\text{ft} / \text{sec})^2$  for TLP and  $0.0848 \text{kips} / (\text{ft} / \text{sec})^2$  for SPAR are used to find total wind force on the floating structures.  $F_w$  stands for the total wind force on hull above MWL and  $V_{10}$  represents 1-hour averaged wind velocity at 10m height above MWL. Figure 2-7 shows the 3-hour simulated wind velocity and its spectrum at the height of center of pressure. The API wind spectrum is adopted in this simulation and it is formulated as follows.

$$S(f) = \frac{3444.8 \left( \frac{U_0}{32.8} \right)^2 \left( \frac{z}{32.8} \right)^{0.45}}{\left( 1 + \tilde{f}^n \right)^{(5/3n)}}$$

$$\tilde{f} = 172 f \left( \frac{z}{32.8} \right)^{2/3} \left( \frac{U_0}{32.8} \right)^{-0.75},$$

where  $n = 0.468$  and

- $S(f)(\text{ft}^2 \text{s}^{-2} / \text{Hz})$  is the spectral energy density at frequency  $f(\text{Hz})$
- $z(\text{ft})$  is the height above sea level
- $U_0(\text{ft} / \text{s})$  is the 1-hour mean wind speed at 32.8 ft above sea level.

The 3-sec gust velocity for each hurricane condition is also included in the random wind velocity series. The design wind speed  $u(z,t)(\text{ft} / \text{s})$  at height  $z(\text{ft})$  above sea level for period  $t \leq t_0 = 3600\text{s}$  is given by:

$$u(z,t) = U(z)[1 - 0.41I_u(z) \ln(t/t_0)],$$

where the 1-hour mean wind speed  $U(z)(\text{ft} / \text{s})$  at level  $z$  is given by:

$$U(z) = U_0 \left[ 1 + C \ln \left( \frac{z}{32.8} \right) \right]$$

$$C = 0.0573\sqrt{1 + 0.0457U_0}$$

and where the turbulence intensity  $I_u(z)$  at level  $z$  is given by

$$I_u(z) = 0.06\left[1 + 0.013U_0\right]\left(\frac{z}{32.8}\right)^{-0.22},$$

where  $U_0$  (ft/s) is 1-hour average wind speed at 32.8 ft elevation.

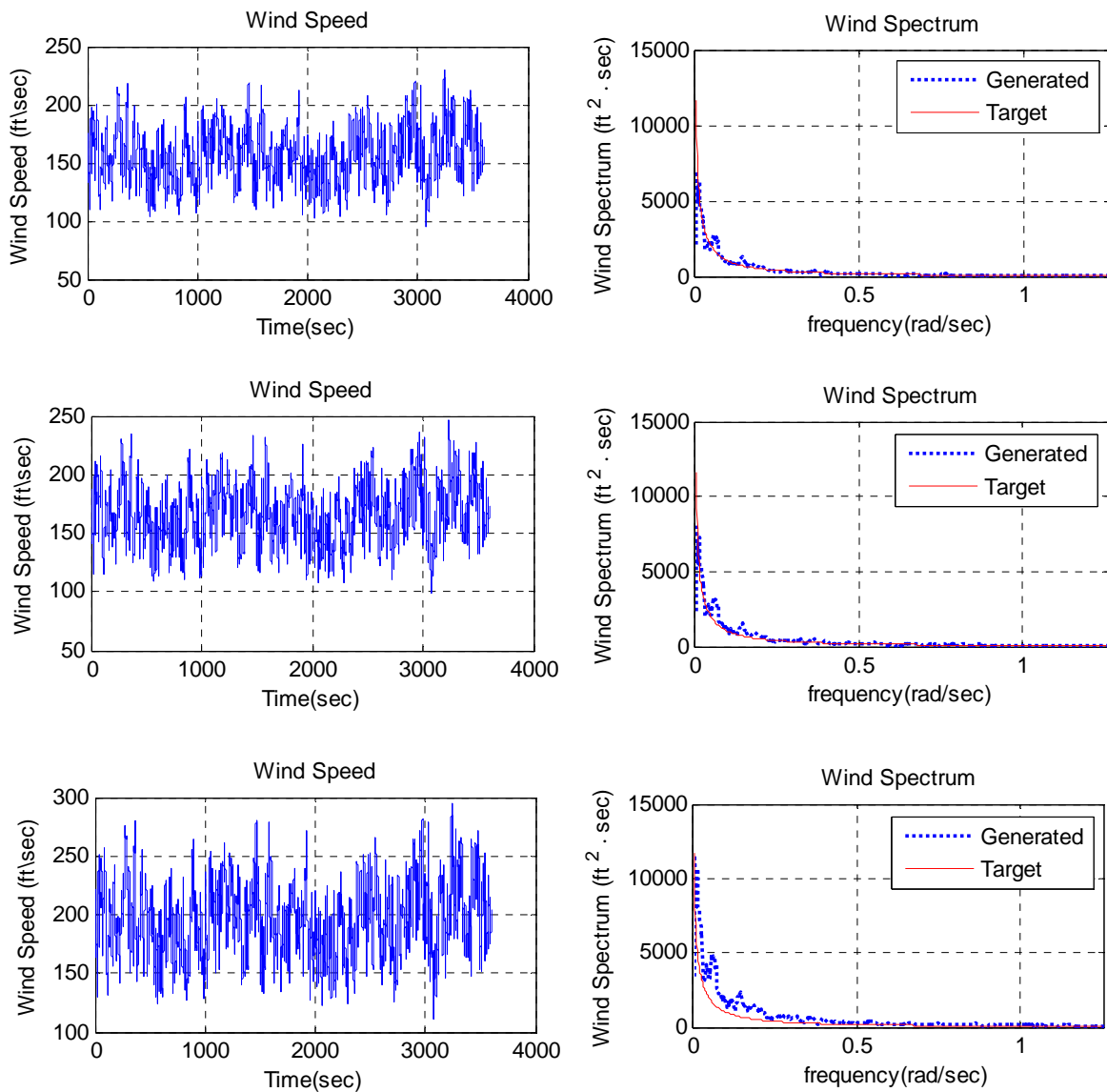


**Fig 2-7 Wind Speed Time Series and Spectrum**

The currents profile for 100-year, 200-year, and 1000-year return period hurricane conditions are depicted in Figure 2-8.

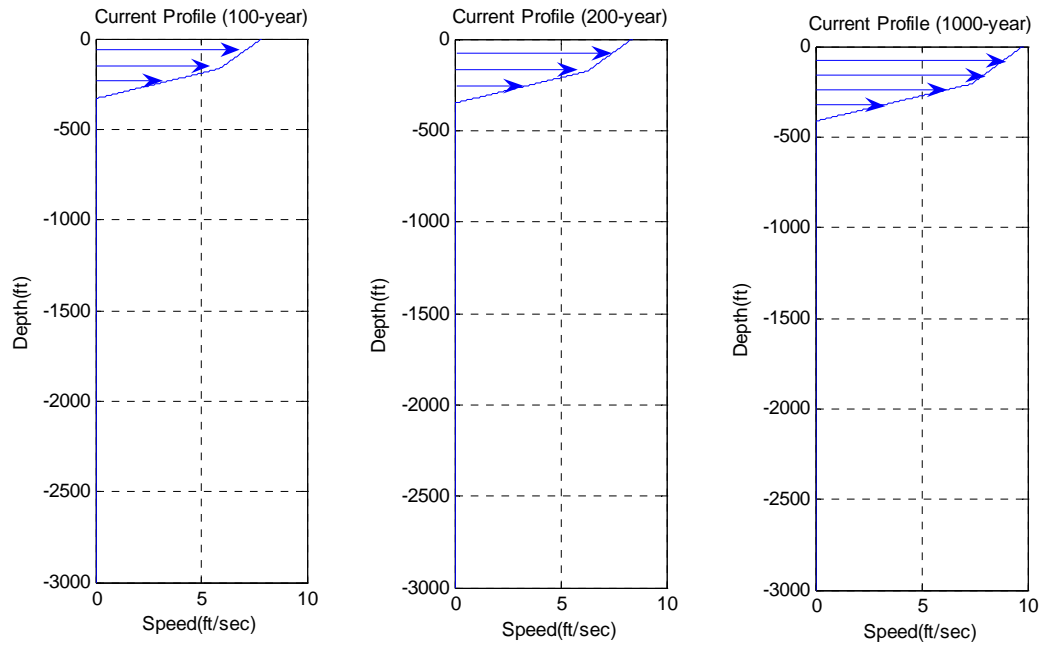


**Fig 2-8 Current Profile in Hurricane Conditions**



## 2.2 Coupled Dynamic Analysis in Time Domain Using CHARM3D

### 2.2.1 Added Mass and Damping Coefficient

If a floating body moves in an ocean, hydrodynamic pressure forces and moment will affect the motion of the body. The hydrodynamic pressure on the body due to the body motion can be regarded as equivalent increment of body mass. That portion of mass is an added mass. Added mass and damping coefficient for both TLP and SPAR are presented in Figures 2-9 and 2-10.

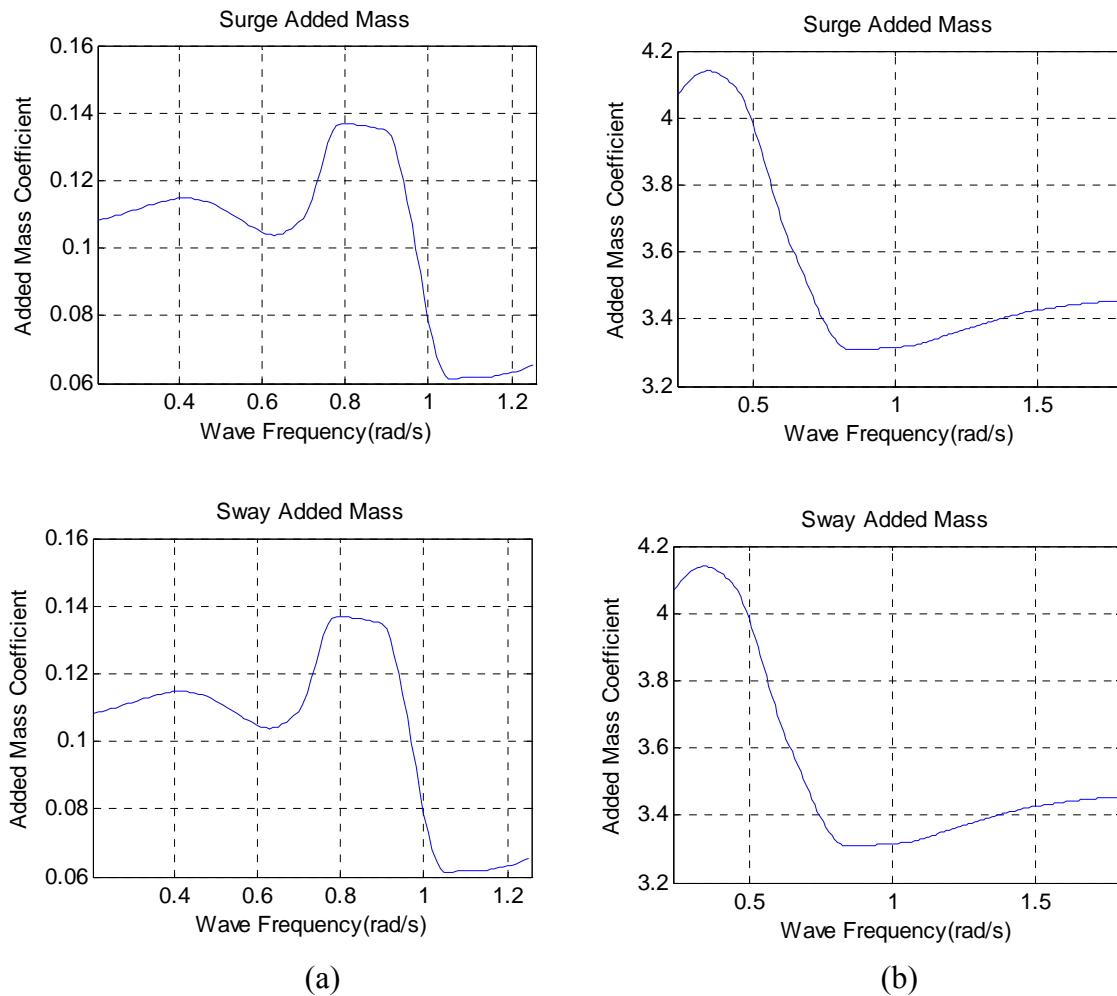


**Fig 2-9 Added Mass Coefficient of (a) TLP and (b) SPAR**

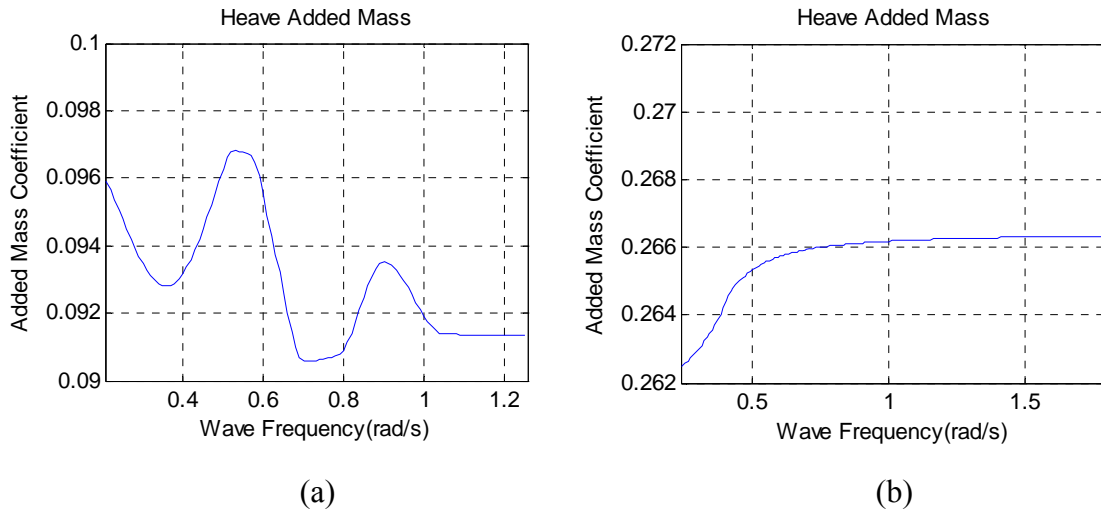


**Fig 2-9 Continued**

The motion of floating structures will generate the radiation waves and this may reduce the energy that the structures have. This effect is quantified by damping coefficient of the structures.

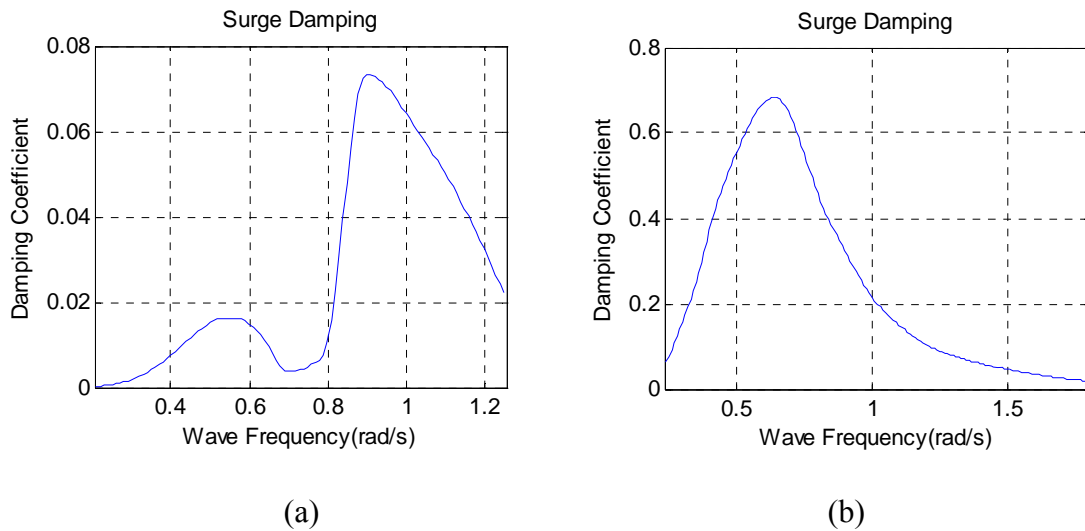


**Fig 2-10 Damping Coefficient of (a) TLP and (b) SPAR**

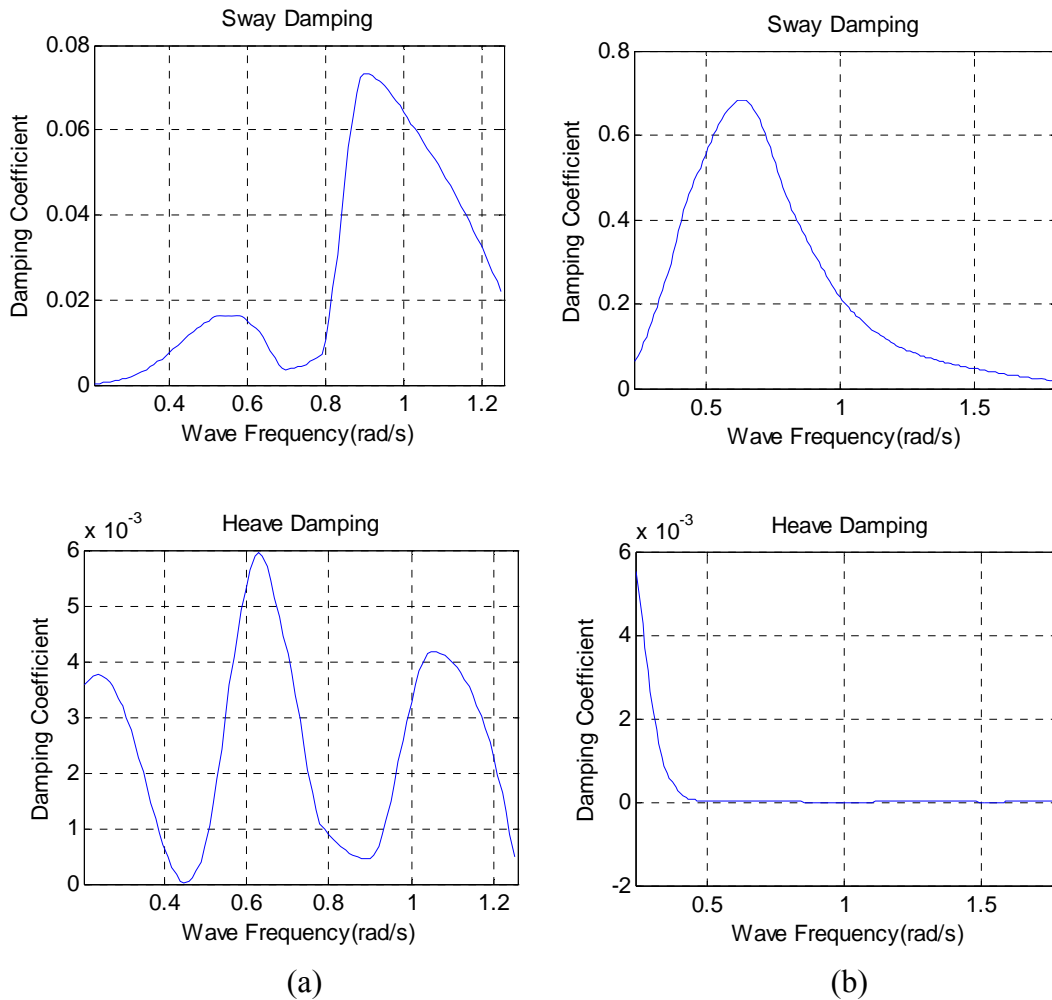


**Fig 2-10 Continued**

### 2.2.2 Forces on Derrick and Skid Base

Once hydrodynamic coefficients are calculated, time domain analysis should be carried out. Only the first order of wave force is implemented and second order sum frequency wave force is neglected. The second order difference frequency wave force can be approximately included by Newman's approximation method. The hydrodynamic coefficient from WAMIT output is converted into CHARM3D input using the interface

software WAMPOST. The mooring lines and risers of the TLP and SPAR are modeled so that we get a more realistic motion of each system. The total force acting on the derrick and skid base consists of 3 different force components which include inertia, wind, and gravity force. In order to calculate the total force for 3-hour duration, all 3 force components are simulated individually and are summed up. Since each individual forces have their own phase characteristics, maximum of simulated total force could not be greater than summation of each maximum. The detail of calculation has been set up by Yang (2009) and whole procedure of calculation in this study follows Yang's methodology except for wind force calculation. Wind forces on the derrick were computed following the recommendations in API 4F. 3-hour random wind velocities are simulated based on the API wind spectrum, and thus 3-second gust velocity for each hurricane condition is also included. The derrick is divided into 4 parts - upper derrick, lower derrick, drill floor and substructure, and wind force is calculated individually with different perm factor which represents a ratio between estimated measures of the total projected areas of all the members in an area to the total area. The wind force of the skid base is also calculated in the same way as wind force of the derrick. Total wind force at the center of pressure was computed for respective wind velocities, projected areas, and heading angles.

### 2.2.3 Reaction Forces on the Footings

The reaction force on the footings of derrick or skid base can be calculated from the force and moment equilibrium. If we assume that the derrick is a rigid body, then reaction force at each direction can be calculated as follows. In general, lateral reaction

force is mostly occurred by horizontal force such as wind force and inertia force, but vertical uplift reaction force is caused by vertical force like gravity force and overturning moment due to horizontal forces. The reaction force for derrick and skid base will be separately considered, and these reaction forces are also simulated during 3-hour simulation period. Design engineer should take maximum and minimum reaction forces into consideration to guarantee proper stability of structures.

- Reaction Force of X and Y Direction

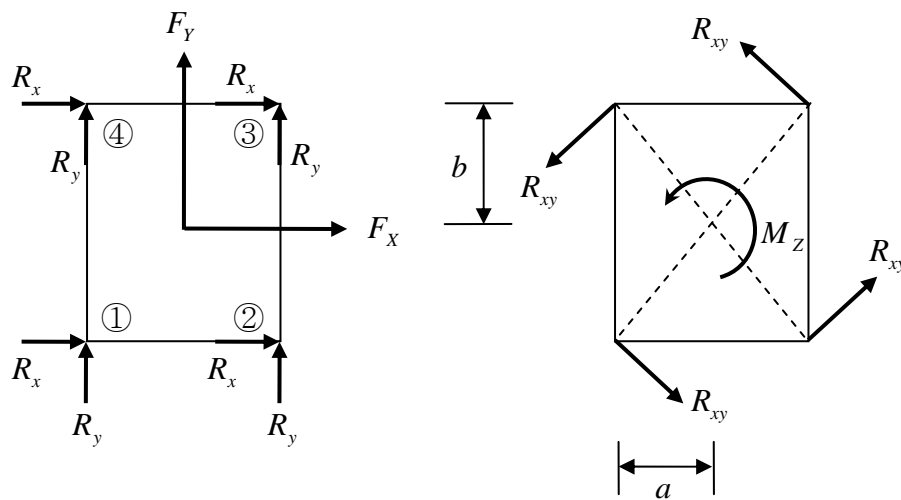


**Fig 2-11 Horizontal Reaction Forces**

The reaction force of x-direction consists of the external force of x direction and external moment of z direction as shown in Figure 2-11. The force and moment equilibrium can be expressed by

$$F_x + 4R_x = 0$$

$$F_Y + 4R_y = 0$$

$$M_Z + 4R_{xy} \cdot \sqrt{a^2 + b^2} = 0$$

Thus, the reaction forces  $R_x$ ,  $R_y$ , and  $R_{xy}$  will be

$$R_x = -\frac{F_X}{4}$$

$$R_y = -\frac{F_Y}{4}$$

$$R_{xy} = -\frac{M_Z}{4\sqrt{a^2 + b^2}}$$

Total reaction force of each footing would be

$$\text{Point ① : } R_{1x} = R_x + R_{xy} \frac{b}{\sqrt{a^2 + b^2}} = -\frac{F_X}{4} - \frac{b \cdot M_Z}{4(a^2 + b^2)}$$

$$\text{Point ② : } R_{2x} = R_x + R_{xy} \frac{b}{\sqrt{a^2 + b^2}} = -\frac{F_X}{4} - \frac{b \cdot M_Z}{4(a^2 + b^2)}$$

$$\text{Point ③ : } R_{3x} = R_x - R_{xy} \frac{b}{\sqrt{a^2 + b^2}} = -\frac{F_X}{4} + \frac{b \cdot M_Z}{4(a^2 + b^2)}$$

$$\text{Point ④ : } R_{4x} = R_x - R_{xy} \frac{b}{\sqrt{a^2 + b^2}} = -\frac{F_X}{4} + \frac{b \cdot M_Z}{4(a^2 + b^2)}$$

Similarly, the reaction force of y direction can be calculated as follows

$$\text{Point ① : } R_{1y} = R_y - R_{xy} \frac{a}{\sqrt{a^2 + b^2}} = -\frac{F_Y}{4} + \frac{a \cdot M_Z}{4(a^2 + b^2)}$$

$$\text{Point ② : } R_{2y} = R_y + R_{xy} \frac{a}{\sqrt{a^2 + b^2}} = -\frac{F_Y}{4} - \frac{a \cdot M_Z}{4(a^2 + b^2)}$$

$$\text{Point ③ : } R_{3y} = R_y + R_{xy} \frac{a}{\sqrt{a^2 + b^2}} = -\frac{F_y}{4} - \frac{a \cdot M_z}{4(a^2 + b^2)}$$

$$\text{Point ④ : } R_{4y} = R_y - R_{xy} \frac{a}{\sqrt{a^2 + b^2}} = -\frac{F_y}{4} + \frac{a \cdot M_z}{4(a^2 + b^2)}$$

- Reaction Force of Z Direction

The reaction force of z direction consists of external force on the vertical direction and overturning moment along x and y directions as shown in Figure 2-12.

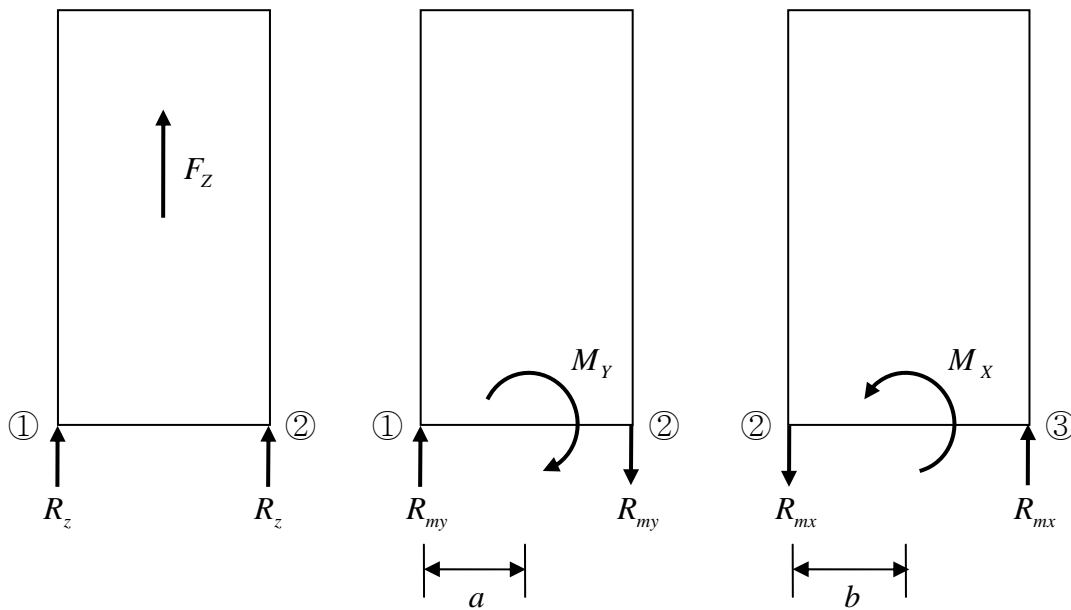


**Fig 2-12 Vertical Reaction Forces**

The force and moment equilibrium of vertical direction is

$$F_z + 4R_z = 0$$

$$M_y + 4aR_{my} = 0$$

$$M_x + 4bR_{mx} = 0$$

Thus,

$$R_z = -\frac{F_z}{4}$$

$$R_{my} = -\frac{M_y}{4a}$$

$$R_{mx} = -\frac{M_x}{4b}$$

Total reaction force of vertical direction would be

$$\text{Point ① : } R_{1z} = R_z + R_{my} - R_{mx} = -\frac{F_z}{4} - \frac{M_y}{4a} + \frac{M_x}{4b}$$

$$\text{Point ② : } R_{2z} = R_z - R_{my} - R_{mx} = -\frac{F_z}{4} + \frac{M_y}{4a} + \frac{M_x}{4b}$$

$$\text{Point ③ : } R_{3z} = R_z - R_{my} + R_{mx} = -\frac{F_z}{4} + \frac{M_y}{4a} - \frac{M_x}{4b}$$

$$\text{Point ④ : } R_{4z} = R_z + R_{my} + R_{mx} = -\frac{F_z}{4} - \frac{M_y}{4a} - \frac{M_x}{4b}$$

All calculations are conducted by the motion information of hull structures and wind velocity time history. Engineering mathematical software MATLAB is used to calculate 3-hour external force and reaction force simulation.



### 3 TLP CASE STUDY

#### 3.1 TLP Motion Analysis

As we discussed in the previous section, both frequency domain and time domain analysis tools are utilized to analyze the motion of TLP. The TLP model adopted in this study is an identical model analyzed by Kim et al, (2001), so the physical characteristics of motion are also supposed to be the same, once the environmental conditions are kept the same.

#### 3.2 External Forces and Moments

Inertia force, wind force and gravity force are calculated separately, and summed up to get a total external force on the derrick and skid base. Since the initial study and calculation have been done by Yang (2009), only reproduced data which are calculated with different environmental conditions and different wind force calculation method are presented in Appendix. In this study, 2 different directions of incident angle for wind, wave and current ( $0^\circ$  and  $45^\circ$ ) are computed as conducted in the initial research, and the selected return period of hurricane is 100-year for TLP.

#### 3.3 Reaction Forces

Engineers responsible for derrick design should consider maximum or minimum reaction force of each footing when they decide the strength of footings. Positive and negative signs stand for the direction of reaction force. That is to say, maximum of absolute value of each reaction force is significant. To see the tendency of reaction force

of each footing, mean reaction forces for 0 degree incident angle case are presented in Figures 3-1 and 3-2. Since the derrick and skid base are assumed as a rigid body, the longitudinal or lateral reaction forces for derrick or skid base show the similar tendency for 4 footings.

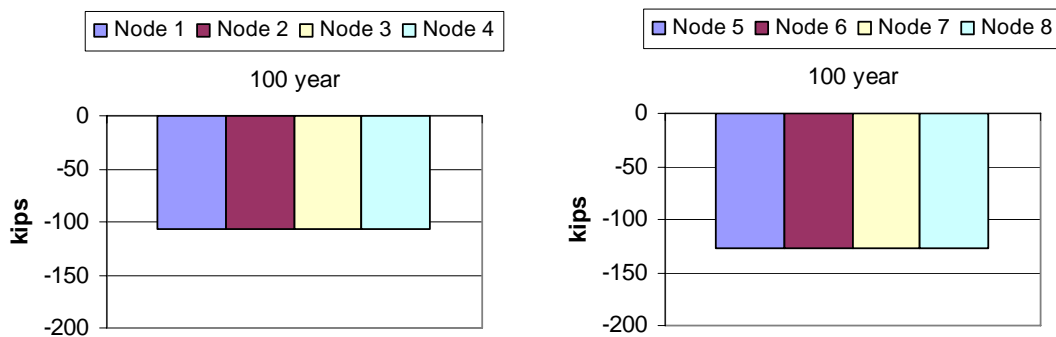


**Fig 3-1 TLP Mean Surge Reaction Force (0 Degrees)**

The tendency of uplift reaction force of footings can be intuitively predicted if the direction of external forces is given. Apparently, the footings located in the weather side (Node 1 and 4) will experience the tensile force if the weight do not have enough force to overcome overturning moment. The footings in the lee side (Node 2 and 3) will experience the compression force during all the simulation time. In Figure 3-2, this tendency can be verified. The negative sign of reaction force represent the uplift reaction force, and positive sign means the compression force.

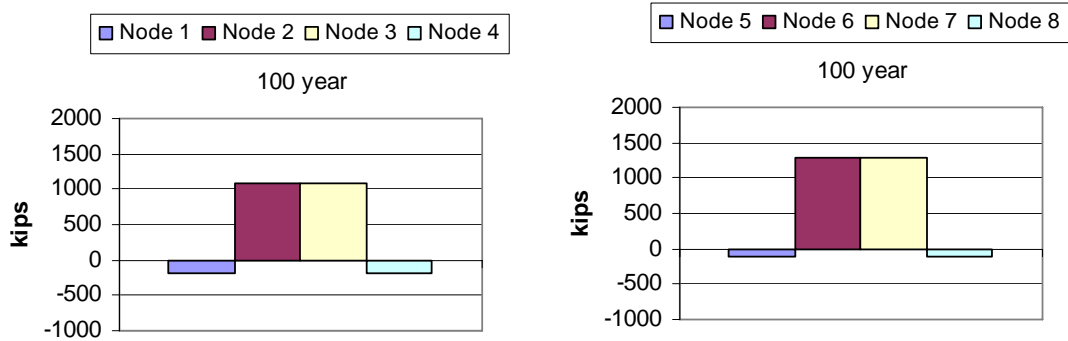


**Fig 3-2 TLP Mean Heave Reaction Force (0 Degrees)**

The simulation data for TLP are attached in the Appendix section and the key result and significant data along with the data of SPAR case study will be analyzed and presented.

#### 4 CASE 1. SPAR (3000FT) WITH DERRICK AA – 0 DEGREE CASE

##### 4.1 SPAR Motion Time History

In this case, the reaction force on derrick footings and skid base footings for SPAR will be analyzed. Wind, wave and current are coming from the 0 degree incident angle. The SPAR motion time series for 100-year, 200-year and 1000-year hurricane conditions will be presented. In general, SPAR is more vulnerable to roll and pitch. So, inertia force of derrick could be greater than that of TLP. Due to the large inclination angle, gravity force of surge component could also be bigger than that of TLP. Figures 4-1 to 4-3 show the 3-hour simulation result of SPAR motion and its spectral density for 100-year hurricane condition.

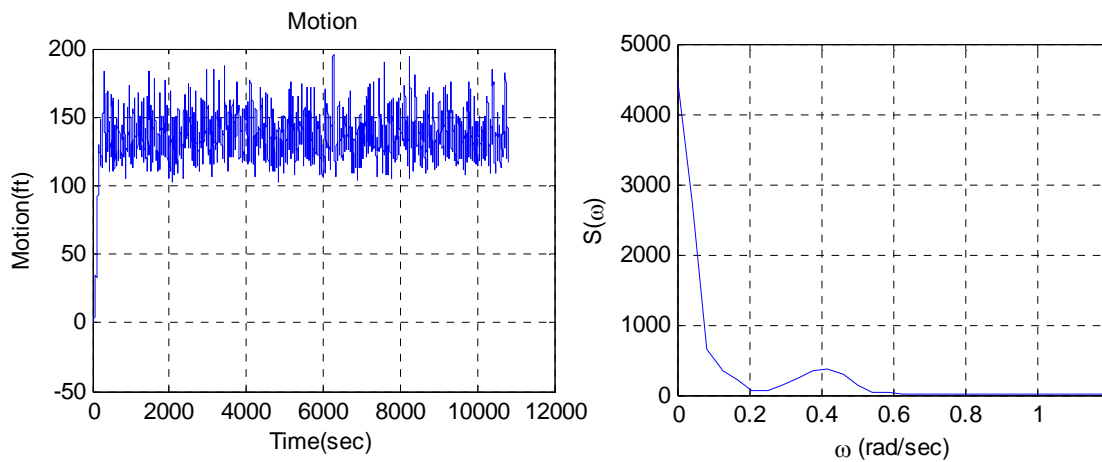


**Fig 4-1 SPAR Surge Motion and Spectrum (0 Degrees)**

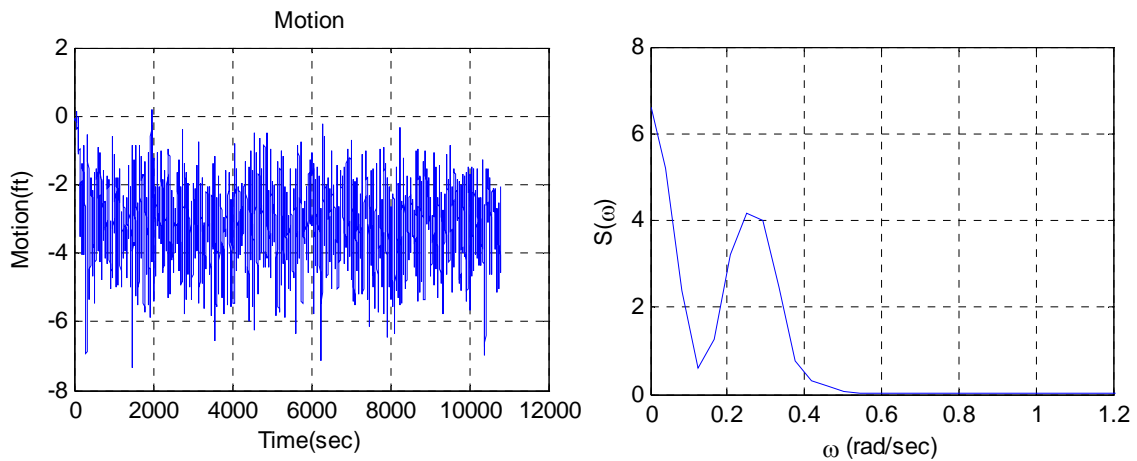


**Fig 4-2 SPAR Heave Motion and Spectrum (0 Degrees)**

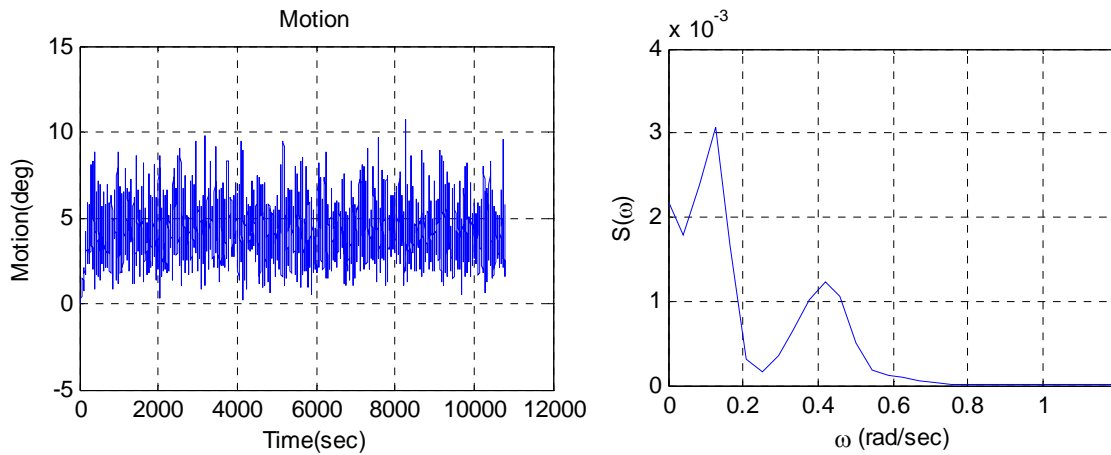


**Fig 4-3 SPAR Pitch Motion and Spectrum (0 Degrees)**

#### 4.2 Inertia Force

Inertia force of SPAR derrick is relatively bigger than that of TLP derrick, because the rotational motion of SPAR including pitch and roll is more severe. Large inertia force can contribute to the increase of uplift reaction force, so the SPAR derrick footings will experience bigger reaction forces compared to TLP derrick footings. The

inertial force of derrick and skid base are calculated based on the hull motion, and are summarized in Figures 4-4 to 4-5 and Table 4-1.

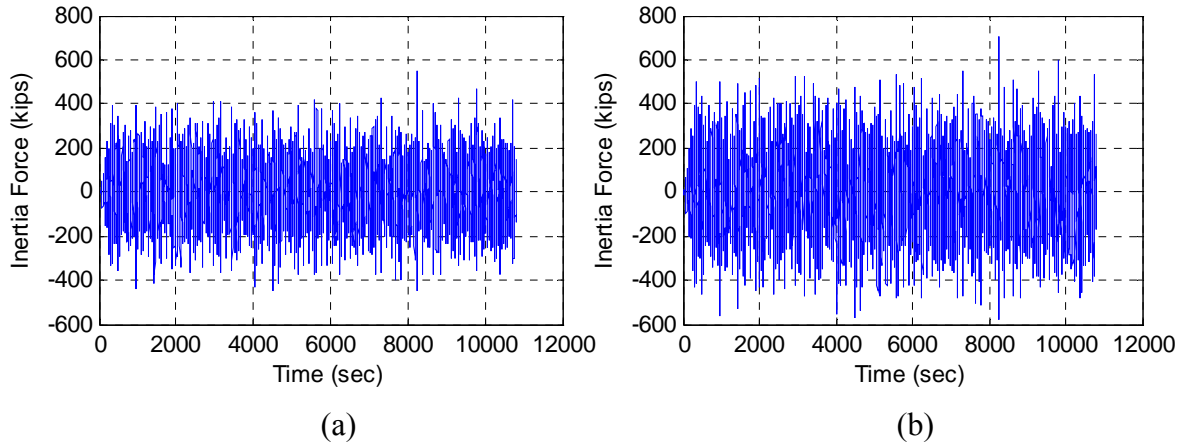


**Fig 4-4 Surge Inertia Force of (a) Derrick and (b) Derrick + Skid Base (0 Degrees)**

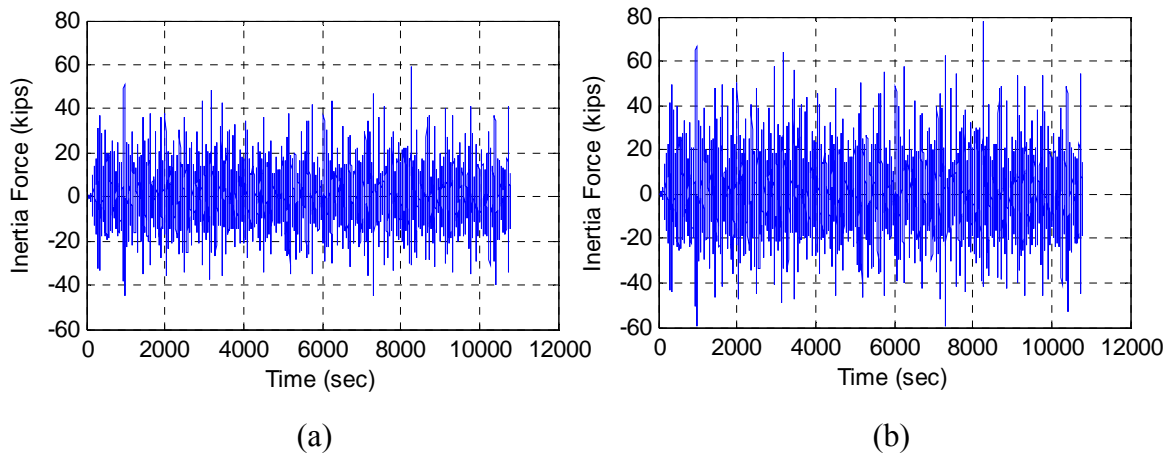


**Fig 4-5 Heave Inertia Force of (a) Derrick and (b) Derrick + Skid Base (0 Degrees)**

**Table 4-1 Inertia Force Statistics for (a) Derrick and (b) Derrick + Skid Base (0 Degrees)**

<b>Inertia</b>	Surge	Sway	Heave
MAX	546	1	59
MIN	-451	-1	-45
MEAN	0	0	1

(a)

<b>Inertia</b>	Surge	Sway	Heave
MAX	698	1	78
MIN	-577	-1	-60
MEAN	0	0	1

(b)

### 4.3 Wind Force

The derrick and skid base of SPAR is located 140ft above MWL, and for this reason, derrick wind force of SPAR is less than that of TLP. The wind force on each component of the derrick and skid base is tabulated below. Mean pressure of derrick is 399 kips, while mean pressure of TLP derrick is 422 kips. Total wind force on derrick including skid base is 467 kips. A detail list of wind force component is tabulated in Table 4-2.

**Table 4-2 Wind Force of Derrick and Skid Base (0 Degrees)**

<b>100 YEAR</b>	z elev above MWL to Mid-Point	U(z) 1-hr ave	C <sub>shape</sub>	Unit Pressure	Perm Factor	Projected Area	Pressure	Moment
Upper derrick	343	218	1.25	70	0.6	2805	118	23984
Lower derrick	258	211	1.25	66	0.6	2975	117	13787
Drill floor	208	205	1.50	75	1.0	750	56	3783
Substructure	175	201	1.50	72	0.6	2500	107	3756
<b>Derrick</b>							<b>399</b>	<b>45310</b>
Skid base	145	196	1.50	68	1.0	1000	68	341
<b>Derrick + Skid Base</b>							<b>467</b>	<b>45651</b>

The time history of wind force and statistics of force are shown in Figures 4-6 to 4-7 and Table 4-3.

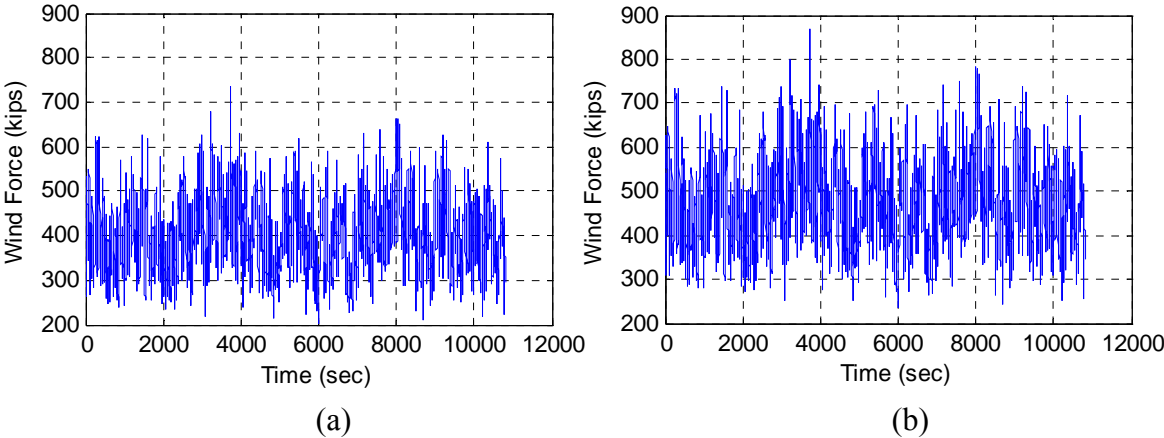


**Fig 4-6 Surge Wind Force of (a) Derrick and (b) Derrick + Skid Base (0 Degrees)**

Heave component of wind force of SPAR is considerably bigger than that of TLP case, as the large tilted angle of derrick can generate vertical uplift force on derrick. Compared with TLP case, the maximum heave component of derrick is 93 kips, while it is 5 kips for TLP.

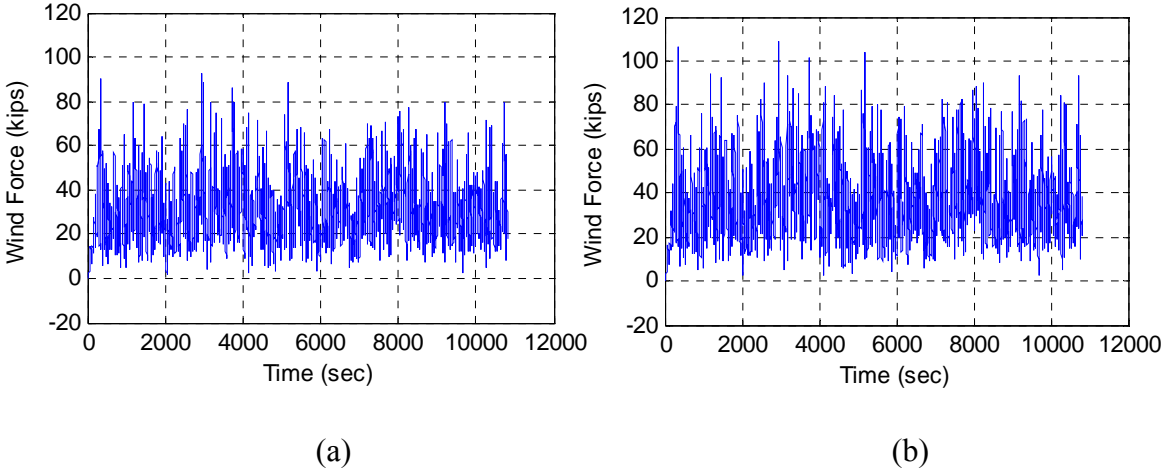


**Fig 4-7 Heave Wind Force of (a) Derrick and (b) Derrick + Skid Base (0 Degrees)**



**Table 4-3 Wind Force Statistics for (a) Derrick and (b) Derrick + Skid Base (0 Degrees)**

Wind	Surge	Sway	Heave
MAX	736	1	93
MIN	203	-1	0
MEAN	400	0	31

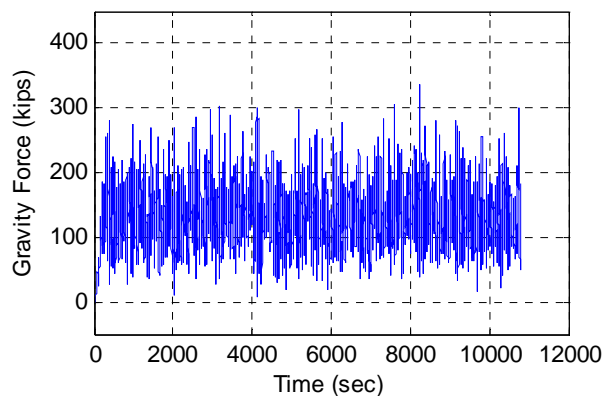
(a)

Wind	Surge	Sway	Heave
MAX	868	1	109
MIN	235	-2	0
MEAN	468	0	36

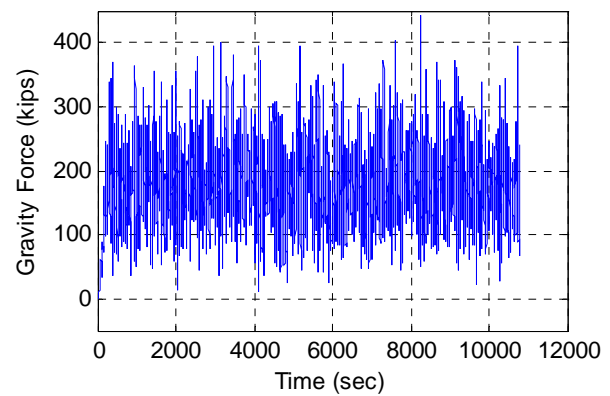
(b)

#### 4.4 Gravity Force

Most of the gravity force on footings is applied in a vertical direction due to its weight. If the hull is tilted, then horizontal component of gravity force will also rise. For TLP case, this horizontal component of gravity force is negligible because pitch and roll of hull is so small. However, horizontal component of gravity force for SPAR is significant relative to TLP due to large motion of pitch or roll. The maximum surge component of gravity force of TLP derrick is only 19 kips, but the maximum of SPAR is 335 kips which is comparable to the inertia force of TLP derrick. Figures 4-8 to 4-9 and Table 4-4 show the time history of gravity force.



(a)



(b)

**Fig 4-8 Surge Gravity Force of (a) Derrick and (b) Derrick + Skid Base (0 Degrees)**

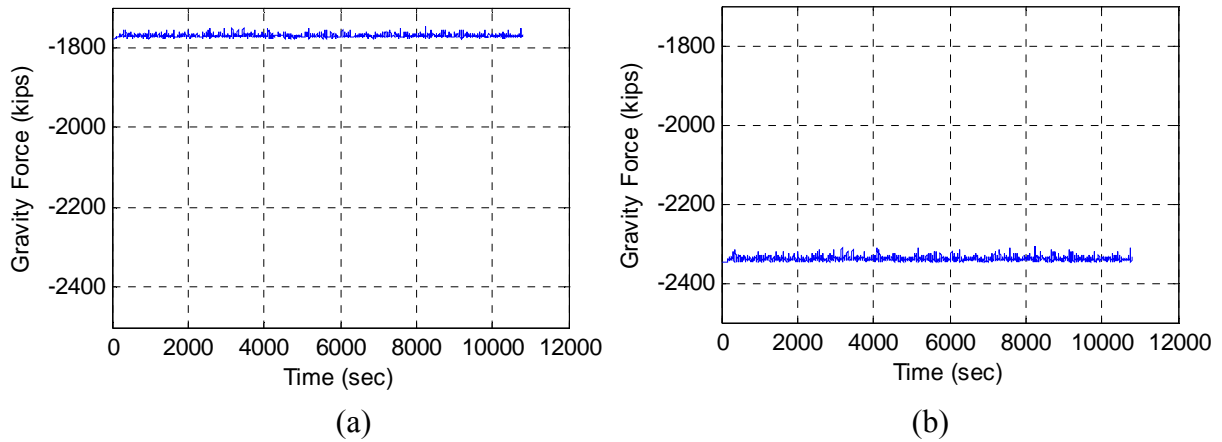


**Fig 4-9 Heave Gravity Force of (a) Derrick and (b) Derrick + Skid Base (0 Degrees)**

**Table 4-4 Gravity Force Statistics for (a) Derrick and (b) Derrick + Skid Base (0 Degrees)**

Gravity	Surge	Sway	Heave
MAX	335	0	-1745
MIN	0	0	-1777
MEAN	134	0	-1771

(a)

Gravity	Surge	Sway	Heave
MAX	443	0	-2305
MIN	0	0	-2347
MEAN	177	0	-2340

(b)

#### 4.5 Total Force

The summation of inertia force, wind force and gravitational force is regarded as total force, and it is presented in Figures 4-10 to 4-11 and Table 4-5.

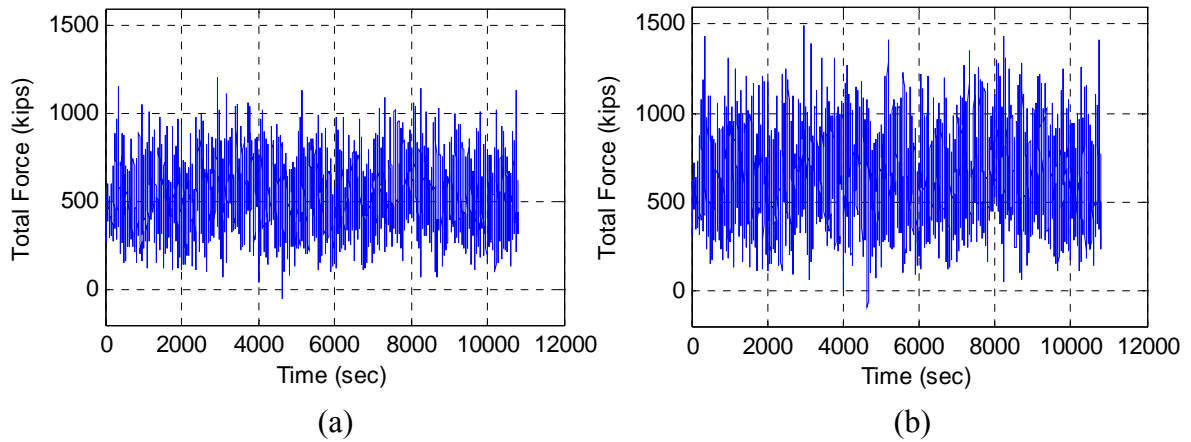


**Fig 4-10 Surge Total Force of (a) Derrick and (b) Derrick + Skid Base (0 Degrees)**

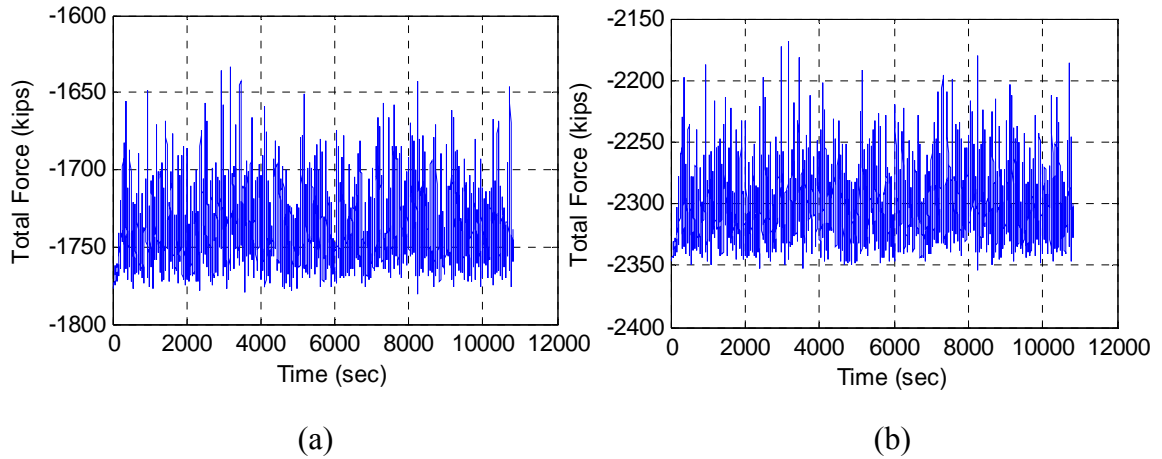


**Fig 4-11 Heave Total Force of (a) Derrick and (b) Derrick + Skid Base (0 Degrees)**

Except for wind force, both inertia force and gravity force on SPAR derrick are larger than those of TLP derrick, so total force on derrick and skid base of SPAR is admittedly large.

**Table 4-5 Total Force Statistics for (a) Derrick and (b) Derrick + Skid Base (0 Degrees)**

Total	Surge	Sway	Heave
MAX	1207	1	-1633
MIN	-53	-2	-1780
MEAN	534	0	-1740

(a)

Total	Surge	Sway	Heave
MAX	1493	1	-2169
MIN	-96	-2	-2354
MEAN	645	0	-2303

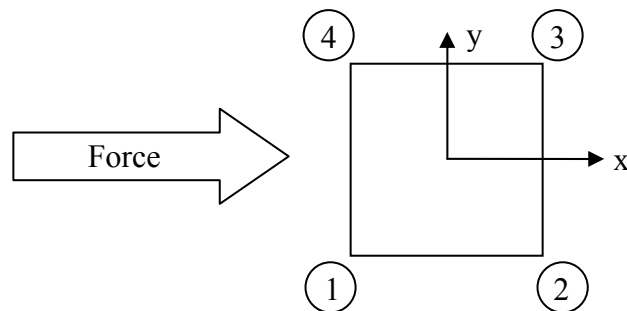
(b)

#### 4.6 Reaction Force

The reaction forces of each footing are calculated according to the methodology described in the previous section. The node number for derrick ranges from 1 to 4 and from 5 to 8 for skid base. The time histories of derrick reaction force of each footing are listed below. Since the total force applied on derrick and skid base is bigger than that of TLP, we expect that the reaction force of each footing will be bigger as well.

##### 4.6.1 Derrick Reaction Force

The location of derrick footings and node number is shown in Figure 4-12. The external force including wind, wave, and current is coming from 0 degree of positive x-direction.

**Fig 4-12 Direction of Force and Node Location of Derrick (0 Degrees)**

The time history of total reaction force is shown in Figures 4-13 to 4-16, and the statistics of reaction force for derrick footings are tabulated in Table 4-6.

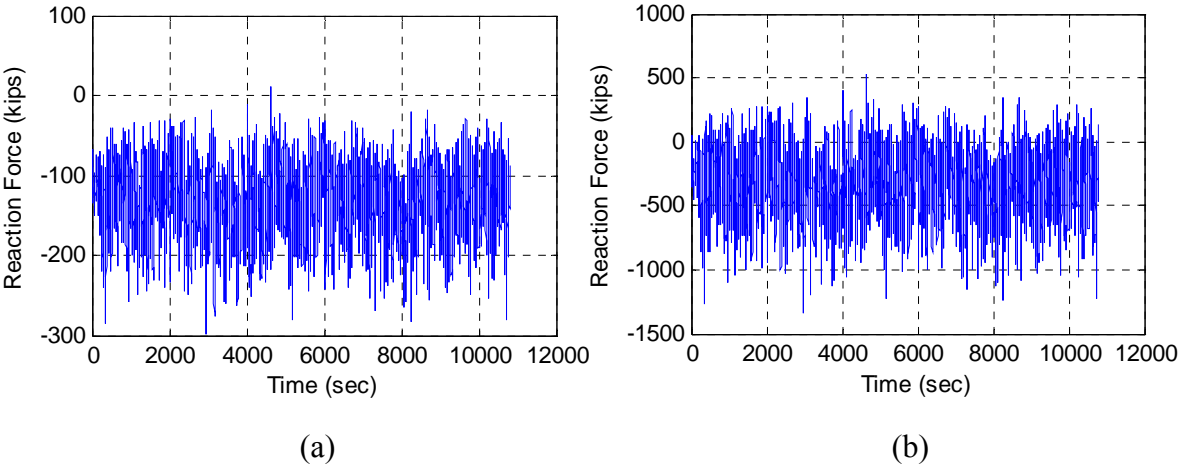


**Fig 4-13 (a) Surge Reaction (b) Heave Reaction on Footing 1 (0 Degrees)**

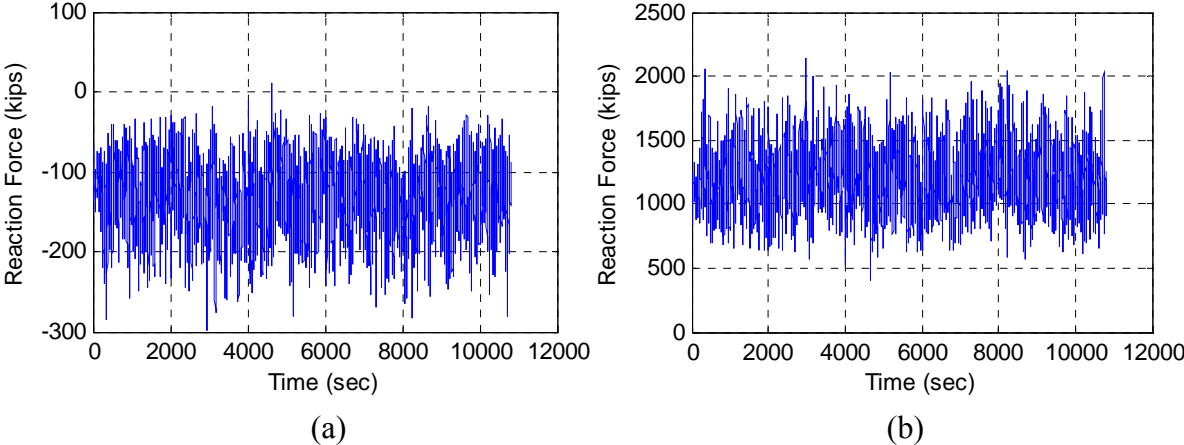


**Fig 4-14 (a) Surge Reaction (b) Heave Reaction on Footing 2 (0 Degrees)**

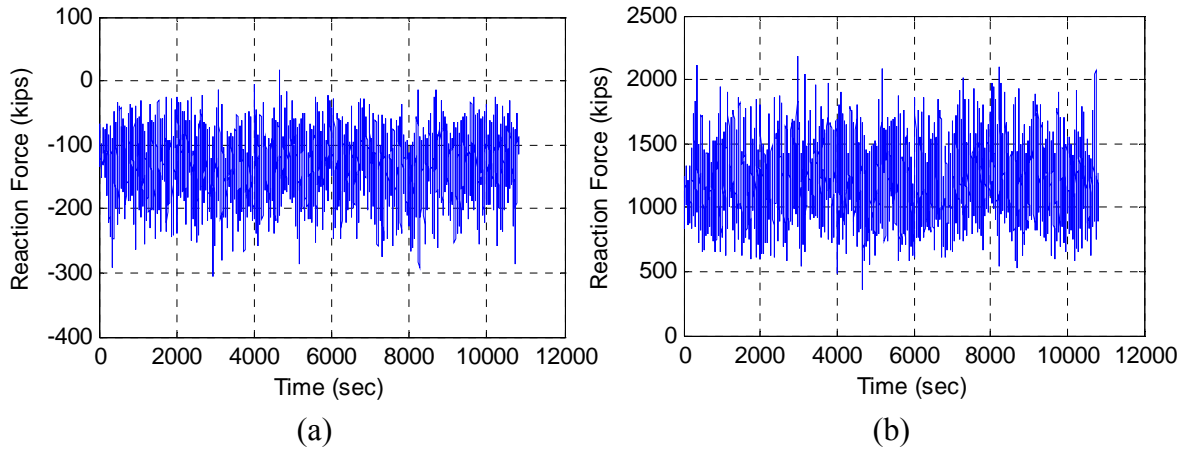


**Fig 4-15 (a) Surge Reaction (b) Heave Reaction on Footing 3 (0 Degrees)**

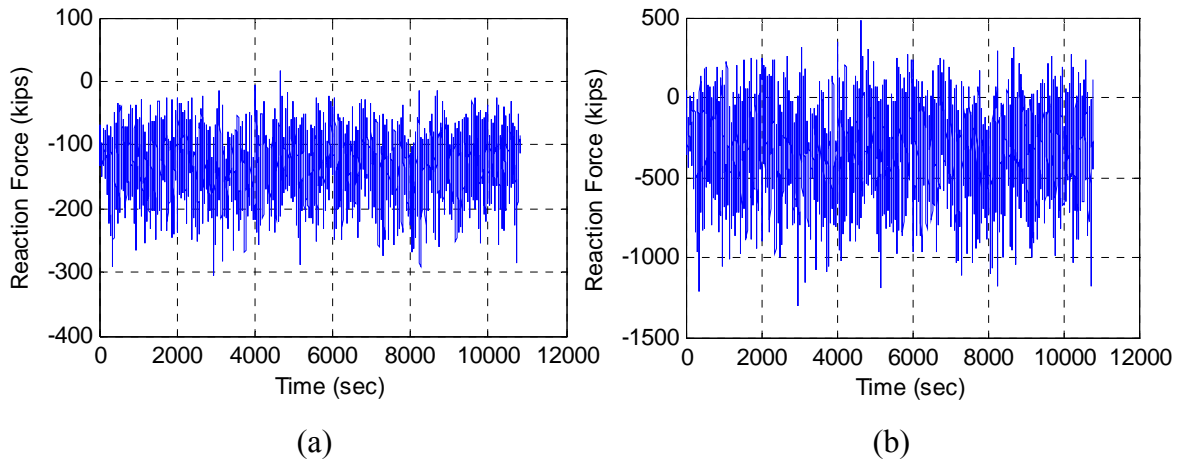


**Fig 4-16 (a) Surge Reaction (b) Heave Reaction on Footing 4 (0 Degrees)**

**Table 4-6 Derrick Reaction Force Statistics (0 Degrees)**

Node	Reaction	X	Y	Z
1	MAX	10	3	530
	MIN	-299	-4	-1351
	MEAN	-133	0	-341

Node	Reaction	X	Y	Z
2	MAX	10	4	2131
	MIN	-299	-3	406
	MEAN	-133	0	1211

**Table 4-6 Continued**

Node	Reaction	X	Y	Z
3	MAX	16	4	2175
	MIN	-305	-3	359
	MEAN	-133	0	1211

Node	Reaction	X	Y	Z
4	MAX	16	3	482
	MIN	-305	-4	-1308
	MEAN	-133	0	-341

The mean uplifting force on node 1 and 4 is 341 kips and mean compression force on node 2 and 3 is 1211 kips. For node 1 and 4, the maximum positive reaction force of 527 kips and 479 kips stands for compression force. This means that upstream node 1 and 4 experiences both tensile and compression force.

#### 4.6.2 Skid Base Reaction Force

The skid base footings are not located at the squared position as shown in Figure 4-17 and the mean reaction force would be greater than derrick footing reaction force, because both weight and projected area are increased.

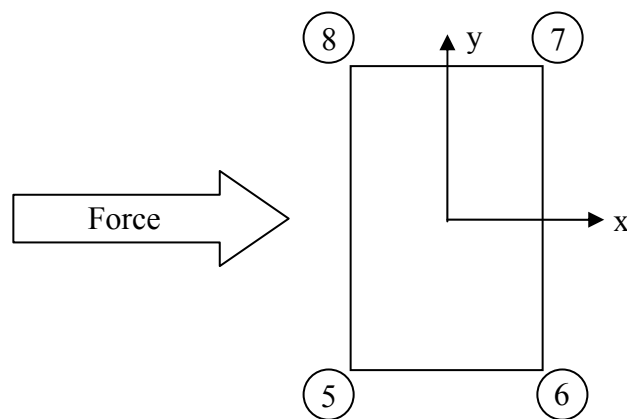


**Fig 4-17 Direction of Force and Node Location of Skid Base (0 Degrees)**

The time history of total reaction force is shown in Figures 4-18 to 4-21, and the statistics of reaction force for skid base footings are tabulated in Table 4-7.

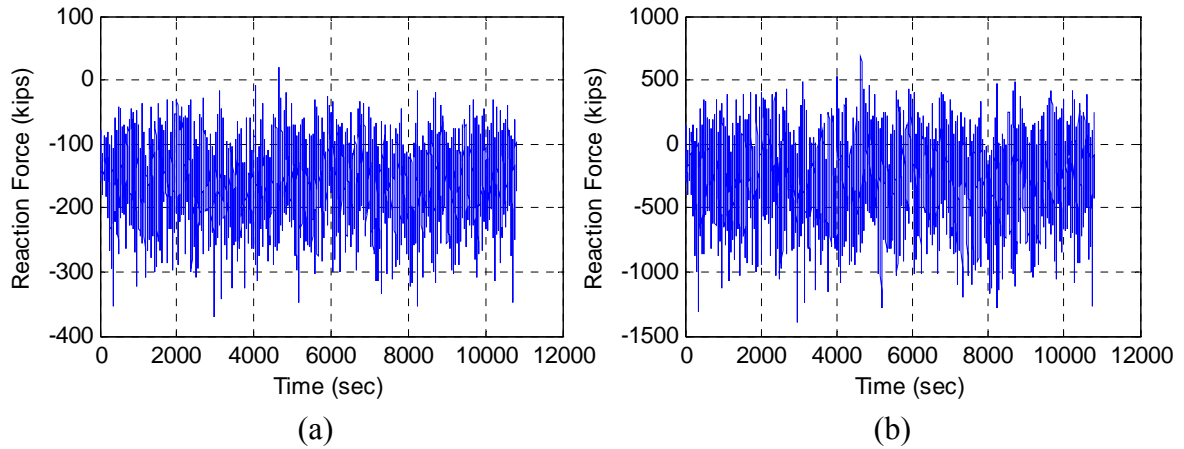


**Fig 4-18 (a) Surge Reaction (b) Heave Reaction on Footing 5 (0 Degrees)**

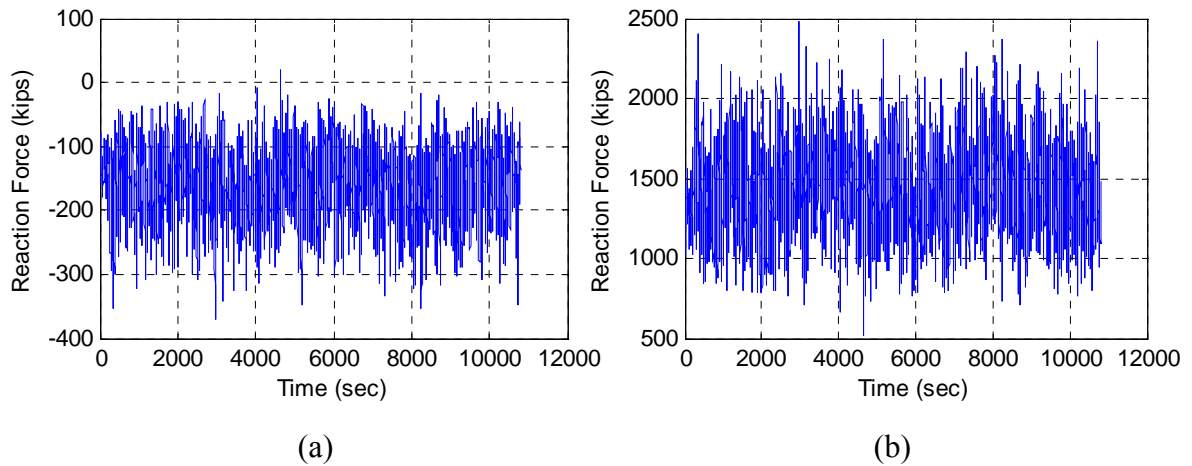


**Fig 4-19 (a) Surge Reaction (b) Heave Reaction on Footing 6 (0 Degrees)**



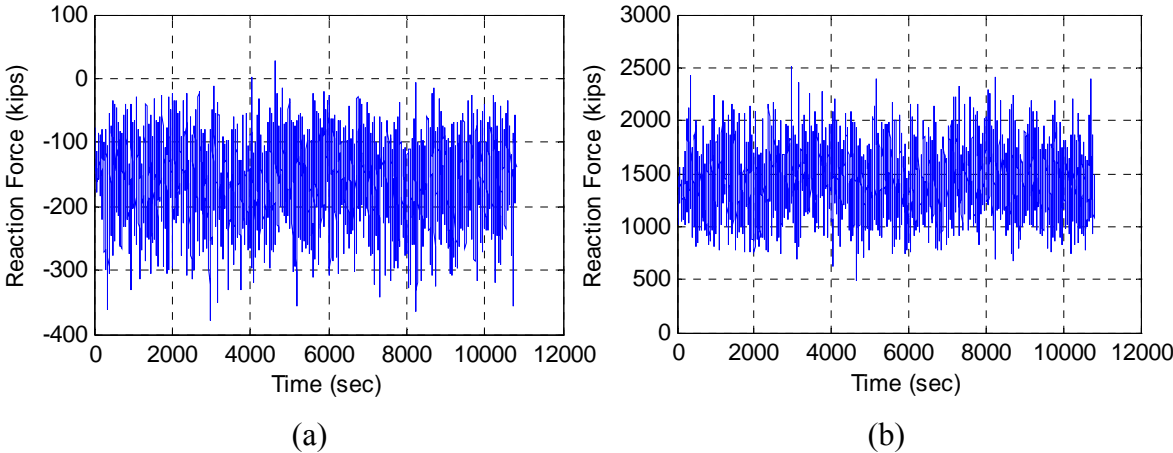


Fig 4-20 (a) Surge Reaction (b) Heave Reaction on Footing 7 (0 Degrees)

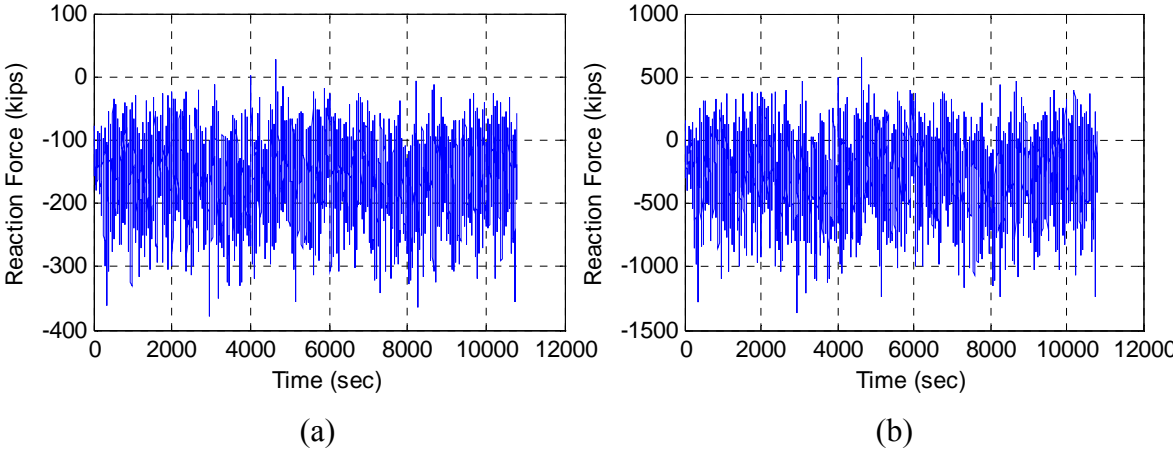


Fig 4-21 (a) Surge Reaction (b) Heave Reaction on Footing 8 (0 Degrees)

Table 4-7 Skid Base Reaction Force Statistics (0 Degrees)

Node	Reaction	X	Y	Z
5	MAX	20	2	684
	MIN	-369	-2	-1411
	MEAN	-161	0	-284

Node	Reaction	X	Y	Z
6	MAX	20	2	2472
	MIN	-369	-2	525
	MEAN	-161	0	1435

**Table 4-7 Continued**

Node	Reaction	X	Y	Z
7	MAX	28	2	2504
	MIN	-377	-2	490
	MEAN	-161	0	1435

Node	Reaction	X	Y	Z
8	MAX	28	2	650
	MIN	-377	-2	-1378
	MEAN	-161	0	-284

The absolute value of mean reaction force on upstream footings node 5 and 8 is decreased relative to the reaction force of derrick footings because a portion of increased weight of skid base plays a role in resisting overturning moment. Similarly, the footings on downstream footings node 6 and 7 experience more compression force than derrick footing at the same location.

#### 4.7 200-year and 1000-year Hurricane Conditions

A similar analysis is carried out for 200-year and 1000-year hurricane conditions. Each force component and reaction force will be presented.

##### 4.7.1 200-year Hurricane Condition

Table 4-8 shows the force components of derrick and skid base footings for 200-year hurricane condition.

**Table 4-8 Force Statistics for (a) Derrick and (b) Derrick + Skid Base  
(0 Degrees, 200-year Hurricane Condition)**

<b>Inertia</b>	Surge	Sway	Heave
MAX	568	1	69
MIN	-457	-1	-52
MEAN	0	0	1

<b>Inertia</b>	Surge	Sway	Heave
MAX	726	1	91
MIN	-585	-1	-68
MEAN	0	0	1

<b>Wind</b>	Surge	Sway	Heave
MAX	848	1	113
MIN	229	-2	0
MEAN	457	0	39

<b>Wind</b>	Surge	Sway	Heave
MAX	1001	2	133
MIN	266	-2	0
MEAN	536	0	46

<b>Gravity</b>	Surge	Sway	Heave
MAX	363	0	-1740
MIN	0	0	-1777
MEAN	148	0	-1770

<b>Gravity</b>	Surge	Sway	Heave
MAX	479	0	-2298
MIN	0	0	-2347
MEAN	196	0	-2338

<b>Total</b>	Surge	Sway	Heave
MAX	1317	1	-1603
MIN	-21	-2	-1779
MEAN	605	0	-1730

<b>Total</b>	Surge	Sway	Heave
MAX	1626	2	-2131
MIN	-59	-2	-2352
MEAN	731	0	-2291

(a)

(b)

The reaction force of each footing for 200-year hurricane condition is shown in Table 4-9.

**Table 4-9 Reaction Force Statistics (0 Degrees, 200-year Hurricane Condition)**

Node	Reaction	X	Y	Z
1	MAX	2	3	483
	MIN	-326	-4	-1521
	MEAN	-151	0	-448

Node	Reaction	X	Y	Z
2	MAX	2	4	2286
	MIN	-326	-3	454
	MEAN	-151	0	1313

Node	Reaction	X	Y	Z
3	MAX	8	4	2330
	MIN	-332	-3	405
	MEAN	-151	0	1313

Node	Reaction	X	Y	Z
4	MAX	8	3	434
	MIN	-332	-4	-1479
	MEAN	-151	0	-448

Node	Reaction	X	Y	Z
5	MAX	10	2	632
	MIN	-403	-2	-1601
	MEAN	-183	0	-403

Node	Reaction	X	Y	Z
6	MAX	10	2	2643
	MIN	-403	-2	577
	MEAN	-183	0	1549

Node	Reaction	X	Y	Z
7	MAX	19	2	2677
	MIN	-410	-2	541
	MEAN	-183	0	1548

Node	Reaction	X	Y	Z
8	MAX	19	2	597
	MIN	-410	-2	-1570
	MEAN	-183	0	-403

#### 4.7.2 1000-year Hurricane Condition

Table 4-10 shows the force components of derrick and skid base footings for 1000-year hurricane condition.

**Table 4-10 Force Statistics for (a) Derrick and (b) Derrick + Skid Base  
(0 Degrees, 1000-year Hurricane Condition)**

<b>Inertia</b>	Surge	Sway	Heave
MAX	654	1	117
MIN	-516	-1	-87
MEAN	0	0	1

<b>Inertia</b>	Surge	Sway	Heave
MAX	837	1	155
MIN	-660	-1	-115
MEAN	0	0	2

<b>Wind</b>	Surge	Sway	Heave
MAX	1236	2	229
MIN	319	-2	0
MEAN	655	0	79

<b>Wind</b>	Surge	Sway	Heave
MAX	1457	2	269
MIN	369	-3	0
MEAN	766	0	92

<b>Gravity</b>	Surge	Sway	Heave
MAX	486	0	-1709
MIN	0	0	-1777
MEAN	209	0	-1764

<b>Gravity</b>	Surge	Sway	Heave
MAX	642	0	-2257
MIN	0	0	-2347
MEAN	275	0	-2329

<b>Total</b>	Surge	Sway	Heave
MAX	1694	2	-1450
MIN	94	-2	-1784
MEAN	863	0	-1683

<b>Total</b>	Surge	Sway	Heave
MAX	2098	2	-1942
MIN	74	-3	-2359
MEAN	1041	0	-2236

(a)

(b)

The reaction force of each footing for 1000-year hurricane condition is shown in Table 4-11.

**Table 4-11 Reaction Force Statistics (0 Degrees, 1000-year Hurricane Condition)**

Node	Reaction	X	Y	Z
1	MAX	-27	4	313
	MIN	-420	-4	-2115
	MEAN	-216	0	-835

Node	Reaction	X	Y	Z
2	MAX	-27	5	2811
	MIN	-420	-4	623
	MEAN	-216	0	1678

Node	Reaction	X	Y	Z
3	MAX	-20	5	2856
	MIN	-427	-4	569
	MEAN	-216	0	1677

Node	Reaction	X	Y	Z
4	MAX	-20	4	259
	MIN	-427	-4	-2060
	MEAN	-216	0	-836

Node	Reaction	X	Y	Z
5	MAX	-23	2	447
	MIN	-520	-2	-2265
	MEAN	-260	0	-831

Node	Reaction	X	Y	Z
6	MAX	-23	3	3222
	MIN	-520	-2	760
	MEAN	-260	0	1949

Node	Reaction	X	Y	Z
7	MAX	-14	3	3255
	MIN	-529	-2	720
	MEAN	-260	0	1949

Node	Reaction	X	Y	Z
8	MAX	-14	2	408
	MIN	-529	-2	-2225
	MEAN	-260	0	-831

The mean reaction forces of each footing are compared in Figures 4-22 and 4-23.

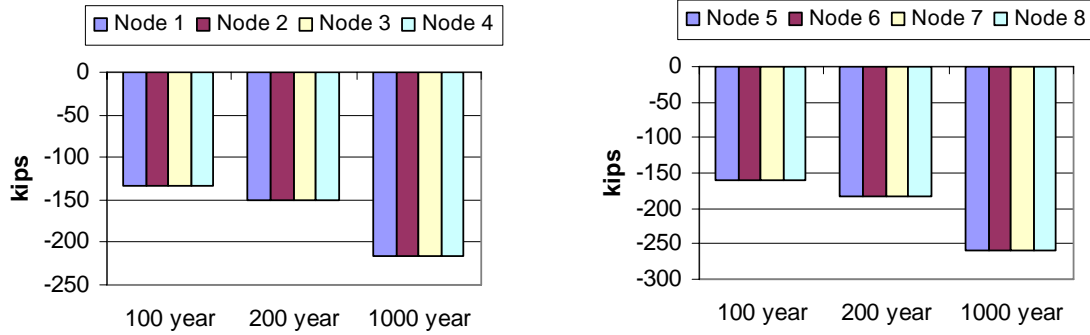


Fig 4-22 SPAR Mean Surge Reaction Force (0 Degrees)

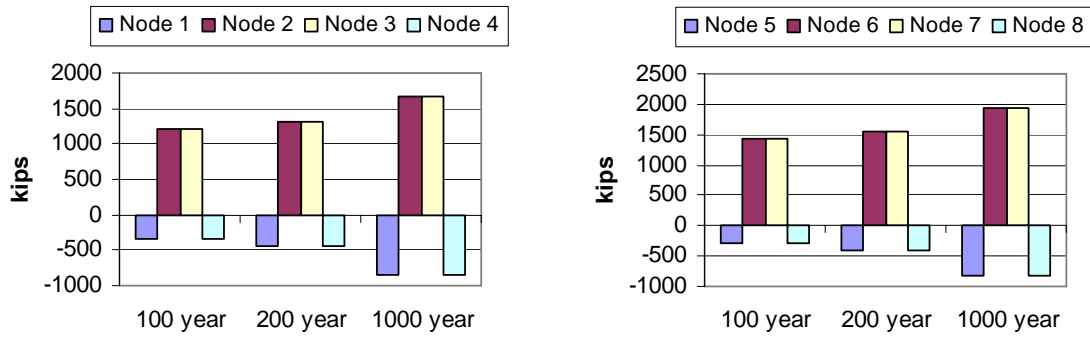
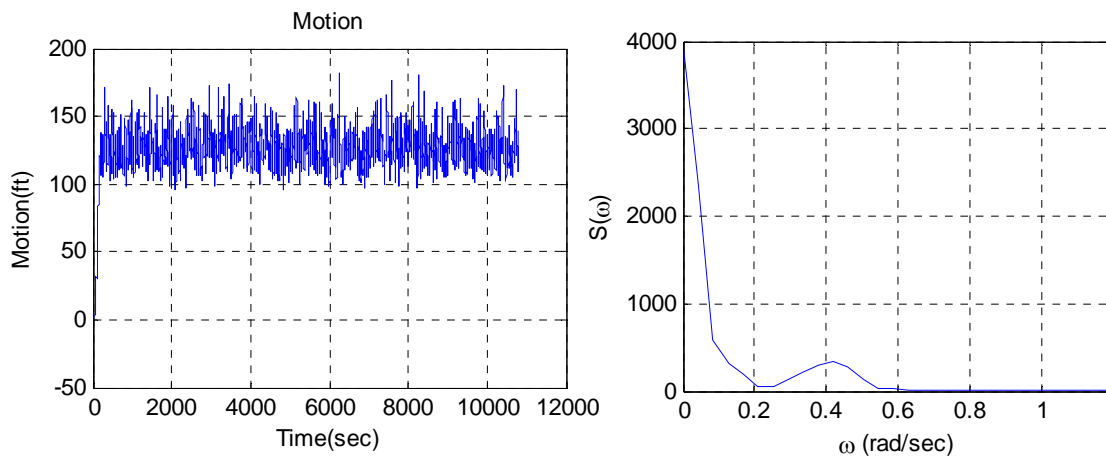


Fig 4-23 SPAR Mean Heave Reaction Force (0 Degrees)

## 5 CASE 2. SPAR (3000FT) WITH DERRICK AA – 21.25 DEGREE CASE

### 5.1 SPAR Motion Time History

If wind, wave and current are coming from 21.25 degree of X axis, then the uplift force on the skid base footing (Node 5) will be maximum because the incident angle is perpendicular to tip line between Node 6 and 8. The purpose of this case study is to investigate the uplift force of skid base footings and the result will be compared with the 45 degree case study. The different characteristics of motion between TLP and SPAR cause a different magnitude of reaction force, but basically the pattern of force distribution is quite similar. Figures 5-1 to 5-6 show the 3-hour simulation result of SPAR motion and its spectral density for 100-year hurricane condition.



**Fig 5-1 SPAR Surge Motion and Spectrum (21.25 Degrees)**



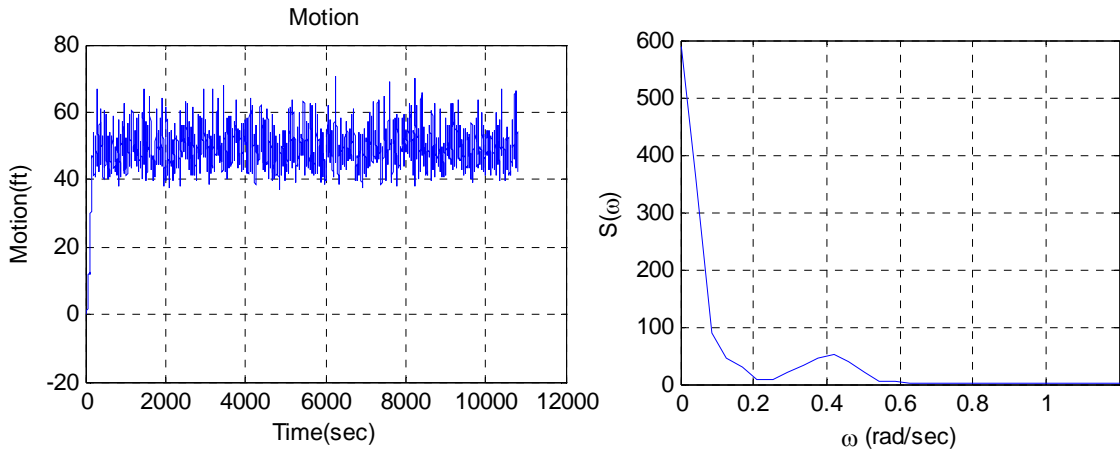


**Fig 5-2 SPAR Sway Motion and Spectrum (21.25 Degrees)**

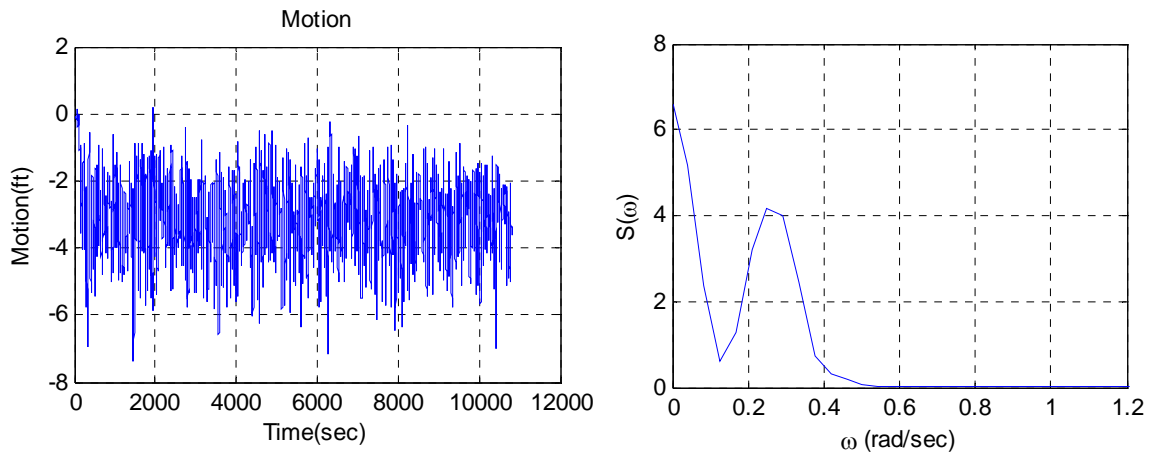


**Fig 5-3 SPAR Heave Motion and Spectrum (21.25 Degrees)**

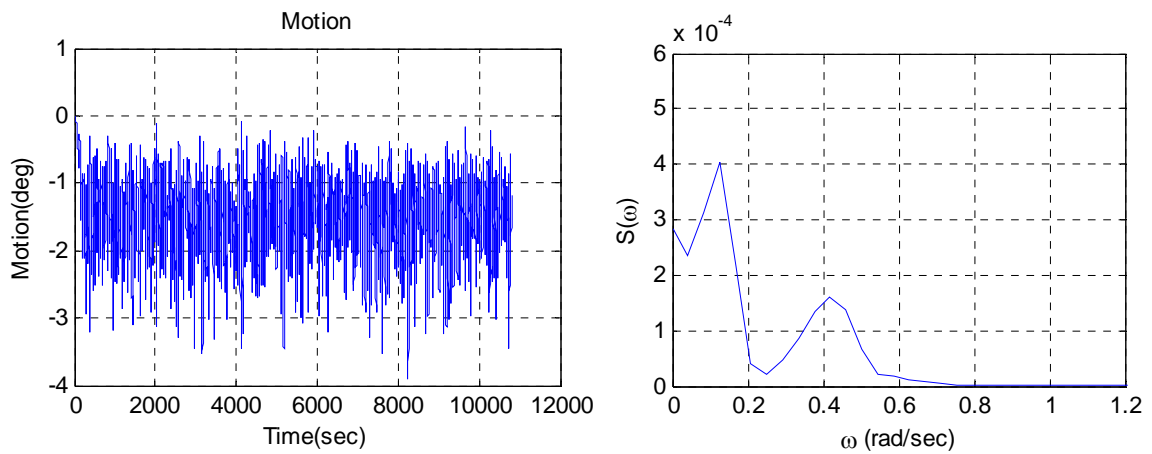


**Fig 5-4 SPAR Roll Motion and Spectrum (21.25 Degrees)**

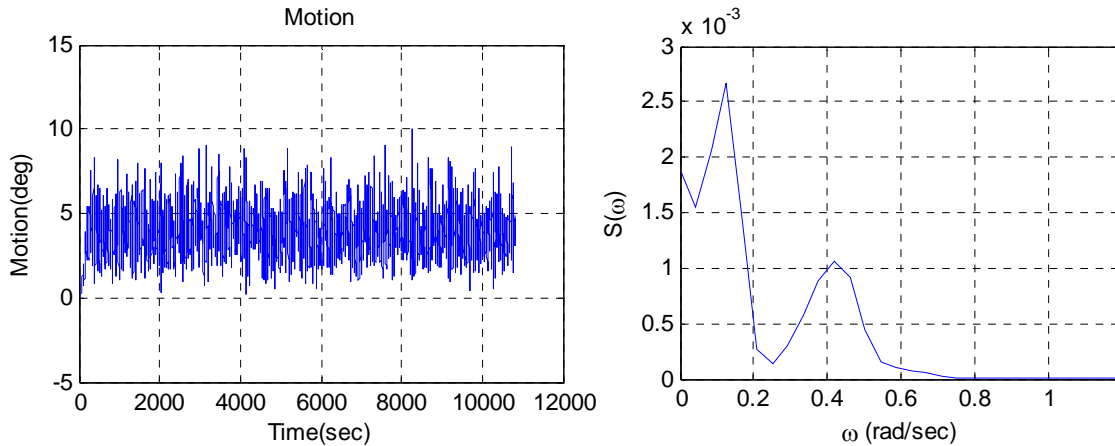


**Fig 5-5 SPAR Pitch Motion and Spectrum (21.25 Degrees)**

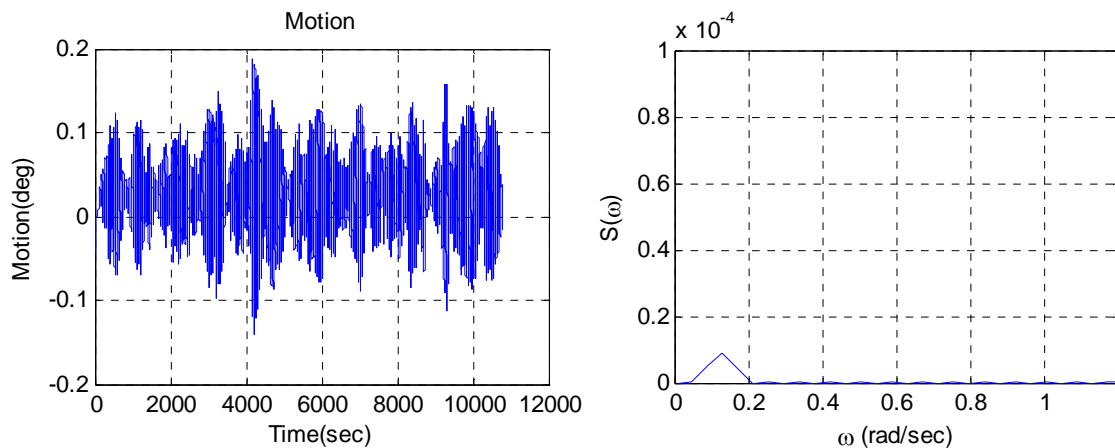


**Fig 5-6 SPAR Yaw Motion and Spectrum (21.25 Degrees)**

The motions of all 6 degrees of freedom are plotted below since incident wave angle of 21.25 degree will affect all motions. The hull is shifted more by the surge direction than sway direction due to the angle of external forces. For the same reason, pitch angle is larger than roll angle. In this case, the distinct differences of SPAR motion compared to TLP motion are roll and pitch motion. Pitch motion shows that the static heel angle is around 4 degrees and it sometimes increases up to 8 ~ 9 degrees. This big pitch and roll motion will cause large inertia and gravity force.

5.2 Inertia Force

The inertial force of derrick and skid base are calculated based on the hull motion, and are summarized in Figures 5-7 to 5-9 and Table 5-1.

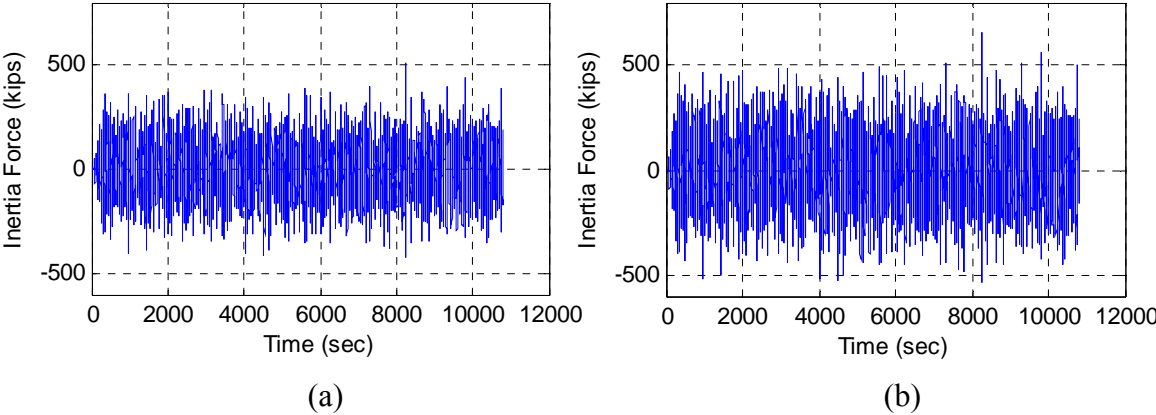


Fig 5-7 Surge Inertia Force of (a) Derrick and (b) Derrick + Skid Base (21.25 Degrees)

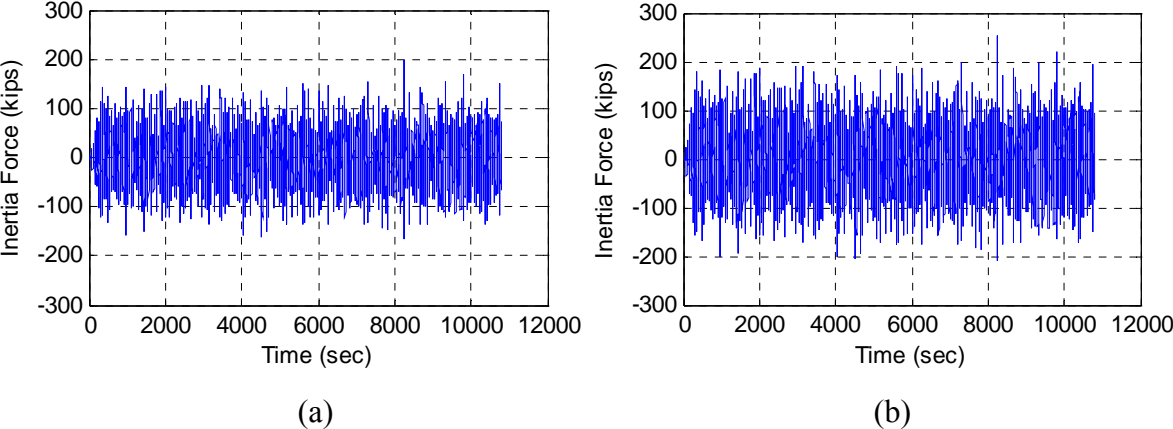
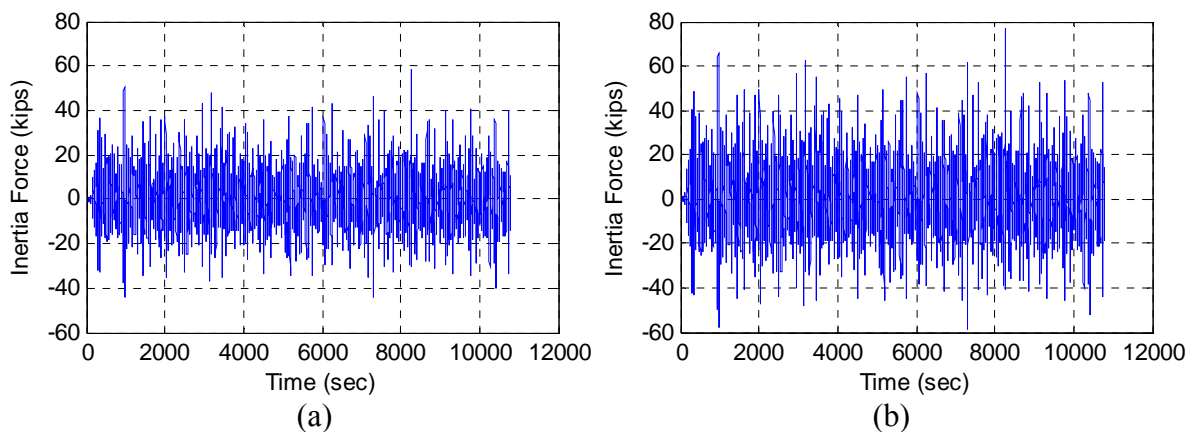


Fig 5-8 Sway Inertia Force of (a) Derrick and (b) Derrick + Skid Base (21.25 Degrees)



**Fig 5-9 Heave Inertia Force of (a) Derrick and (b) Derrick + Skid Base (21.25 Degrees)**

**Table 5-1 Inertia Force Statistics for (a) Derrick and (b) Derrick + Skid Base (21.25 Degrees)**

<b>Inertia</b>	Surge	Sway	Heave
MAX	508	196	59
MIN	-421	-163	-45
MEAN	0	0	1

(a)

<b>Inertia</b>	Surge	Sway	Heave
MAX	650	251	77
MIN	-539	-209	-59
MEAN	0	0	1

(b)

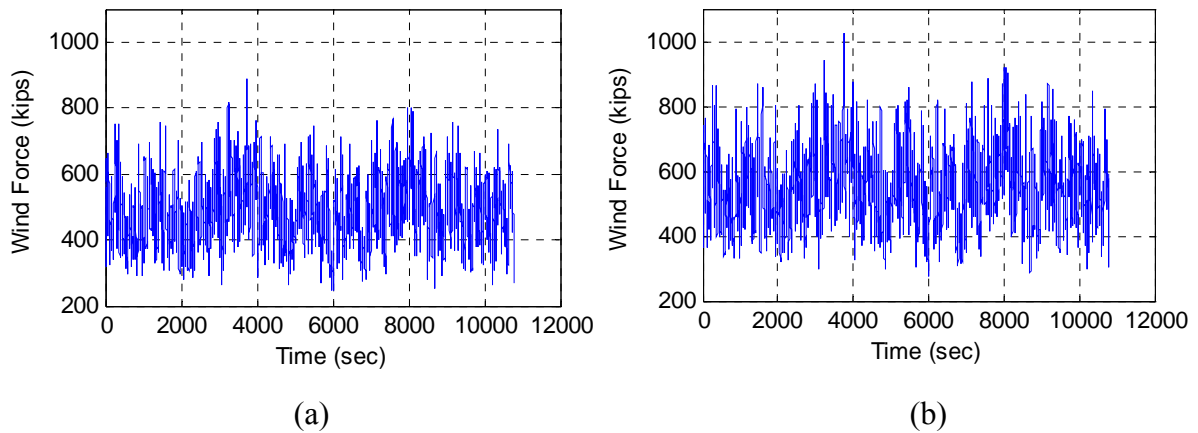
### 5.3 Wind Force

As we already discussed, the projected area of skid base is maximum compared to all other cases. Mean wind force on SPAR derrick is 517 kips, while mean TLP derrick wind force is 546 kip; this difference comes from the different vertical location of derrick and skid base. The mean wind force on derrick and skid base is tabulated in Table 5-2.

**Table 5-2 Wind Force of Derrick and Skid Base (21.25 Degrees)**

<b>100 YEAR</b>	z elev above MWL to Mid-Point	U(z) 1-hr ave	C <sub>shape</sub>	Unit Pressure	Perm Factor	Projected Area	Pressure	Moment
Upper derrick	343	218	1.25	70	0.6	3631	153	31046
Lower derrick	258	211	1.25	66	0.6	3851	152	17847
Drill floor	208	205	1.50	75	1.0	971	73	4896
Substructure	175	201	1.50	72	0.6	3236	139	4862
<b>Derrick</b>							<b>517</b>	<b>58651</b>
Skid base	145	196	1.50	68	1.0	1077	73	367
<b>Derrick + Skid Base</b>							<b>590</b>	<b>59018</b>

The time history of wind force and its statistics are shown in Figures 5-10 to 5-12 and Table 5-3.

**Fig 5-10 Surge Wind Force for (a) Derrick and (b) Derrick + Skid Base (21.25 Degrees)**

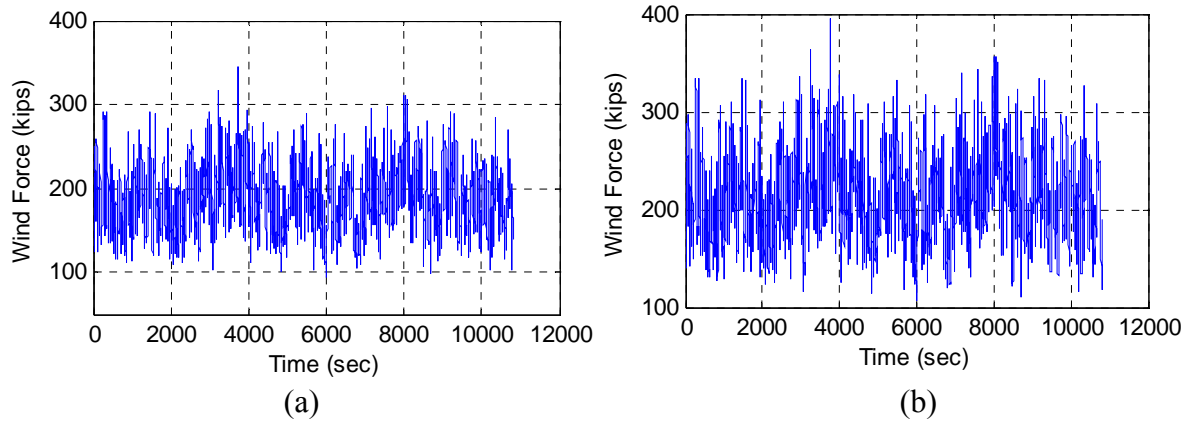


**Fig 5-11 Sway Wind Force for (a) Derrick and (b) Derrick + Skid Base (21.25 Degrees)**

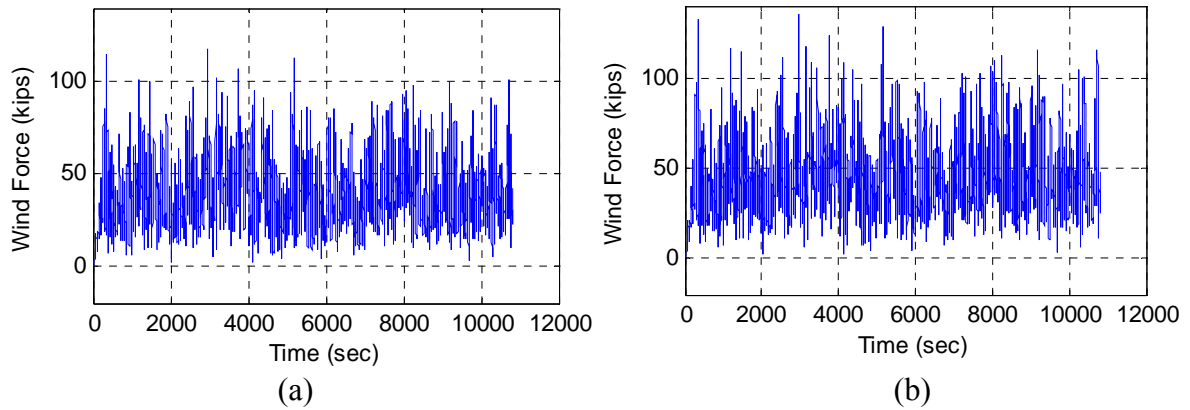


**Fig 5-12 Heave Wind Force for (a) Derrick and (b) Derrick + Skid Base (21.25 Degrees)**

**Table 5-3 Wind Force Statistics for (a) Derrick and (b) Derrick + Skid Base (21.25 Degrees)**

Wind	Surge	Sway	Heave
MAX	890	345	118
MIN	245	95	0
MEAN	483	187	39

(a)

Wind	Surge	Sway	Heave
MAX	1022	396	135
MIN	277	107	0
MEAN	552	214	44

(b)

## 5.4 Gravity Force

Now that SPAR hull rotates with a bigger tilted angle, the footings will experience a larger horizontal component of gravity force. The maximum surge gravity force is 310 kips for derrick and 409 kips for skid base. These forces are even greater than the inertia force of TLP at the same condition. Figures 5-13 to 5-15 and Table 5-4 show 3-hour time history of gravity forces.

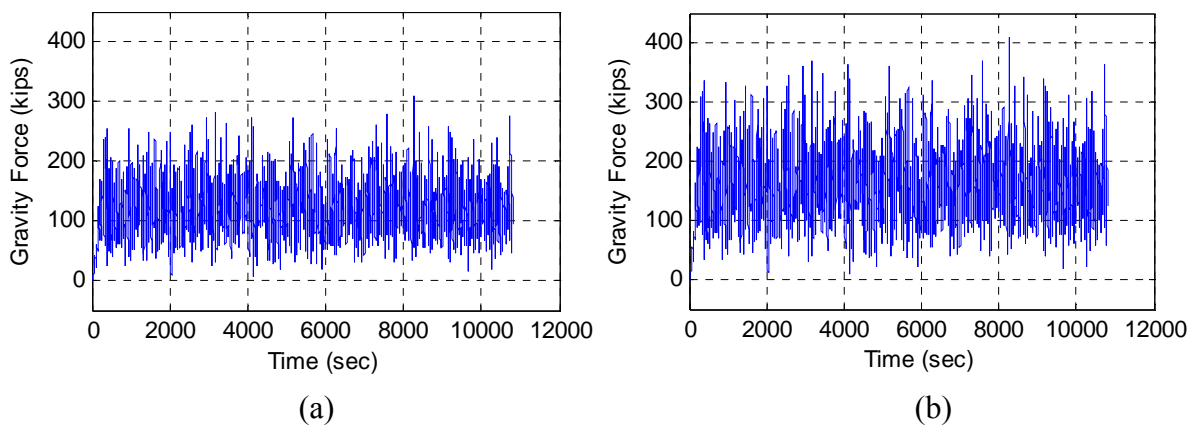


**Fig 5-13 Surge Gravity Force for (a) Derrick and (b) Derrick + Skid Base (21.25 Degrees)**

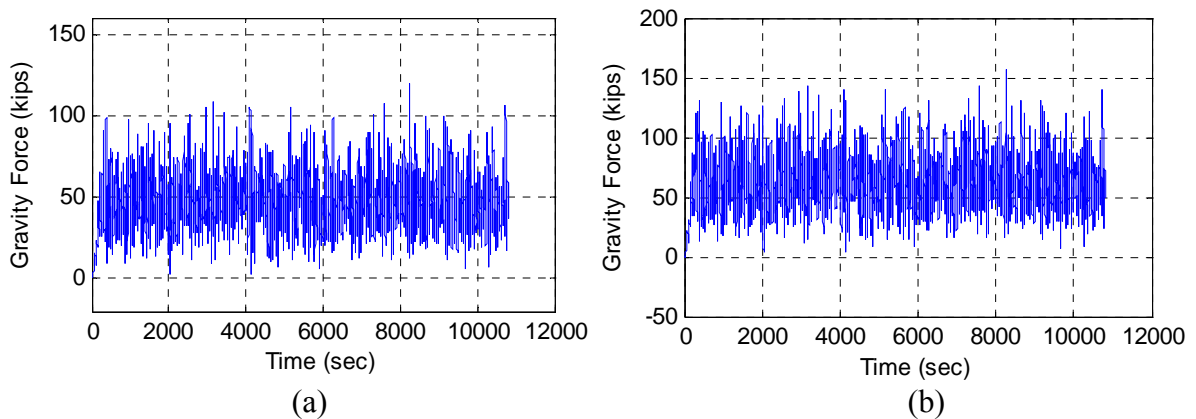


**Fig 5-14 Sway Gravity Force for (a) Derrick and (b) Derrick + Skid Base (21.25 Degrees)**

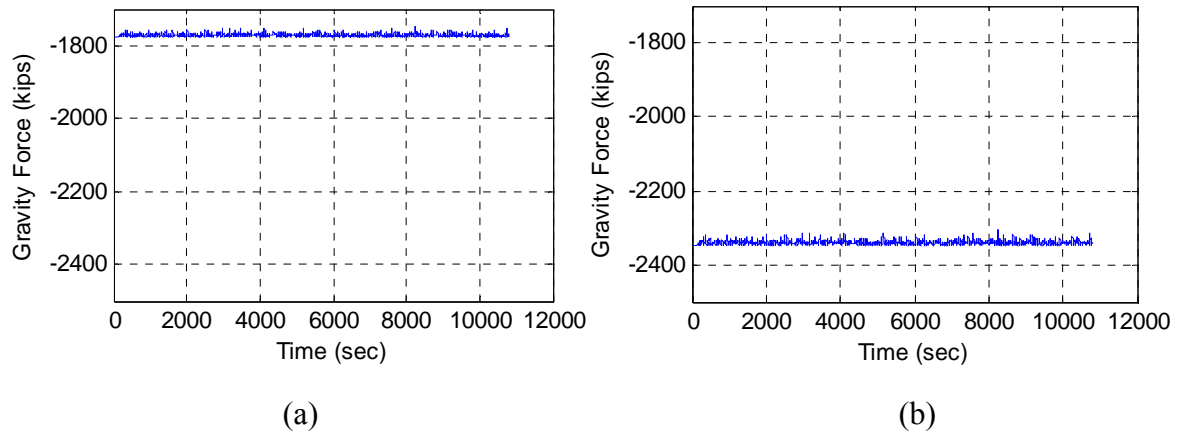


**Fig 5-15 Heave Gravity Force for (a) Derrick and (b) Derrick + Skid Base (21.25 Degrees)**

**Table 5-4 Gravity Force Statistics for (a) Derrick and (b) Derrick + Skid Base (21.25 Degrees)**

Gravity	Surge	Sway	Heave
MAX	310	119	-1746
MIN	0	0	-1777
MEAN	122	47	-1772

(a)

Gravity	Surge	Sway	Heave
MAX	409	157	-2306
MIN	0	0	-2347
MEAN	161	62	-2340

(b)

### 5.5 Total Force

Total force on the derrick and skid base can be expressed by a summation of inertia force, wind force and gravity force. Time history of total force and statistics of force are shown below. All three components of force are presented in this case to show how different the force distribution on derrick and skid base is compared with other cases. Apparently, wider projected area plays an important role in increased total force on derrick and skid base. The time history of total force and statistics of force are shown in Figures 5-16 to 5-18 and Table 5-5.



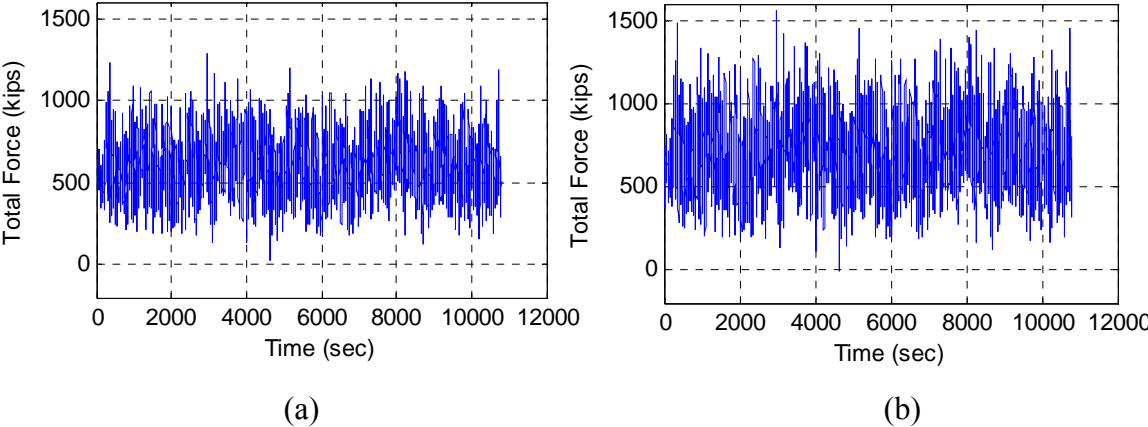


**Fig 5-16 Surge Total Force for (a) Derrick and (b) Derrick + Skid Base (21.25 Degrees)**

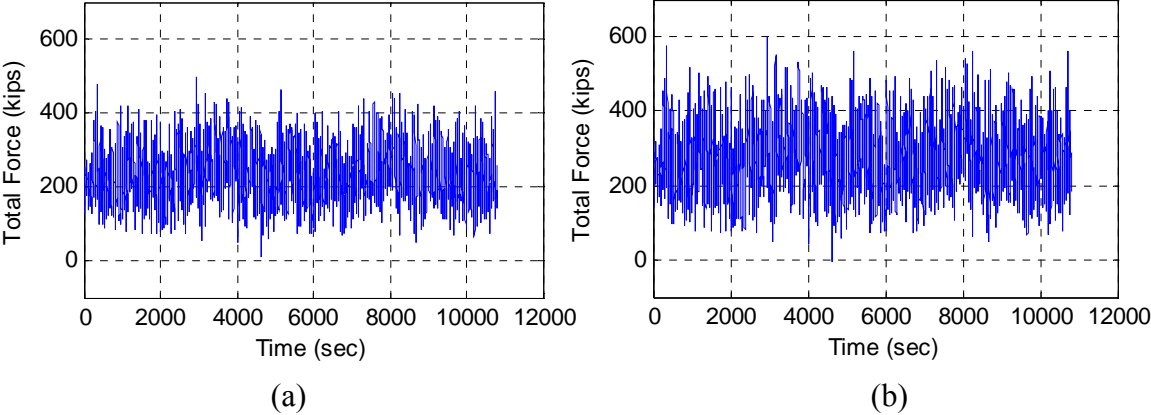


**Fig 5-17 Sway Total Force for (a) Derrick and (b) Derrick + Skid Base (21.25 Degrees)**

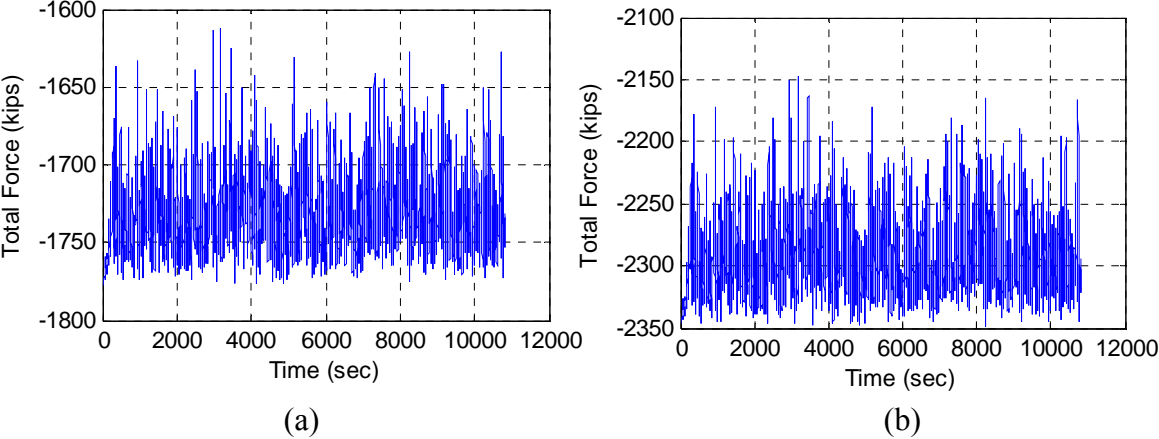


**Fig 5-18 Heave Total Force for (a) Derrick and (b) Derrick + Skid Base (21.25 Degrees)**

**Table 5-5 Total Force Statistics for (a) Derrick and (b) Derrick + Skid Base (21.25 Degrees)**

<b>Total</b>	Surge	Sway	Heave
MAX	1282	494	-1612
MIN	27	10	-1777
MEAN	605	234	-1732

(a)

<b>Total</b>	Surge	Sway	Heave
MAX	1554	599	-2147
MIN	-10	-4	-2349
MEAN	713	276	-2295

(b)

## 5.6 Reaction Force

The reaction force of derrick and skid base will be presented separately, and three directions of reaction force, surge, sway and heave directions are plotted. In this case, sway component of reaction force is less than surge reaction force, but the design engineer should account for both reaction forces in order to decide proper strength of connections since the connection characteristics and design criteria of footing could be different from the longitudinal and lateral directions. The reaction force of SPAR case is presented below.

### 5.6.1 Derrick Reaction Force

The time history of derrick reaction force is shown in Figures 5-19 to 5-22, and the statistics of reaction force for derrick footings are tabulated in Table 5-6.

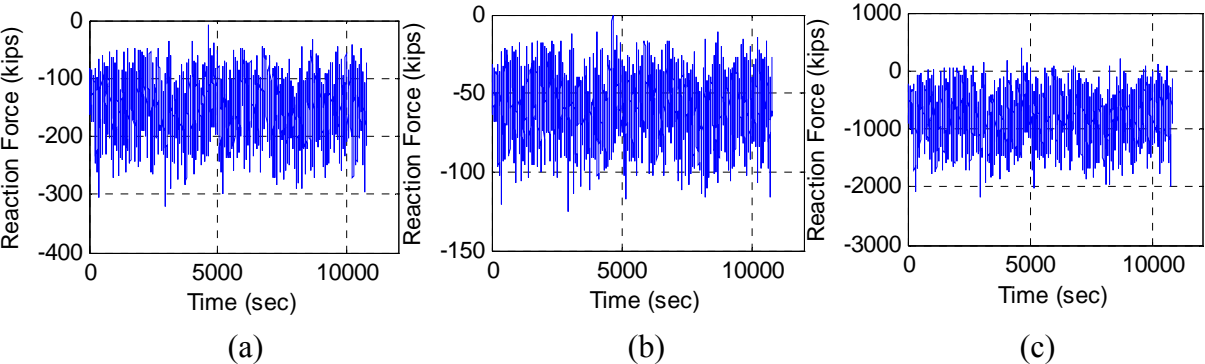


**Fig 5-19 (a) Surge Reaction (b) Sway Reaction (c) Heave Reaction on Footing 1 (21.25 Degrees)**

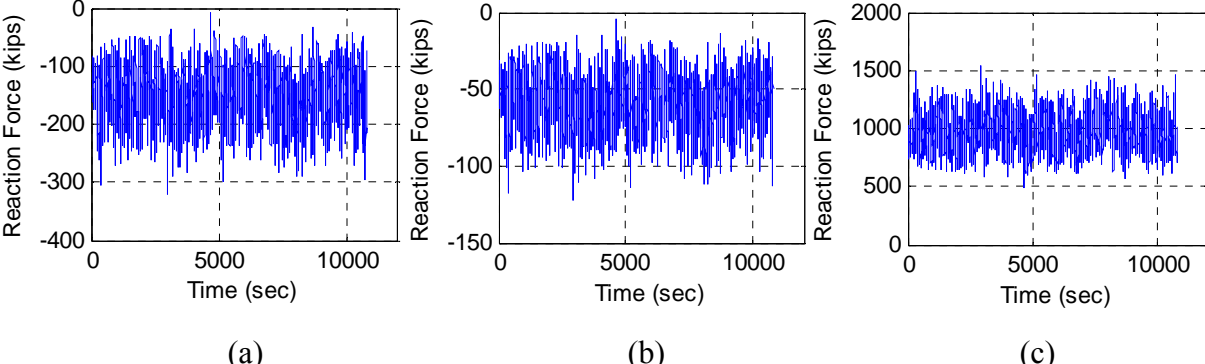


**Fig 5-20 (a) Surge Reaction (b) Sway Reaction (c) Heave Reaction on Footing 2 (21.25 Degrees)**

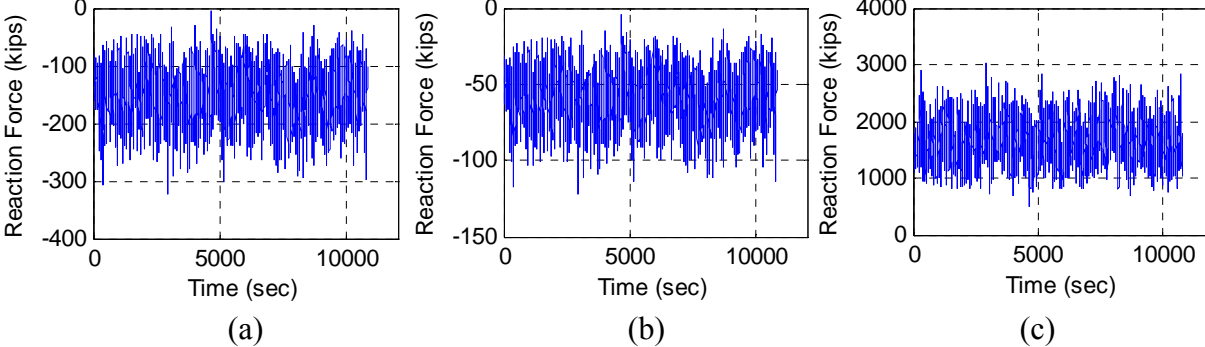


**Fig 5-21 (a) Surge Reaction (b) Sway Reaction (c) Heave Reaction on Footing 3 (21.25 Degrees)**

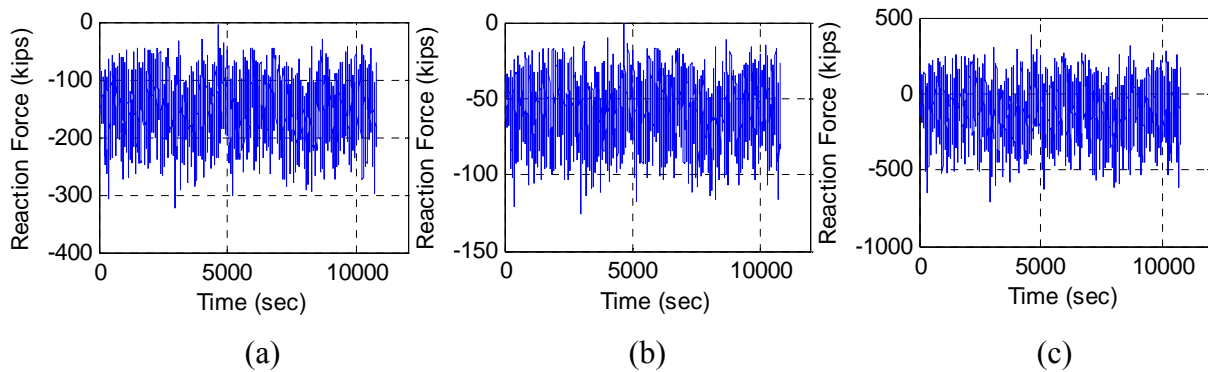


**Fig 5-22 (a) Surge Reaction (b) Sway Reaction (c) Heave Reaction on Footing 4 (21.25 Degrees)**

**Table 5-6 Derrick Reaction Force Statistics (21.25 Degrees)**

Node	Reaction	X	Y	Z
1	MAX	-9	-1	396
	MIN	-319	-125	-2195
	MEAN	-151	-59	-793

Node	Reaction	X	Y	Z
2	MAX	-9	-4	1535
	MIN	-319	-122	492
	MEAN	-151	-59	974

Node	Reaction	X	Y	Z
3	MAX	-5	-4	3010
	MIN	-322	-122	491
	MEAN	-151	-59	1659

Node	Reaction	X	Y	Z
4	MAX	-5	-1	395
	MIN	-322	-125	-720
	MEAN	-151	-59	-108

Two derrick footings located at upstream direction (Node 1 and 4) experience both uplift force and compression force throughout the simulation time. The other footings are under a compression force. The reaction force of skid base footing shows a similar pattern and it is plotted from Figures 5-23 to 5-26 and Table 5-7.

5.6.2 Skid Base Reaction Force

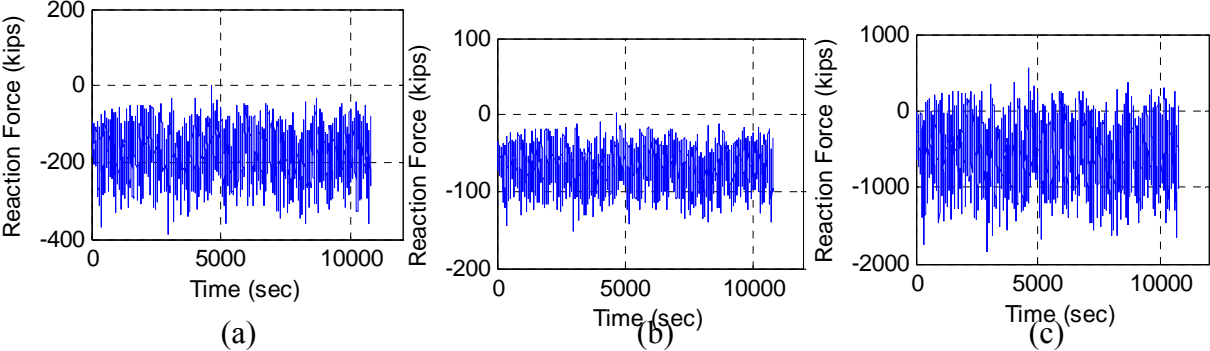


Fig 5-23 (a) Surge Reaction (b) Sway Reaction (c) Heave Reaction on Footing 5 (21.25 Degrees)

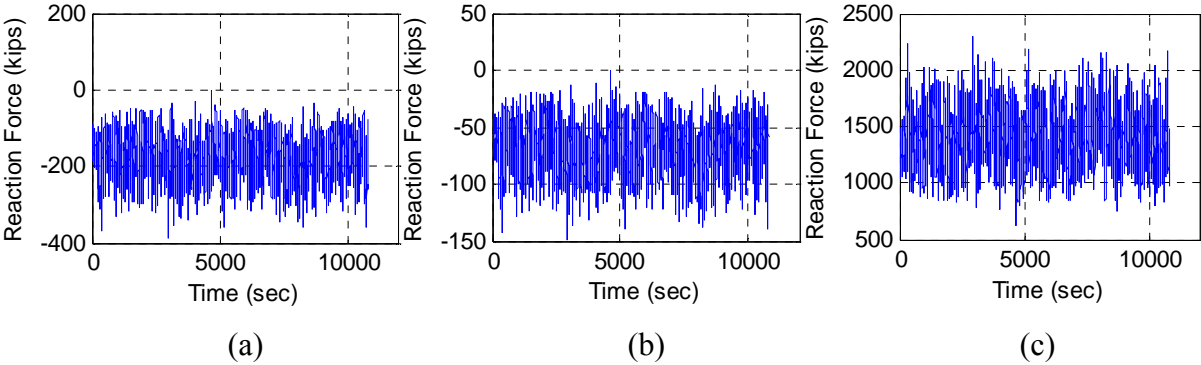


Fig 5-24 (a) Surge Reaction (b) Sway Reaction (c) Heave Reaction on Footing 6 (21.25 Degrees)

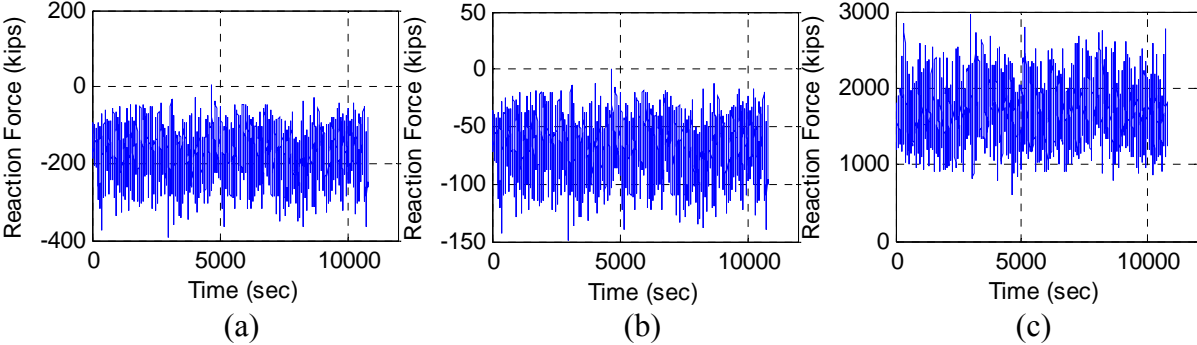
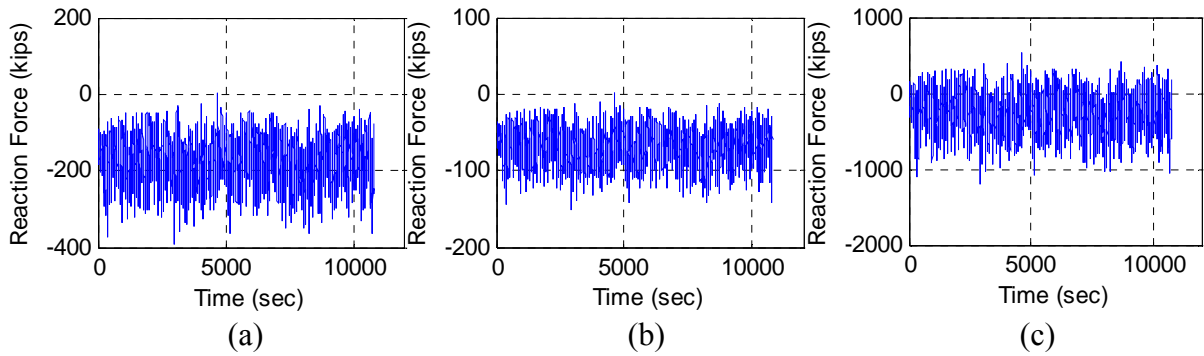


Fig 5-25 (a) Surge Reaction (b) Sway Reaction (c) Heave Reaction on Footing 7 (21.25 Degrees)



**Fig 5-26 (a) Surge Reaction (b) Sway Reaction (c) Heave Reaction on Footing 8 (21.25 Degrees)**

**Table 5-7 Skid Base Reaction Force Statistics (21.25 Degrees)**

Node	Reaction	X	Y	Z
5	MAX	0	2	562
	MIN	-386	-151	-1860
	MEAN	-178	-69	-547

Node	Reaction	X	Y	Z
6	MAX	0	0	2295
	MIN	-386	-149	628
	MEAN	-178	-69	1401

Node	Reaction	X	Y	Z
7	MAX	5	0	2944
	MIN	-391	-149	610
	MEAN	-178	-69	1694

Node	Reaction	X	Y	Z
8	MAX	5	2	545
	MIN	-391	-151	-1211
	MEAN	-178	-69	-253

**5.7 200-year and 1000-year Hurricane Conditions**

The same analysis is carried out for 200-year and 1000-year hurricane conditions.

## 5.7.1 200-year Hurricane Condition

Table 5-8 shows the force components of derrick and skid base footings for 200-year hurricane condition.

**Table 5-8 Force Statistics for (a) Derrick and (b) Derrick + Skid Base  
(21.25 Degrees, 200-year Hurricane Condition)**

<b>Inertia</b>	Surge	Sway	Heave
MAX	530	204	69
MIN	-426	-165	-52
MEAN	0	0	1

<b>Inertia</b>	Surge	Sway	Heave
MAX	677	261	91
MIN	-545	-211	-68
MEAN	0	0	1

<b>Wind</b>	Surge	Sway	Heave
MAX	1025	396	147
MIN	277	107	0
MEAN	553	214	50

<b>Wind</b>	Surge	Sway	Heave
MAX	1177	455	168
MIN	313	121	0
MEAN	630	244	57

<b>Gravity</b>	Surge	Sway	Heave
MAX	339	130	-1740
MIN	0	0	-1777
MEAN	138	54	-1770

<b>Gravity</b>	Surge	Sway	Heave
MAX	447	172	-2298
MIN	0	0	-2347
MEAN	183	71	-2338

**Table 5-8 Continued**

<b>Total</b>	Surge	Sway	Heave
MAX	1414	544	-1574
MIN	68	26	-1777
MEAN	691	267	-1719

(a)

<b>Total</b>	Surge	Sway	Heave
MAX	1709	657	-2102
MIN	36	14	-2348
MEAN	813	315	-2279

(b)

The corresponding reaction force of each position is shown in Table 5-9.

**Table 5-9 Reaction Force Statistics (21.25 Degrees, 200-year Hurricane Condition)**

Node	Reaction	X	Y	Z
1	MAX	-19	-5	314
	MIN	-352	-138	-2471
	MEAN	-173	-67	-969

Node	Reaction	X	Y	Z
2	MAX	-19	-8	1645
	MIN	-352	-134	528
	MEAN	-173	-67	1048

Node	Reaction	X	Y	Z
3	MAX	-15	-8	3266
	MIN	-355	-134	572
	MEAN	-173	-67	1829

Node	Reaction	X	Y	Z
4	MAX	-15	-5	357
	MIN	-355	-138	-852
	MEAN	-173	-67	-189

Node	Reaction	X	Y	Z
5	MAX	-11	-2	489
	MIN	-425	-165	-2116
	MEAN	-203	-79	-708

Node	Reaction	X	Y	Z
6	MAX	-11	-4	2464
	MIN	-425	-164	681
	MEAN	-203	-79	1514



Table 5-9 Continued

Node	Reaction	X	Y	Z
7	MAX	-6	-4	3176
	MIN	-430	-164	682
	MEAN	-203	-79	1848

Node	Reaction	X	Y	Z
8	MAX	-6	-2	490
	MIN	-430	-165	-1406
	MEAN	-203	-79	-374

## 5.7.2 1000-year Hurricane Condition

Table 5-10 shows the force components of derrick and skid base footings for 1000-year hurricane condition.

**Table 5-10 Force Statistics for (a) Derrick and (b) Derrick + Skid Base  
(21.25 Degrees, 1000-year Hurricane Condition)**

<b>Inertia</b>	Surge	Sway	Heave
MAX	611	234	117
MIN	-482	-185	-86
MEAN	0	0	1

<b>Inertia</b>	Surge	Sway	Heave
MAX	782	299	155
MIN	-617	-237	-114
MEAN	0	0	2

<b>Wind</b>	Surge	Sway	Heave
MAX	1495	574	296
MIN	386	149	0
MEAN	792	305	102

<b>Wind</b>	Surge	Sway	Heave
MAX	1717	660	339
MIN	436	168	0
MEAN	903	348	116

<b>Gravity</b>	Surge	Sway	Heave
MAX	454	172	-1709
MIN	0	0	-1777
MEAN	194	75	-1764

<b>Gravity</b>	Surge	Sway	Heave
MAX	599	227	-2258
MIN	0	0	-2347
MEAN	257	99	-2329

Table 5-10 Continued

Total	Surge	Sway	Heave
MAX	1846	707	-1398
MIN	210	81	-1780
MEAN	986	380	-1660

(a)

Total	Surge	Sway	Heave
MAX	2216	849	-1887
MIN	196	76	-2355
MEAN	1160	447	-2211

(b)

The reaction force of each footing for 1000-year hurricane condition is shown in Table 5-11.

Table 5-11 Reaction Force Statistics (21.25 Degrees, 1000-year Hurricane Condition)

Node	Reaction	X	Y	Z
1	MAX	-55	-18	21
	MIN	-460	-178	-3384
	MEAN	-247	-95	-1581

Node	Reaction	X	Y	Z
2	MAX	-55	-22	2011
	MIN	-460	-175	655
	MEAN	-247	-95	1300

Node	Reaction	X	Y	Z
3	MAX	-51	-22	4116
	MIN	-463	-175	857
	MEAN	-247	-95	2411

Node	Reaction	X	Y	Z
4	MAX	-51	-18	223
	MIN	-463	-178	-1280
	MEAN	-247	-95	-470

Node	Reaction	X	Y	Z
5	MAX	-52	-18	225
	MIN	-552	-213	-2963
	MEAN	-290	-112	-1271

Node	Reaction	X	Y	Z
6	MAX	-52	-20	3029
	MIN	-552	-211	871
	MEAN	-290	-112	1901

**Table 5-11 Continued**

Node	Reaction	X	Y	Z
7	MAX	-46	-20	3949
	MIN	-556	-211	938
	MEAN	-290	-112	2377

Node	Reaction	X	Y	Z
8	MAX	-46	-18	292
	MIN	-556	-213	-2043
	MEAN	-290	-112	-796

Mean reactions for node 1 and node 4 are both negative which means those are experiencing uplift force even in 100-year hurricane conditions as shown in Figures 5-27 to 5-29.

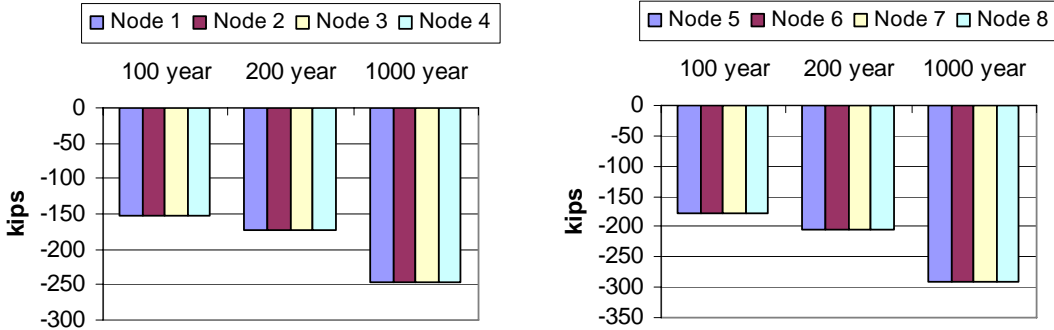


**Fig 5-27 SPAR Mean Surge Reaction Force (21.25 Degrees)**

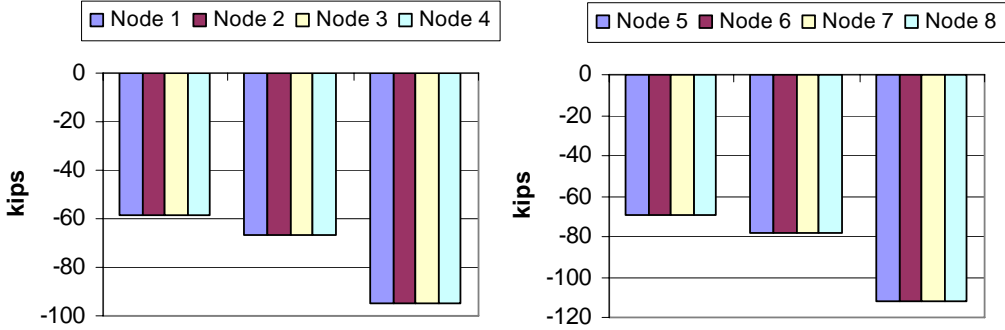


**Fig 5-28 SPAR Mean Sway Reaction Force (21.25 Degrees)**

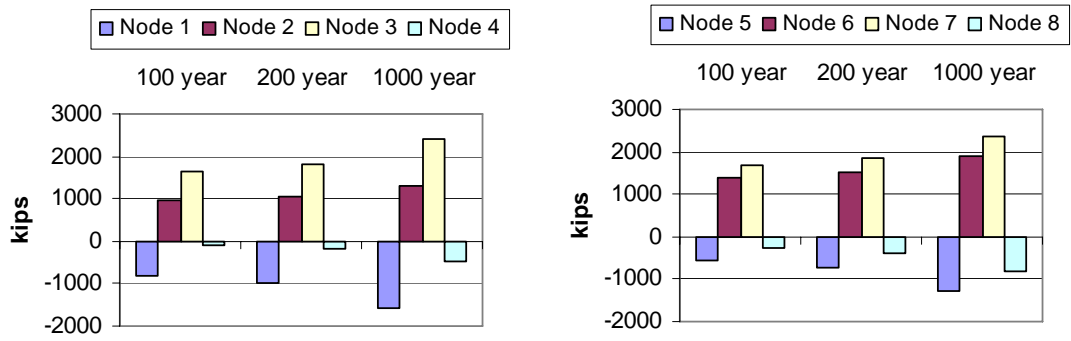


**Fig 5-29 SPAR Mean Heave Reaction Force (21.25 Degrees)**

## 6 CASE 3. SPAR (3000FT) WITH DERRICK AA – 45 DEGREE CASE

### 6.1 SPAR Motion Time History

In this case, we are going to look into 45 degree incident wave case. Of course, this case is a collinear case which means the direction of incident wind and current are coming from the same direction of wave. Wind force on derrick and skid base would be bigger than 0 degree and 21.25 degree cases due to increased projected area of derrick. For this reason, the uplift or compression force of derrick footing will be more severe. However, the reaction force of skid base footing should be investigated and compared to 21.25 degree case because the projected area of skid base in this case is less than 21.25 degree case. Total projected area of those two cases also does not make a big difference. The motion of sway and roll will be same with surge and pitch respectively due to symmetry, so only surge, heave and pitch motion will be presented.

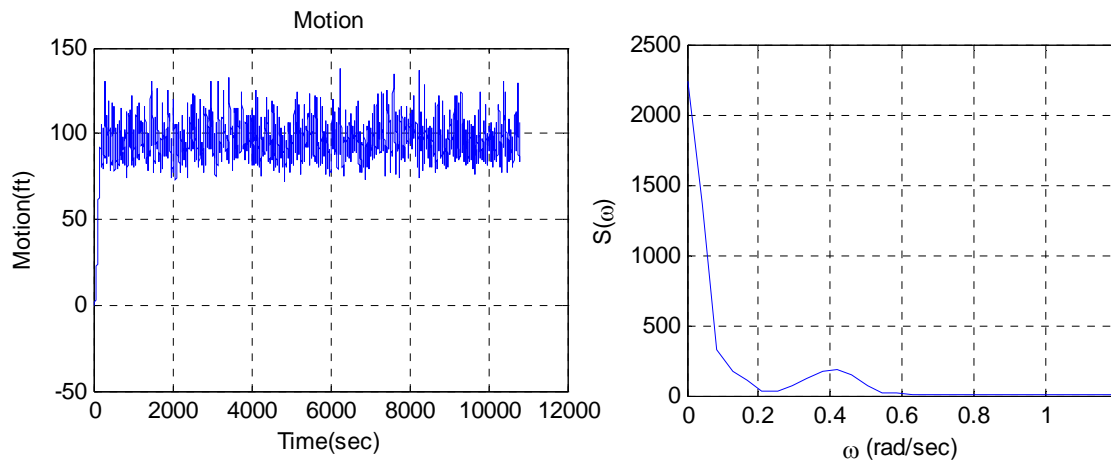


**Fig 6-1 SPAR Surge Motion and Spectrum (45 Degrees)**

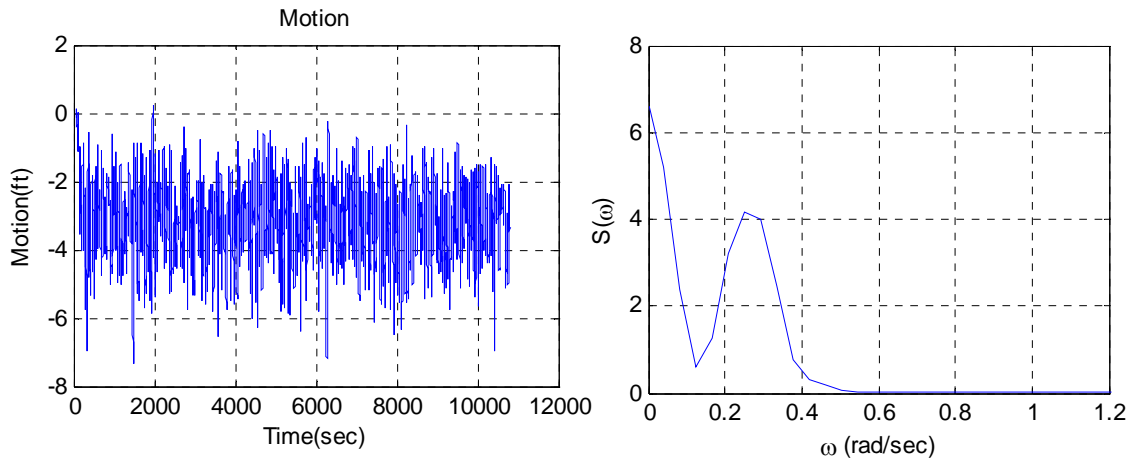


**Fig 6-2 SPAR Heave Motion and Spectrum (45 Degrees)**

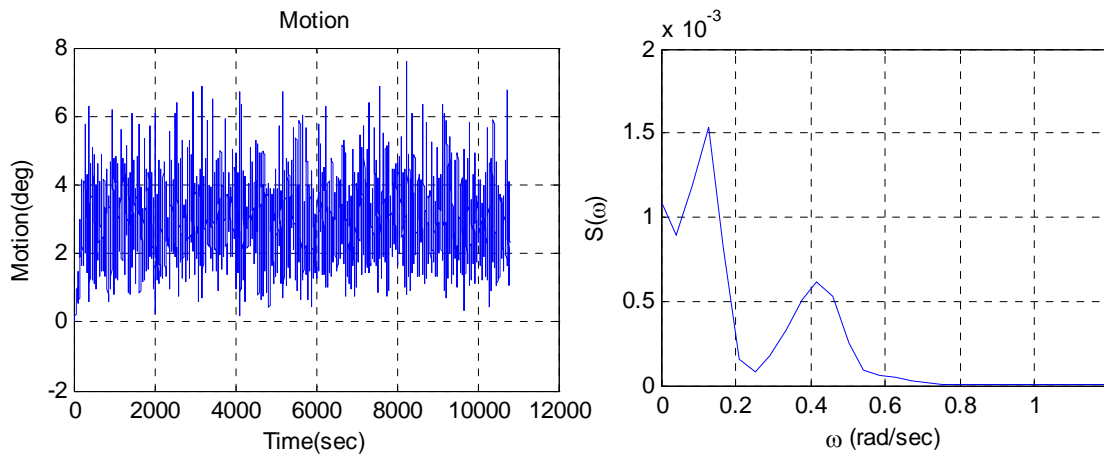


**Fig 6-3 SPAR Pitch Motion and Spectrum (45 Degrees)**

Figures 6-1 to 6-3 show the 3-hour simulation result of SPAR motion and its spectral density for 100-year hurricane condition.

## 6.2 Inertia Force

For the same reason, the inertia force of 3-hour time history is plotted for only surge and heave cases. SPAR is more likely to roll and pitch so the resultant inertia force is bigger than inertia force of TLP.

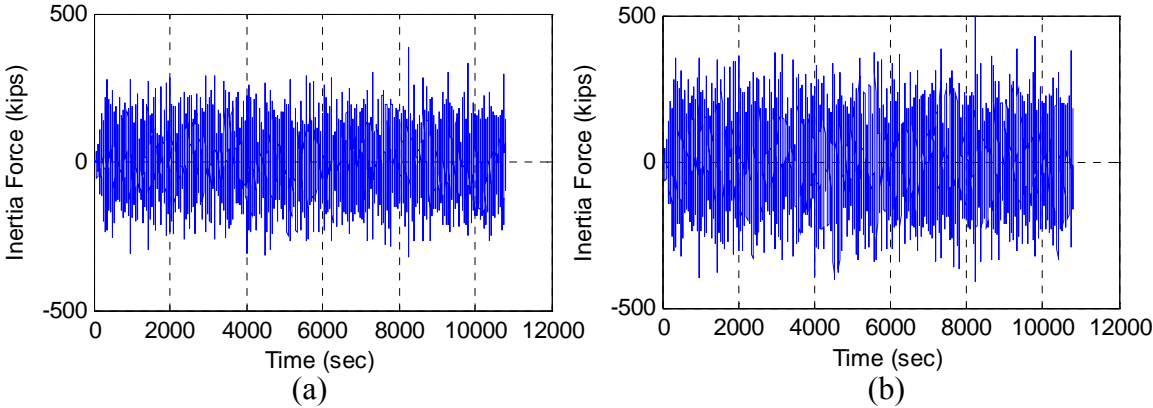


**Fig 6-4 Surge Inertia Force of (a) Derrick and (b) Derrick + Skid Base (45 Degrees)**

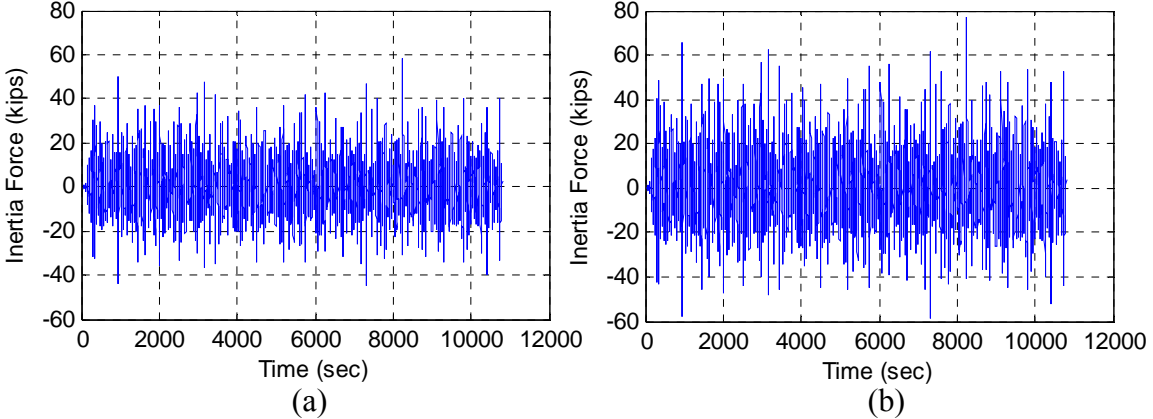


**Fig 6-5 Heave Inertia Force of (a) Derrick and (b) Derrick + Skid Base (45 Degrees)**

The inertial force of derrick and skid base are calculated based on the hull motion, and are summarized in Figures 6-4 to 6-5 and Table 6-1.

**Table 6-1 Inertia Force Statistics for (a) Derrick and (b) Derrick + Skid Base (45 Degrees)**

<b>Inertia</b>	Surge	Sway	Heave
MAX	386	384	59
MIN	-320	-319	-45
MEAN	0	0	1

(a)

<b>Inertia</b>	Surge	Sway	Heave
MAX	494	491	77
MIN	-409	-408	-59
MEAN	0	0	1

(b)

### 6.3 Wind Force

The wind force on derrick and skid base of SPAR is less than wind force of TLP, due to the same reason mentioned above. Detail of wind force component and simulated time history is shown in Table 6-2 and Figures 6-6 to 6-7.

**Table 6-2 Wind Force of Derrick and Skid Base (45 Degrees)**

<b>100 YEAR</b>	z elev above MWL to Mid-Point	U(z) 1-hr ave	C <sub>shape</sub>	Unit Pressure	Perm Factor	Projected Area	Pressure	Moment
Upper derrick	343	218	1.25	70	0.6	3995	169	34159
Lower derrick	258	211	1.25	66	0.6	4165	164	19302
Drill floor	208	205	1.50	75	1.0	1065	80	5371
Substructure	175	201	1.50	72	0.6	3550	152	5334
<b>Derrick</b>							<b>565</b>	<b>64166</b>
Skid base	145	196	1.50	68	1.0	990	67	337
<b>Derrick + Skid Base</b>							<b>632</b>	<b>64504</b>

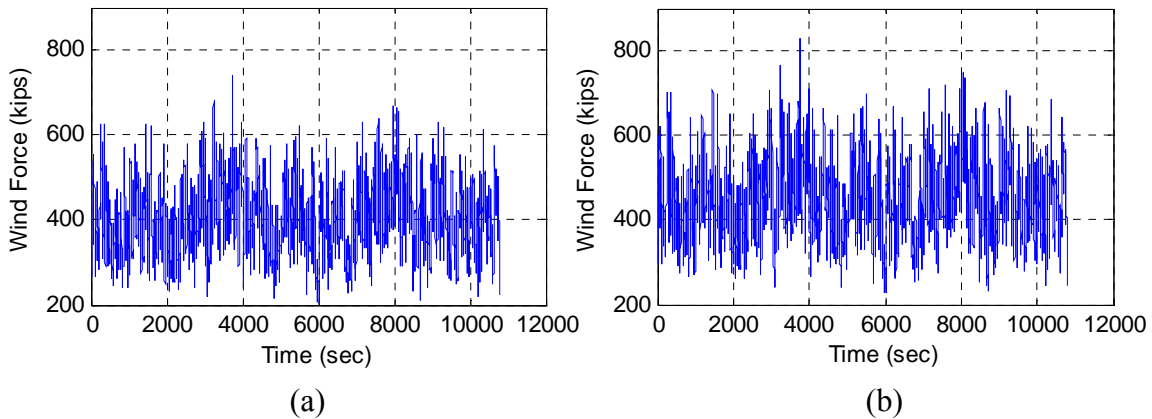


**Fig 6-6 Surge Wind Force of (a) Derrick and (b) Derrick + Skid Base (45 Degrees)**



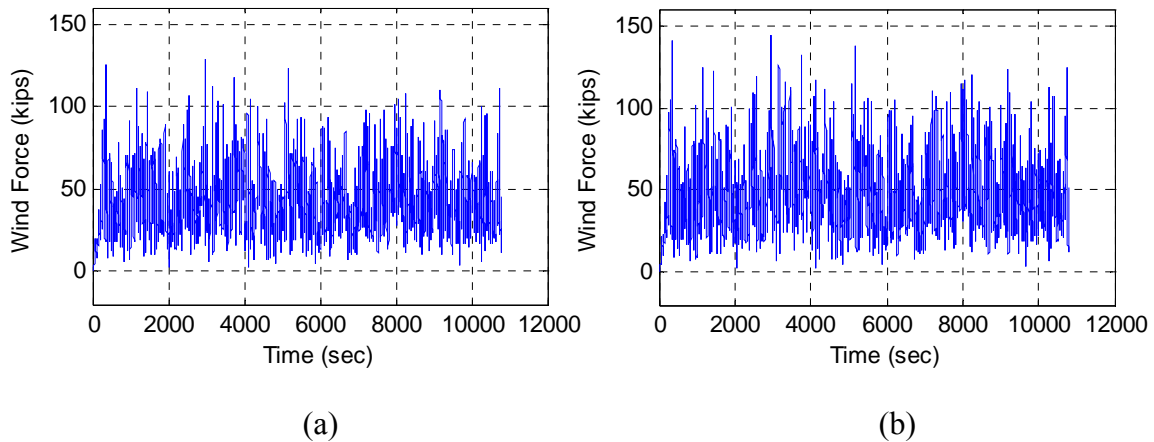


**Fig 6-7 Heave Wind Force of (a) Derrick and (b) Derrick + Skid Base (45 Degrees)**

**Table 6-3 Wind Force Statistics for (a) Derrick and (b) Derrick + Skid Base (45 Degrees)**

Wind	Surge	Sway	Heave
MAX	739	735	129
MIN	203	202	0
MEAN	401	400	42

(a)

Wind	Surge	Sway	Heave
MAX	832	827	145
MIN	226	225	0
MEAN	449	447	47

(b)

The mean wind force of derrick is 565 kips and it approximately coincides with time domain simulation result, meaning that 401 kips of surge and sway direction wind force are applied on the derrick at the same time as shown in Table 6-3.

#### 6.4 Gravity Force

Gravity force of SPAR is simulated and presented. The pattern of gravity force of SPAR follows its general characteristics that we have seen before. Figures 6-8 to 6-9 and Table 6-4 show the time history of gravity force and its statistics.

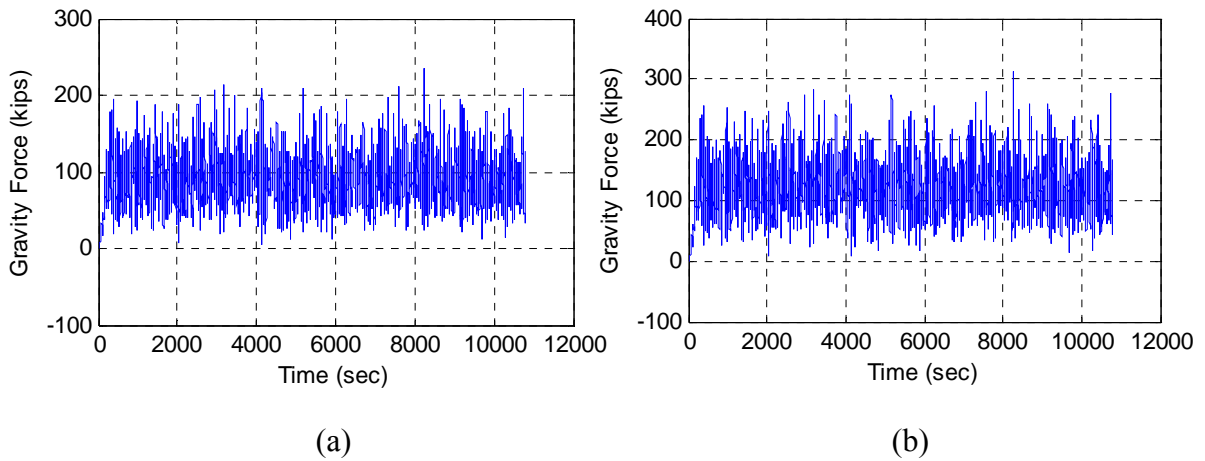


**Fig 6-8 Surge Gravity Force of (a) Derrick and (b) Derrick + Skid Base (45 Degrees)**

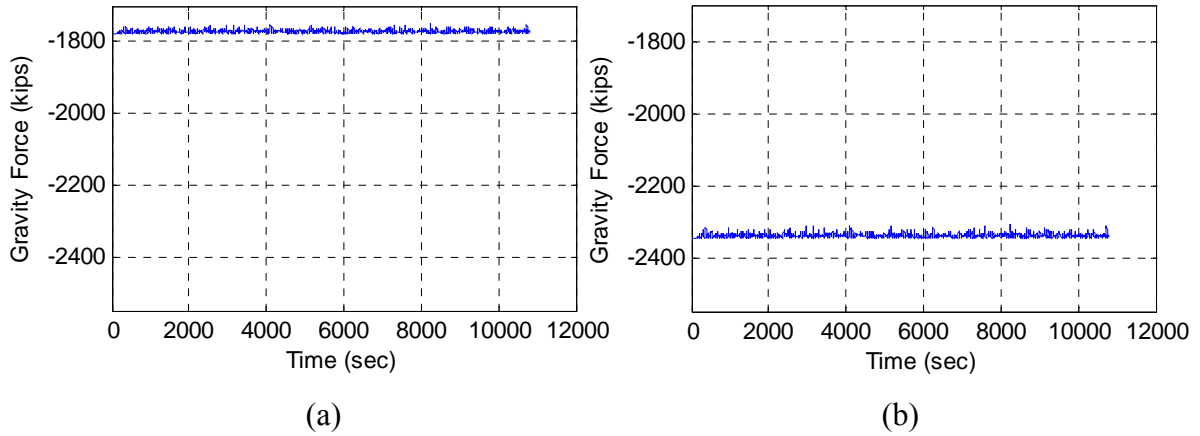


**Fig 6-9 Heave Gravity Force of (a) Derrick and (b) Derrick + Skid Base (45 Degrees)**

**Table 6-4 Gravity Force Statistics for (a) Derrick and (b) Derrick + Skid Base (45 Degrees)**

Gravity	Surge	Sway	Heave
MAX	236	234	-1746
MIN	0	0	-1777
MEAN	93	92	-1772

(a)

Gravity	Surge	Sway	Heave
MAX	311	309	-2306
MIN	0	0	-2347
MEAN	122	122	-2340

(b)

6.5 Total Force

Total force on the derrick and skid base can be expressed by a summation of inertia force, wind force and gravity force. The time history of total force and statistics of force are shown in Figures 6-10, 6-11 and Table 6-5.

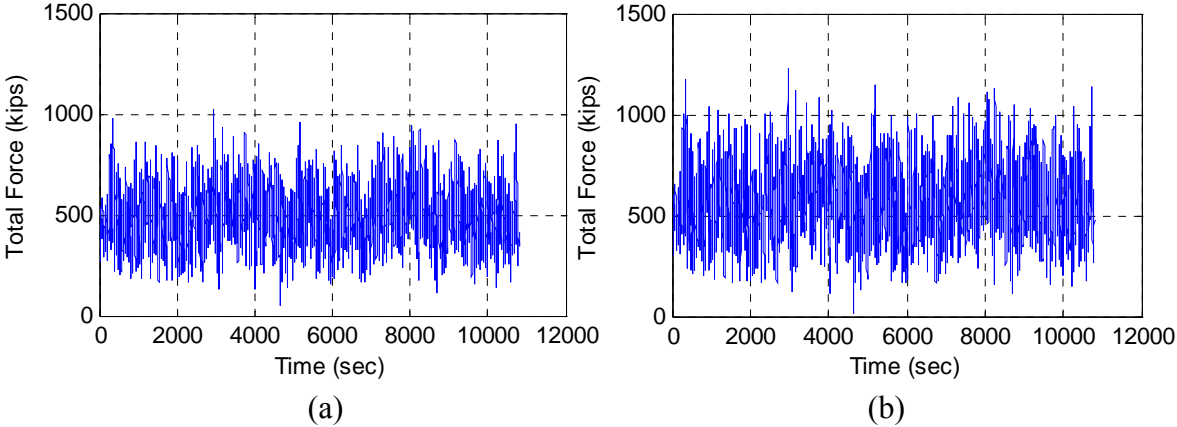


Fig 6-10 Surge Total Force of (a) Derrick and (b) Derrick + Skid Base (45 Degrees)

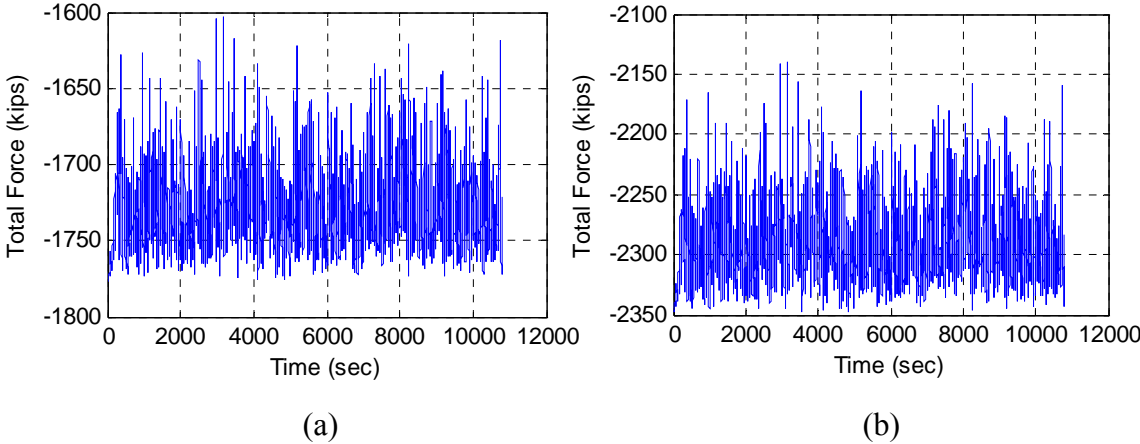


Fig 6-11 Heave Total Force of (a) Derrick and (b) Derrick + Skid Base (45 Degrees)

**Table 6-5 Total Force Statistics for (a) Derrick and (b) Derrick + Skid Base (45 Degrees)**

Total	Surge	Sway	Heave
MAX	1024	1017	-1603
MIN	45	44	-1777
MEAN	494	492	-1728

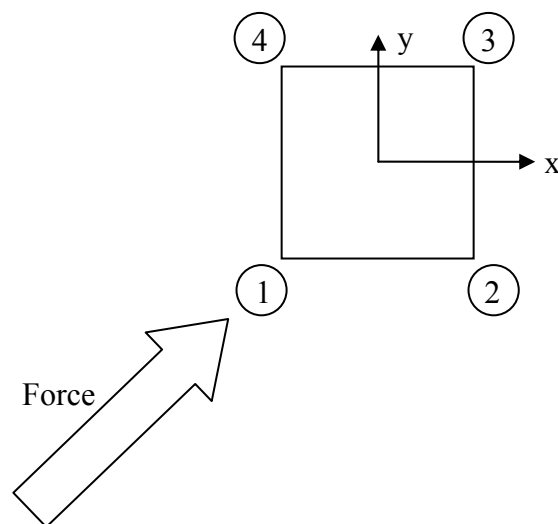
(a)

Total	Surge	Sway	Heave
MAX	1225	1216	-2139
MIN	13	13	-2347
MEAN	571	569	-2292

(b)

### 6.6 Reaction Force

Figure 6-12 shows the location of derrick footing and node numbers. External force is applied with incident angle of 45 degree, so maximum uplift force will take place on the node 1. Accordingly, node 3 will experience maximum compression force. Time history of reaction force for both derrick and skid base footings is illustrated. The derrick footing node 1 is experiencing uplift force during most of the simulation time, while all other footings are under a compression force status.

**Fig 6-12 Direction of Force and Node Location of Derrick (45 Degrees)**

6.6.1 Derrick Reaction Force

The time history of derrick reaction force is shown in Figures 6-13 to 6-16, and the statistics of reaction force for derrick footings are tabulated in Table 6-6.

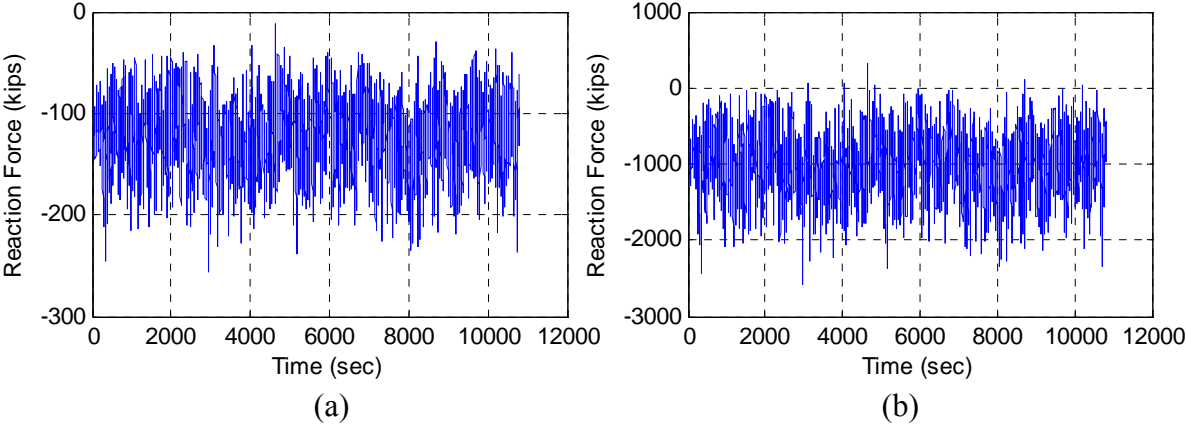


Fig 6-13 (a) Surge Reaction (b) Heave Reaction on Footing 1 (45 Degrees)

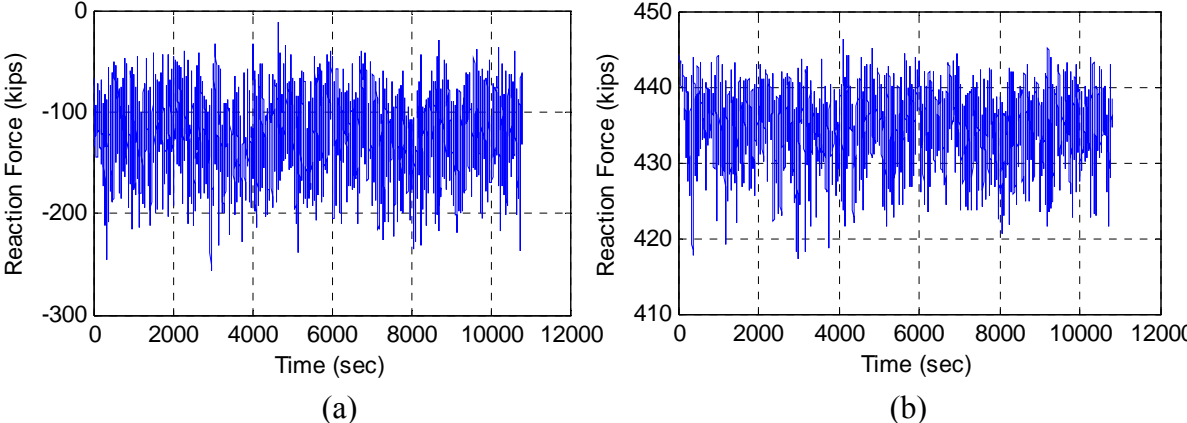
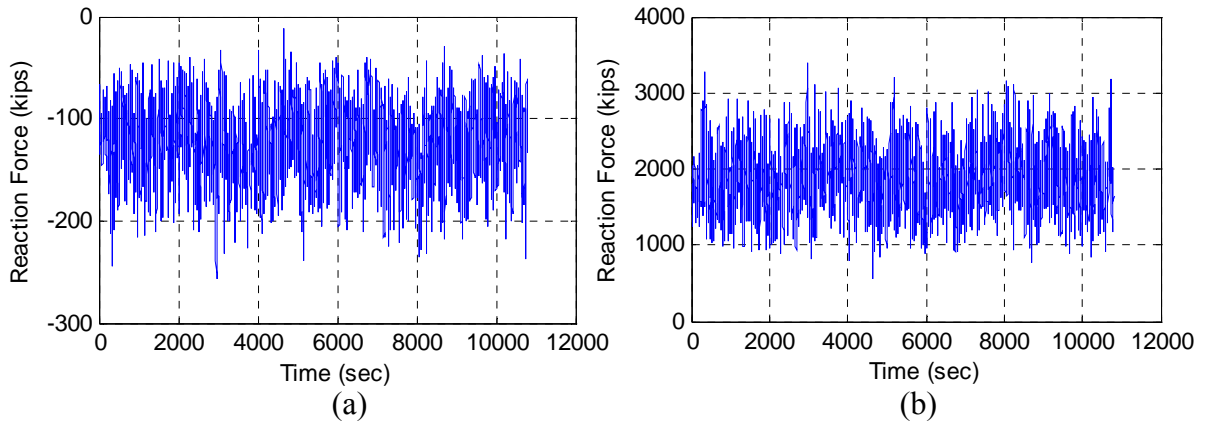
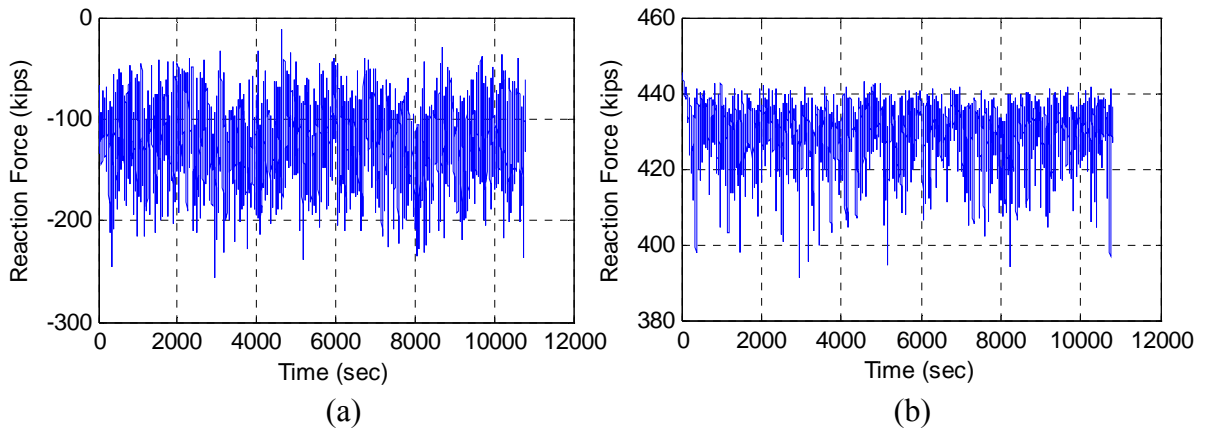


Fig 6-14 (a) Surge Reaction (b) Heave Reaction on Footing 2 (45 Degrees)



**Fig 6-15 (a) Surge Reaction (b) Heave Reaction on Footing 3 (45 Degrees)**



**Fig 6-16 (a) Surge Reaction (b) Heave Reaction on Footing 4 (45 Degrees)**

**Table 6-6 Derrick Reaction Force Statistics (45 Degrees)**

Node	Reaction	X	Y	Z
1	MAX	-11	-11	320
	MIN	-256	-254	-2588
	MEAN	-123	-123	-1009

Node	Reaction	X	Y	Z
2	MAX	-11	-11	446
	MIN	-256	-254	413
	MEAN	-123	-123	435

Table 6-6 Continued

Node	Reaction	X	Y	Z
3	MAX	-11	-11	3398
	MIN	-256	-254	566
	MEAN	-123	-123	1873

Node	Reaction	X	Y	Z
4	MAX	-11	-11	445
	MIN	-256	-254	387
	MEAN	-123	-123	429

### 6.6.2 Skid Base Reaction Force

The external forces are coming from the 45 degree of positive x direction, and this angle is not perpendicular with the diagonal line from node 6 to node 8 as shown in Figure 6-17. Intuitively, we can figure out that node 5 will experience maximum uplift force, but the result should be compared with 21.25 degree case. The time history of skid base reaction force is shown in Figures 6-18 to 6-21, and the statistics of reaction force are tabulated in Table 6-7.

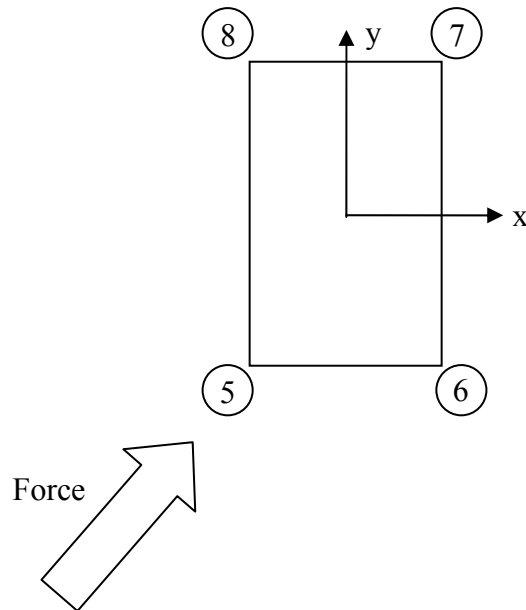


**Fig 6-17 Direction of Force and Node Location of Skid Base (45 Degrees)**

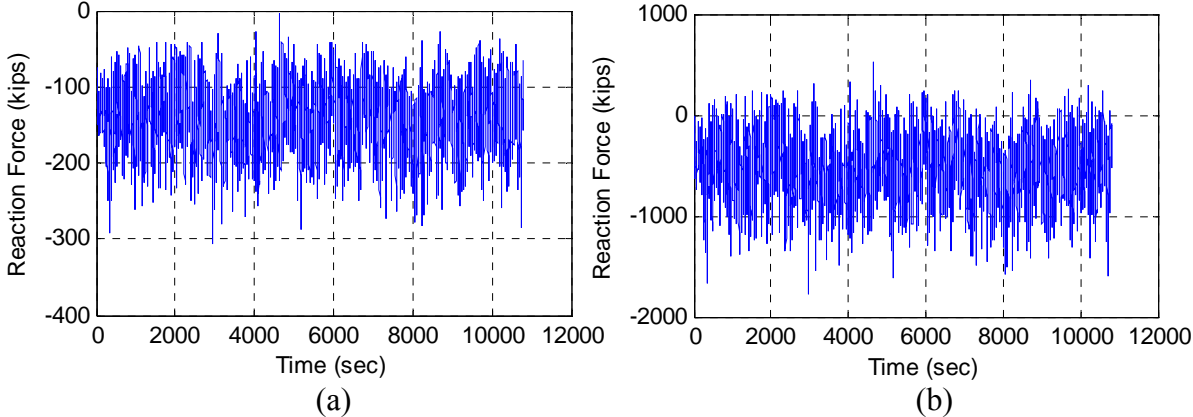


**Fig 6-18 (a) Surge Reaction (b) Heave Reaction on Footing 5 (45 Degrees)**

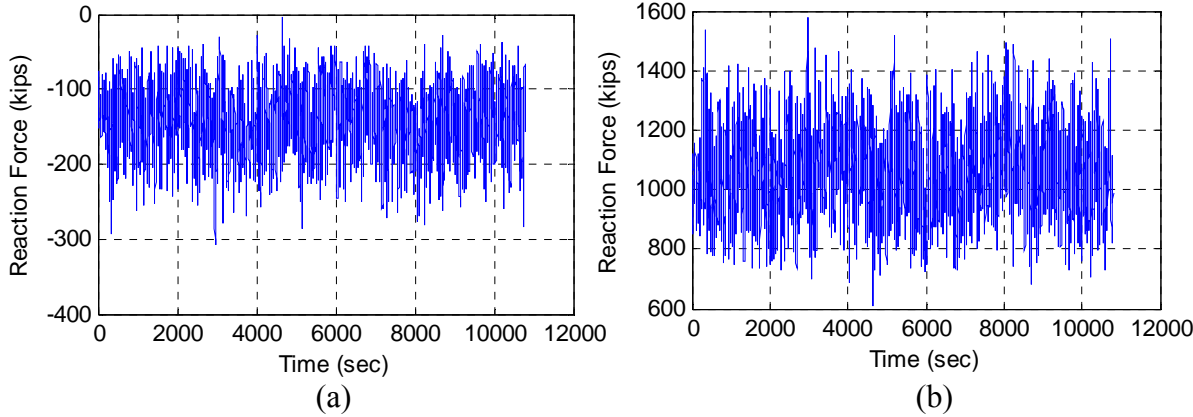


**Fig 6-19 (a) Surge Reaction (b) Heave Reaction on Footing 6 (45 Degrees)**

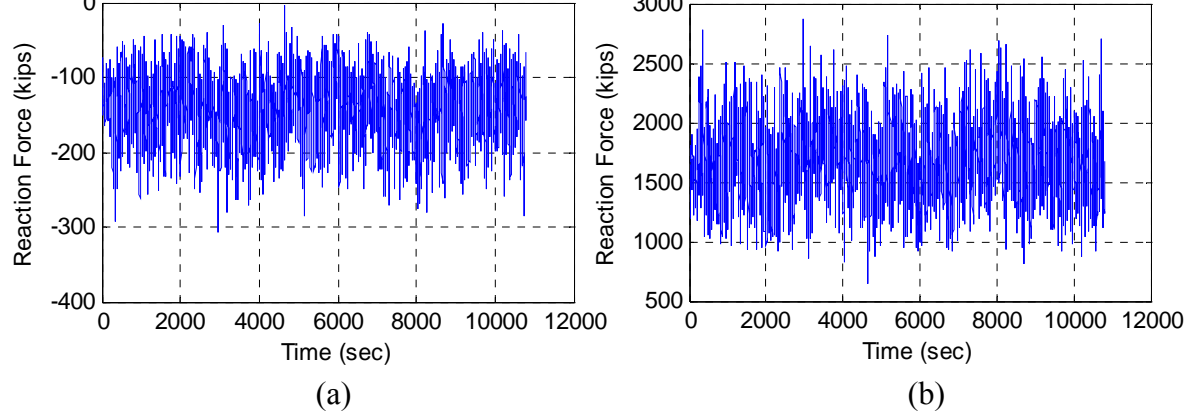


**Fig 6-20 (a) Surge Reaction (b) Heave Reaction on Footing 7 (45 Degrees)**



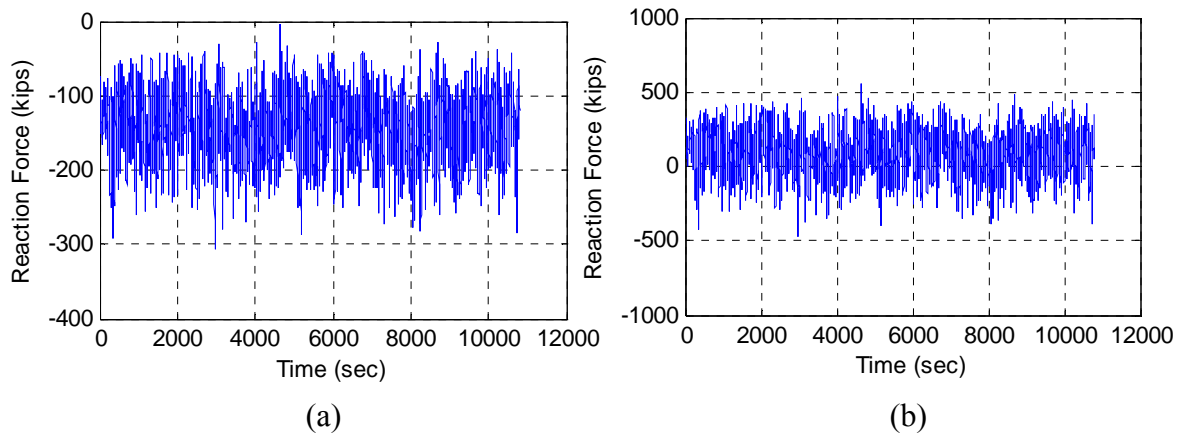


**Fig 6-21 (a) Surge Reaction (b) Heave Reaction on Footing 8 (45 Degrees)**

**Table 6-7 Skid Base Reaction Force Statistics (45 Degrees)**

Node	Reaction	X	Y	Z
5	MAX	-3	-3	524
	MIN	-306	-304	-1787
	MEAN	-143	-142	-530

Node	Reaction	X	Y	Z
6	MAX	-3	-3	1571
	MIN	-306	-304	613
	MEAN	-143	-142	1060

Node	Reaction	X	Y	Z
7	MAX	-3	-3	2867
	MIN	-306	-304	648
	MEAN	-143	-142	1676

Node	Reaction	X	Y	Z
8	MAX	-3	-3	559
	MIN	-306	-304	-491
	MEAN	-143	-142	86

The lateral reaction forces of skid base shows a similar pattern for all 4 footings, but the vertical reaction force shows different characteristics for 4 footings. Two footings located at the diagonal position, node 6 and 8 will experience a different pattern of reaction force because the location of footings is not a squared position and that makes the distribution of force asymmetric.

## 6.7 200-year and 1000-year Hurricane Conditions

The same analysis is carried out for 200-year and 1000-year hurricane conditions.

### 6.7.1 200-year Hurricane Condition

Table 6-8 shows the force components of derrick and skid base footings for 200-year hurricane condition.

**Table 6-8 Force Statistics for (a) Derrick and (b) Derrick + Skid Base  
(45 Degrees, 200-year Hurricane Condition)**

<b>Inertia</b>	Surge	Sway	Heave
MAX	403	400	69
MIN	-324	-323	-52
MEAN	0	0	1

<b>Inertia</b>	Surge	Sway	Heave
MAX	515	512	91
MIN	-414	-413	-68
MEAN	0	0	1

<b>Wind</b>	Surge	Sway	Heave
MAX	852	846	160
MIN	230	229	0
MEAN	459	457	55

<b>Wind</b>	Surge	Sway	Heave
MAX	959	953	180
MIN	256	254	0
MEAN	514	511	62

<b>Gravity</b>	Surge	Sway	Heave
MAX	258	255	-1740
MIN	0	0	-1777
MEAN	105	105	-1770

<b>Gravity</b>	Surge	Sway	Heave
MAX	340	337	-2298
MIN	0	0	-2347
MEAN	139	138	-2338

**Table 6-8 Continued**

<b>Total</b>	Surge	Sway	Heave
MAX	1133	1122	-1563
MIN	79	78	-1777
MEAN	564	562	-1714

(a)

<b>Total</b>	Surge	Sway	Heave
MAX	1352	1339	-2092
MIN	51	51	-2347
MEAN	653	650	-2275

(b)

The corresponding reaction force of each position is shown in Table 6-9.

**Table 6-9 Reaction Force Statistics (45 Degrees, 200-year Hurricane Condition)**

Node	Reaction	X	Y	Z
1	MAX	-20	-20	221
	MIN	-283	-280	-2914
	MEAN	-141	-140	-1217

Node	Reaction	X	Y	Z
2	MAX	-20	-20	446
	MIN	-283	-281	408
	MEAN	-141	-140	432

Node	Reaction	X	Y	Z
3	MAX	-20	-20	3701
	MIN	-283	-281	663
	MEAN	-141	-140	2074

Node	Reaction	X	Y	Z
4	MAX	-20	-20	445
	MIN	-283	-280	372
	MEAN	-141	-140	425

Node	Reaction	X	Y	Z
5	MAX	-13	-13	449
	MIN	-338	-335	-2044
	MEAN	-163	-162	-692

Node	Reaction	X	Y	Z
6	MAX	-13	-13	1670
	MIN	-338	-335	645
	MEAN	-163	-162	1126

**Table 6-9 Continued**

Node	Reaction	X	Y	Z
7	MAX	-13	-13	3098
	MIN	-338	-335	721
	MEAN	-163	-162	1829

Node	Reaction	X	Y	Z
8	MAX	-13	-13	525
	MIN	-338	-335	-615
	MEAN	-163	-162	12

### 6.7.2 1000-year Hurricane Condition

Table 6-10 shows the force components of derrick and skid base footings for 1000-year hurricane condition.

**Table 6-10 Force Statistics for (a) Derrick and (b) Derrick + Skid Base  
(45 Degrees, 1000-year Hurricane Condition)**

<b>Inertia</b>	Surge	Sway	Heave
MAX	466	459	117
MIN	-367	-362	-86
MEAN	0	0	1

<b>Inertia</b>	Surge	Sway	Heave
MAX	596	587	155
MIN	-470	-464	-114
MEAN	0	0	2

<b>Wind</b>	Surge	Sway	Heave
MAX	1246	1229	323
MIN	321	319	0
MEAN	659	653	111

<b>Wind</b>	Surge	Sway	Heave
MAX	1402	1384	363
MIN	356	353	0
MEAN	737	731	124

<b>Gravity</b>	Surge	Sway	Heave
MAX	346	339	-1710
MIN	0	0	-1777
MEAN	148	147	-1764

<b>Gravity</b>	Surge	Sway	Heave
MAX	457	448	-2258
MIN	0	0	-2347
MEAN	195	194	-2329

**Table 6-10 Continued**

Total	Surge	Sway	Heave
MAX	1490	1470	-1377
MIN	198	197	-1779
MEAN	806	800	-1651

(a)

Total	Surge	Sway	Heave
MAX	1762	1738	-1869
MIN	183	182	-2353
MEAN	932	925	-2203

(b)

The reaction force of each footing for 1000-year hurricane condition is shown in Table 6-11.

**Table 6-11 Reaction Force Statistics (45 Degrees, 1000-year Hurricane Condition)**

Node	Reaction	X	Y	Z
1	MAX	-49	-49	-131
	MIN	-373	-367	-3989
	MEAN	-202	-200	-1936

Node	Reaction	X	Y	Z
2	MAX	-49	-49	446
	MIN	-373	-368	387
	MEAN	-202	-200	422

Node	Reaction	X	Y	Z
3	MAX	-49	-49	4711
	MIN	-372	-368	1007
	MEAN	-202	-200	2762

Node	Reaction	X	Y	Z
4	MAX	-49	-49	446
	MIN	-372	-367	301
	MEAN	-202	-200	403

Node	Reaction	X	Y	Z
5	MAX	-46	-45	183
	MIN	-441	-434	-2885
	MEAN	-233	-231	-1249

Node	Reaction	X	Y	Z
6	MAX	-46	-45	1992
	MIN	-441	-435	756
	MEAN	-233	-231	1348

**Table 6-11 Continued**

Node	Reaction	X	Y	Z
7	MAX	-46	-45	3863
	MIN	-440	-435	978
	MEAN	-233	-231	2351

Node	Reaction	X	Y	Z
8	MAX	-46	-45	405
	MIN	-440	-434	-1017
	MEAN	-233	-231	-247

Mean reaction force of each footing is listed in Figures 6-22, 6-23.

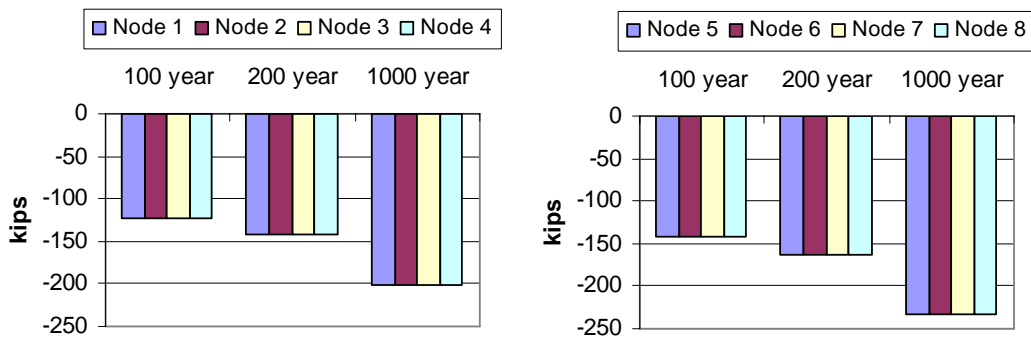


**Fig 6-22 SPAR Mean Surge Reaction Force (45 Degrees)**

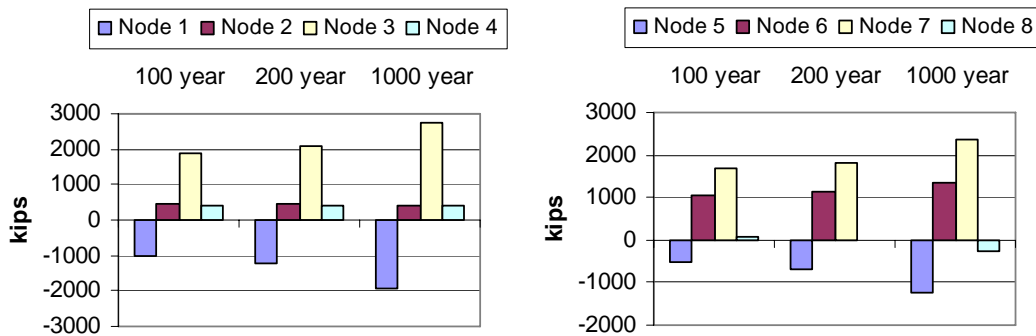


**Fig 6-23 SPAR Mean Heave Reaction Force (45 Degrees)**

Figure 6-23 shows that the mean heave reaction force of derrick footings is positive except for node 1, and it also shows that the reaction force of footing node 2 and

node 4 is constant irrespective of different hurricane conditions. These constant reaction forces are coming from the derrick's gravity force. The pattern of vertical reaction force of skid base is different from the pattern of derrick reaction force, since the skid base is not a squared shape and the incident angle of 45 degrees is not perpendicular to diagonal tip line between node 6 and 8. The interesting thing in this case is the mean reaction force of node 8. For 100-year and 200-year hurricane conditions, this node experiences compression force, but during 1000-year hurricane condition, its mean reaction force turns negative which means this footing will experience uplift tensile force.

## 7 CASE 4. SPAR (3000FT) WITH DERRICK AA – 90 DEGREE CASE

### 7.1 SPAR Motion Time History

The motion of TLP with 90 degree incident wind, wave, and current is exactly the same with the motion of 0 degree numerically, once we regard every motion along the X axis of 0 degree case as the same as the motions along the Y axis of 90 degree case. Thus, the motion history and its spectrum are not reproduced here. The thing we are interested in is how different the reaction forces of skid base footing are compared to 0 degree case.

### 7.2 Inertia Force

Similarly, inertia force of this case is exactly the same as 0 degree incident wave case, but surge motion of 0 degree case is simply expressed as sway motion in this case. The inertial force of derrick and skid base are calculated based on the hull motion, and are summarized in Figures 7-1 to 7-2 and Table 7-1.

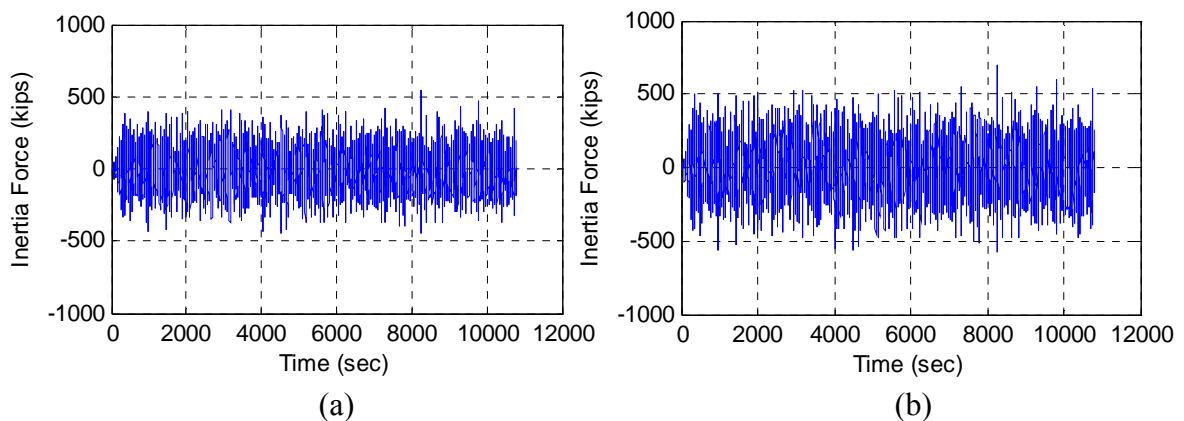


**Fig 7-1 Sway Inertia Force of (a) Derrick and (b) Derrick + Skid Base (90 Degrees)**



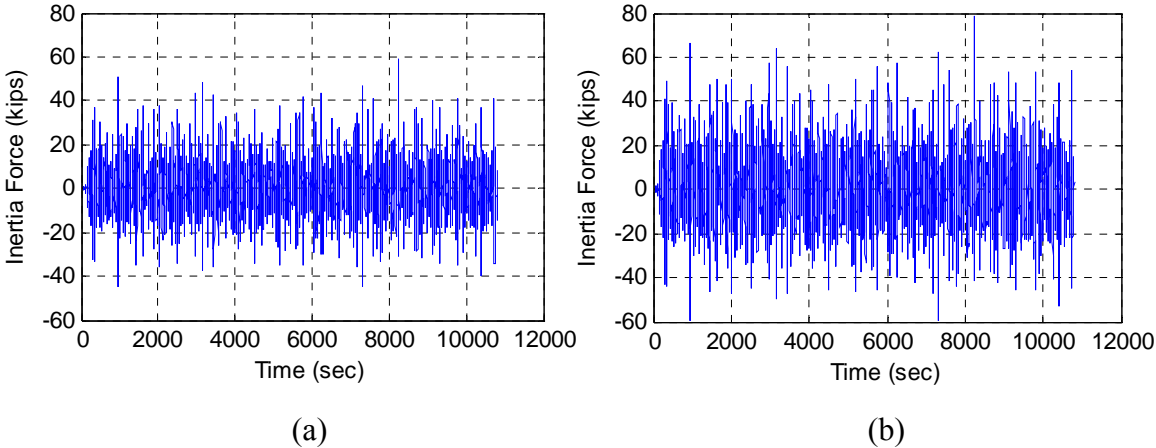


**Fig 7-2 Heave Inertia Force of (a) Derrick and (b) Derrick + Skid Base (90 Degrees)**

**Table 7-1 Inertia Force Statistics for (a) Derrick and (b) Derrick + Skid Base (90 Degrees)**

Inertia	Surge	Sway	Heave
MAX	1	546	59
MIN	-1	-451	-45
MEAN	0	0	1

Inertia	Surge	Sway	Heave
MAX	1	698	78
MIN	-1	-577	-60
MEAN	0	0	1

(a) (b)

7.3 Wind Force

Projected area of derrick is 9030 ft<sup>2</sup> and it is identical with 0 degree case, but the area of skid base in this case is only 400 ft<sup>2</sup>, while it is 1000 ft<sup>2</sup> for 0 degree case. Corresponding mean pressure of the total structure including skid base is 426 kips, but it is 467 kips for 0 degree cases. For this reason, the total structures will experience less wind force. The other difference is that the longitudinal direction of skid base is parallel with upstream direction, so the trend of reaction force of skid base footing would be

different from 0 degree case. Detail of wind force component and simulated time history is shown in Table 7-2 and Figures 7-3 to 7-4.

**Table 7-2 Wind Force of Derrick and Skid Base (90 Degrees)**

<b>100 YEAR</b>		z elev above MWL to Mid-Point	U(z) 1-hr ave	C <sub>shape</sub>	Unit Pressure	Perm Factor	Projected Area	Pressure	Moment
	Upper derrick	343	218	1.25	70	0.6	2805	118	23984
	Lower derrick	258	211	1.25	66	0.6	2975	117	13787
	Drill floor	208	205	1.50	75	1.0	750	56	3783
	Substructure	175	201	1.50	72	0.6	2500	107	3756
<b>Derrick</b>								<b>399</b>	<b>45310</b>
	Skid base	145	196	1.50	68	1.0	400	27	136
<b>Derrick + Skid Base</b>								<b>426</b>	<b>45446</b>

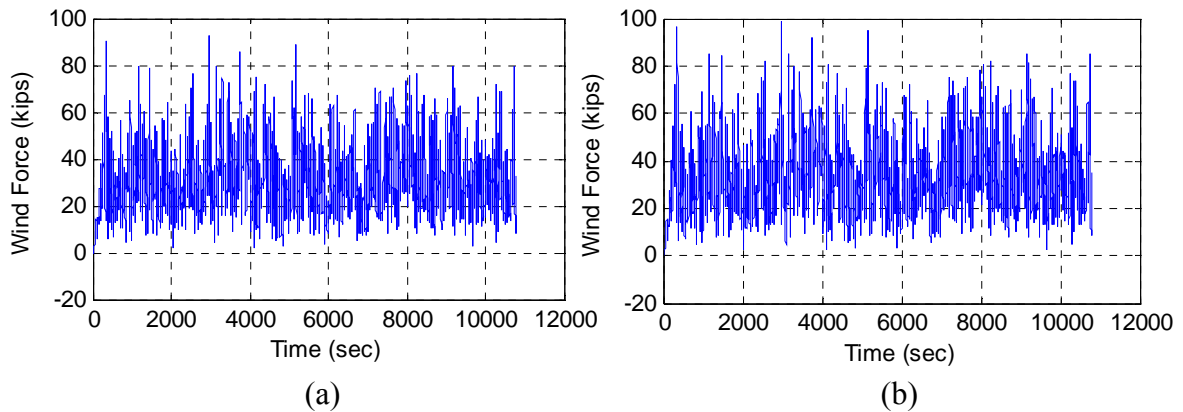


**Fig 7-3 Sway Wind Force of (a) Derrick and (b) Derrick + Skid Base (90 Degrees)**

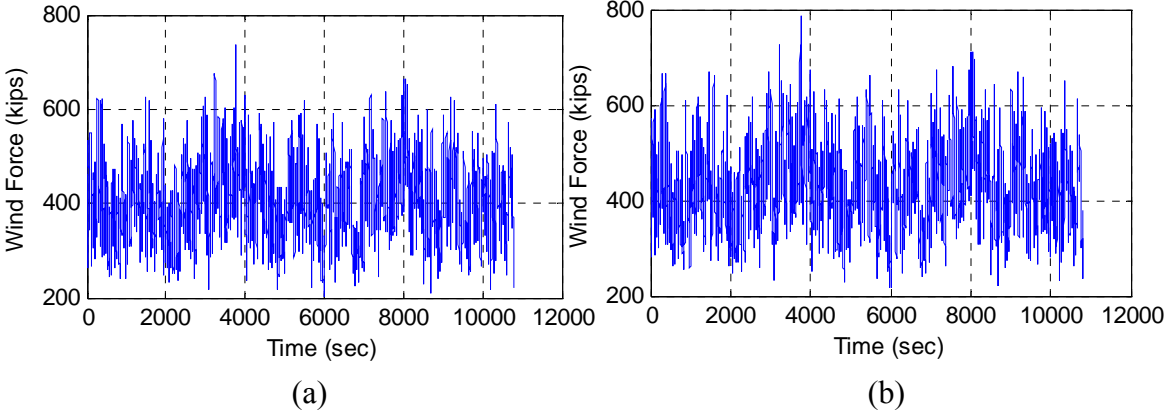


**Fig 7-4 Heave Wind Force of (a) Derrick and (b) Derrick + Skid Base (90 Degrees)**

The maximum and minimum of wind force is tabulated in Table 7-3.

**Table 7-3 Wind Force Statistics for (a) Derrick and (b) Derrick + Skid Base (90 Degrees)**

Wind	Surge	Sway	Heave
MAX	1	736	93
MIN	-1	203	0
MEAN	0	400	31

(a)

Wind	Surge	Sway	Heave
MAX	2	789	99
MIN	-1	215	0
MEAN	0	427	33

(b)

7.4 Gravity Force

Time history of gravity force and statistics of force are shown in Figures 7-5 to 7-6 and Table 7-4.

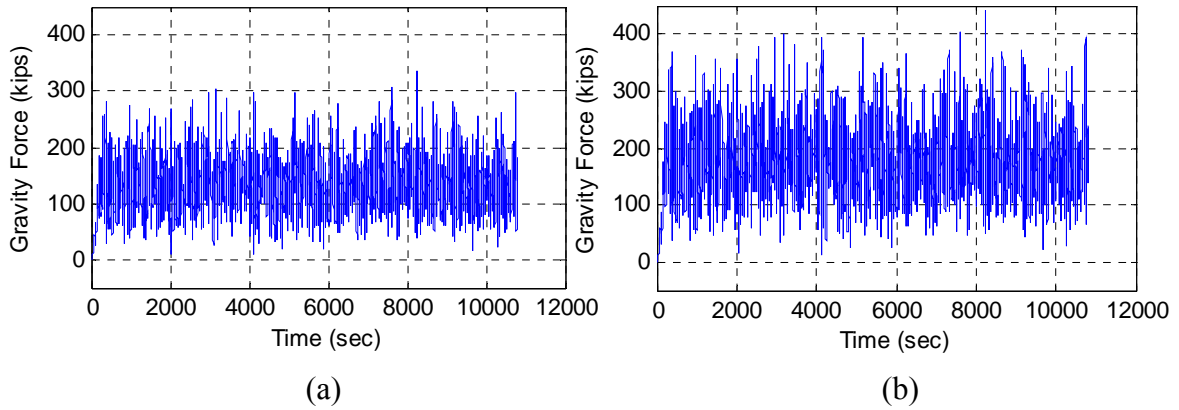


**Fig 7-5 Sway Gravity Force of (a) Derrick and (b) Derrick + Skid Base (90 Degrees)**

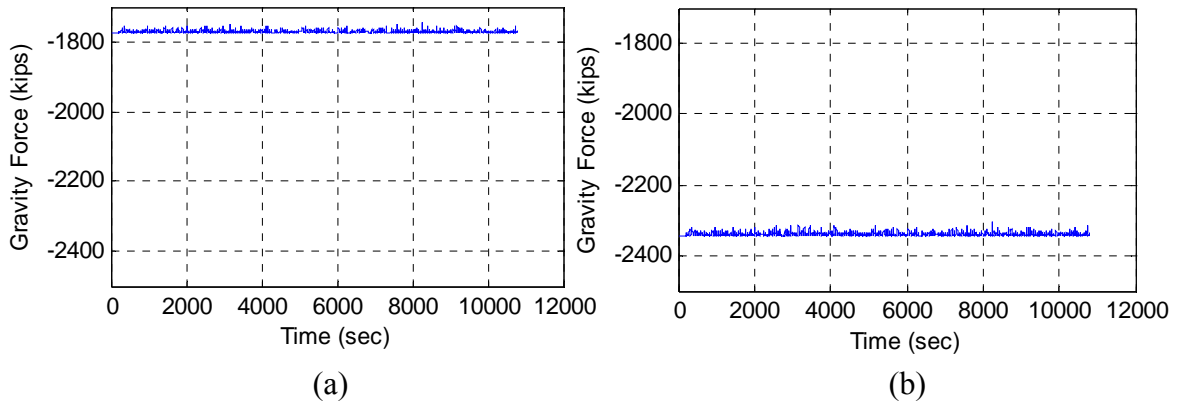


**Fig 7-6 Heave Gravity Force of (a) Derrick and (b) Derrick + Skid Base (90 Degrees)**

**Table 7-4 Gravity Force Statistics for (a) Derrick and (b) Derrick + Skid Base (90 Degrees)**

<b>Gravity</b>	Surge	Sway	Heave
MAX	0	335	-1745
MIN	0	0	-1777
MEAN	0	134	-1771

(a)

<b>Gravity</b>	Surge	Sway	Heave
MAX	0	443	-2305
MIN	0	0	-2347
MEAN	0	177	-2340

(b)

7.5 Total Force

Time history of total force and its statistics are shown in Figures 7-7 to 7-8 and Table 7-5.

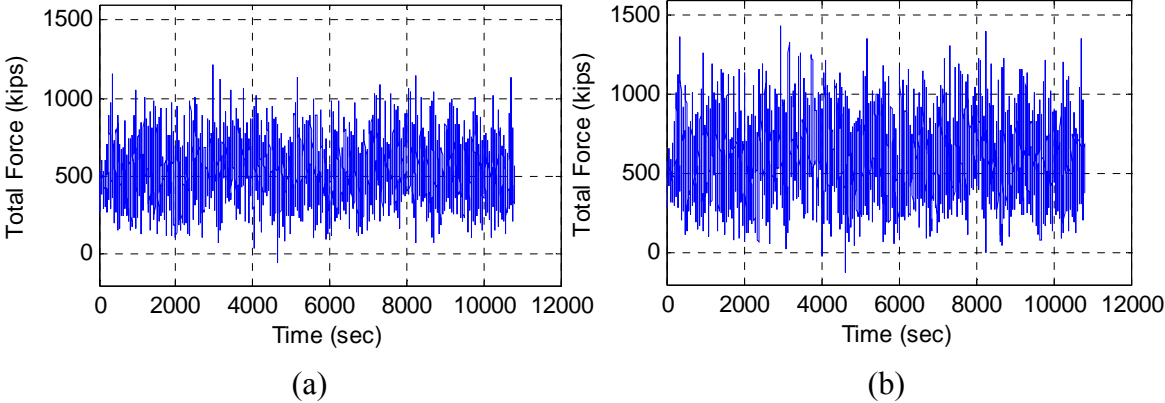


Fig 7-7 Sway Total Force of (a) Derrick and (b) Derrick + Skid Base (90 Degrees)

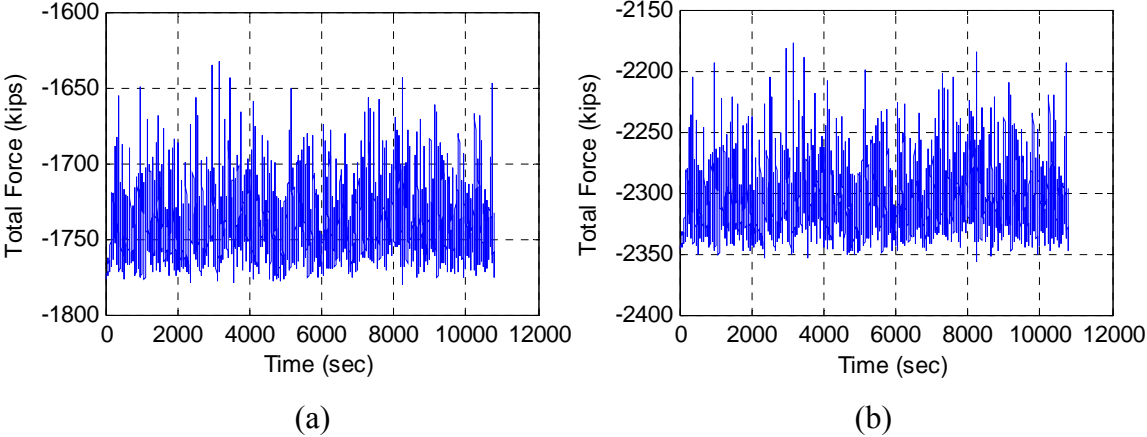


Fig 7-8 Heave Total Force of (a) Derrick and (b) Derrick + Skid Base (90 Degrees)

**Table 7-5 Total Force Statistics for (a) Derrick and (b) Derrick + Skid Base (90 Degrees)**

Total	Surge	Sway	Heave
MAX	2	1207	-1633
MIN	-1	-53	-1780
MEAN	0	534	-1740

(a)

Total	Surge	Sway	Heave
MAX	2	1431	-2177
MIN	-1	-124	-2356
MEAN	0	604	-2306

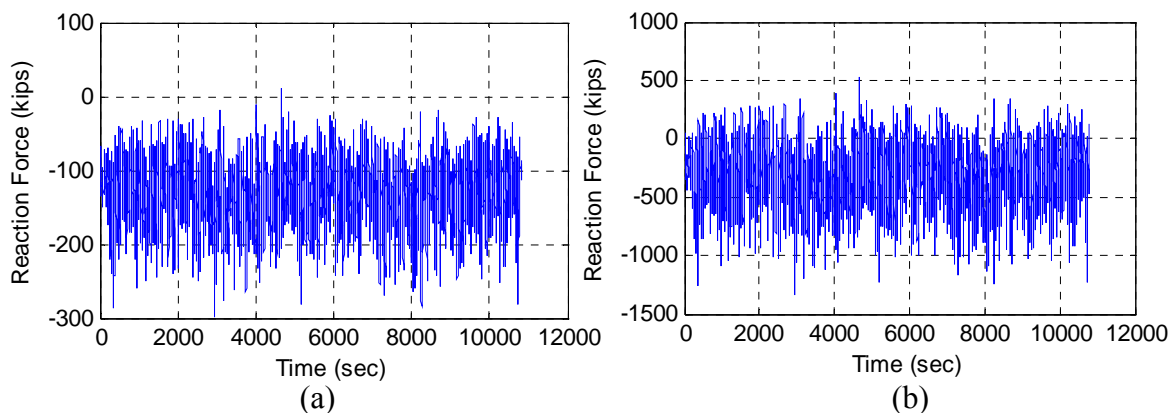
(b)

## 7.6 Reaction Force

Reaction forces of derrick footings and skid base footings are plotted. The derrick reaction force will be similar to that of 0 degree case, but the reaction force of skid base would be quite different as we discussed. The reaction force of SPAR case is presented below.

### 7.6.1 Derrick Reaction Force

The time history of derrick reaction force is shown in Figures 7-9 to 7-12, and the statistics of reaction force for derrick footings are tabulated in Table 7-6.

**Fig 7-9 (a) Surge Reaction (b) Heave Reaction on Footing 1 (90 Degrees)**

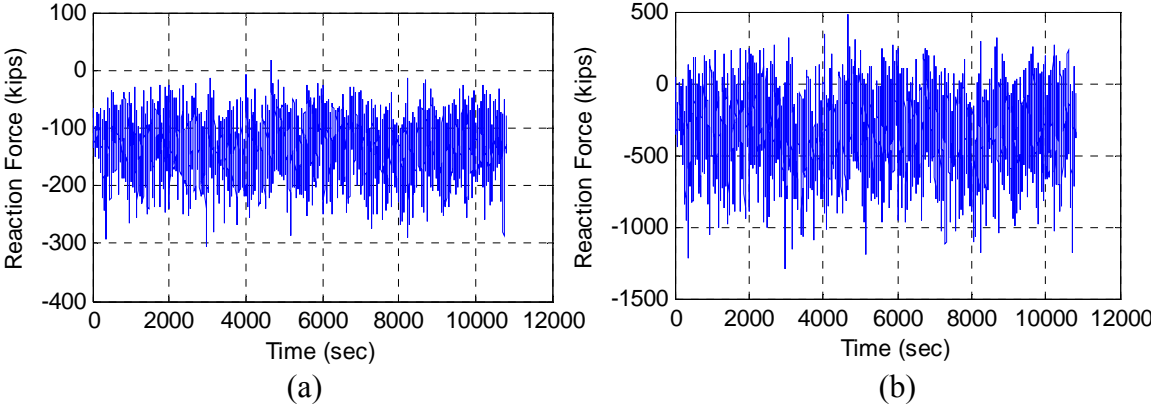


**Fig 7-10 (a) Surge Reaction (b) Heave Reaction on Footing 2 (90 Degrees)**

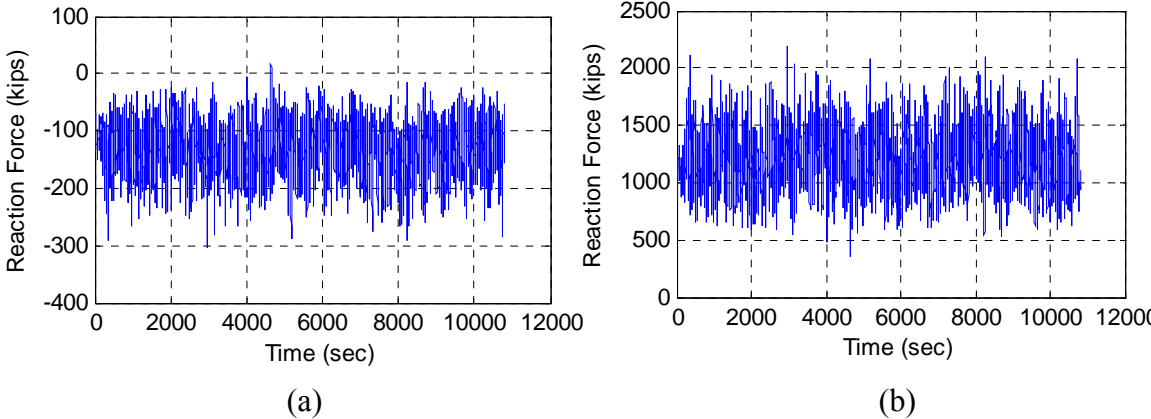


**Fig 7-11 (a) Surge Reaction (b) Heave Reaction on Footing 3 (90 Degrees)**

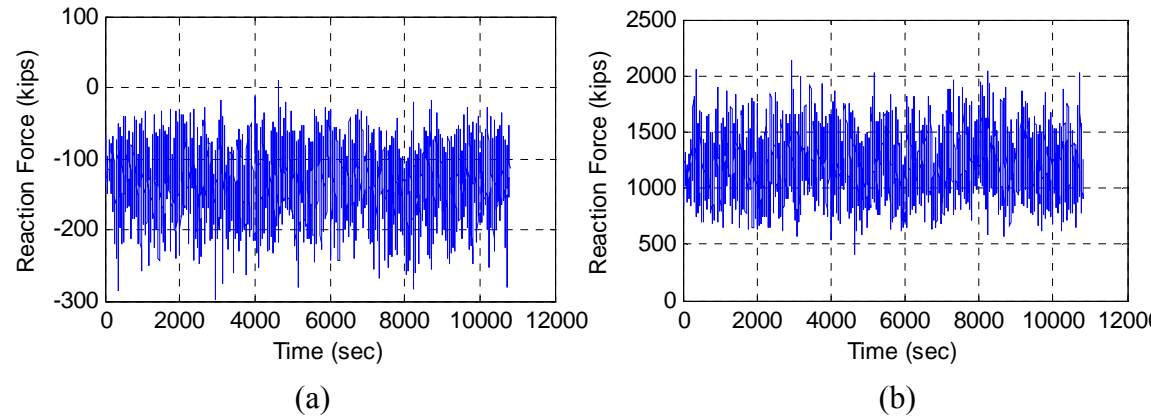


**Fig 7-12 (a) Surge Reaction (b) Heave Reaction on Footing 4 (90 Degrees)**

**Table 7-6 Derrick Reaction Force Statistics (90 Degrees)**

Node	Reaction	X	Y	Z
1	MAX	3	10	529
	MIN	-4	-299	-1354
	MEAN	0	-133	-341

Node	Reaction	X	Y	Z
2	MAX	3	16	482
	MIN	-4	-305	-1305
	MEAN	0	-133	-341

Node	Reaction	X	Y	Z
3	MAX	4	16	2178
	MIN	-3	-305	359
	MEAN	0	-133	1211

Node	Reaction	X	Y	Z
4	MAX	4	10	2129
	MIN	-3	-299	406
	MEAN	0	-133	1211

### 7.6.2 Skid Base Reaction Force

Since the external force is applied from the 90 degrees of x axis direction, the footings of node 5 and node 6 will experience uplift force, and node 7 and node 8 will experience compression force. By investigating this case, we can notice that all 4 nodes experience compression forces for the most part of the time duration, meaning the external forces are not enough to overturn the derrick structures. The time history of skid base reaction force is shown in Figures 7-13 to 7-16, and the statistics of reaction force for derrick footings are tabulated in Table 7-7.



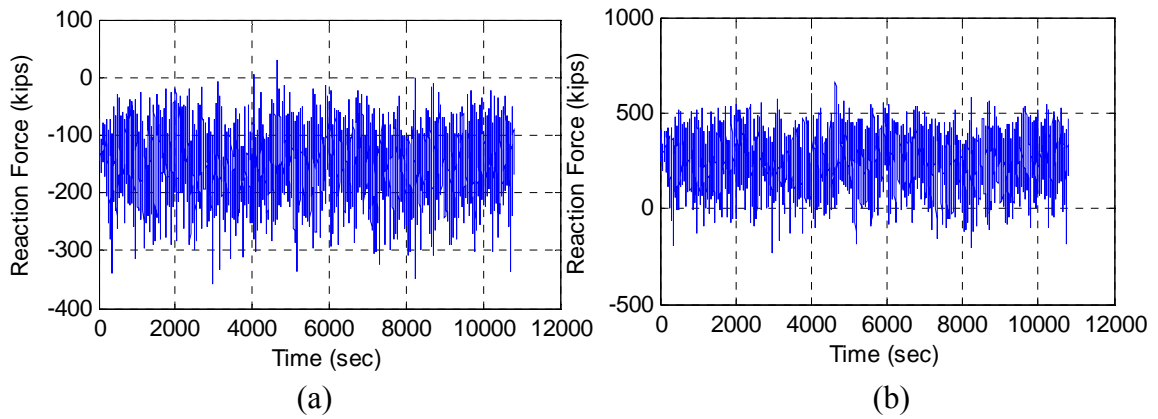


**Fig 7-13 (a) Surge Reaction (b) Heave Reaction on Footing 5 (90 Degrees)**

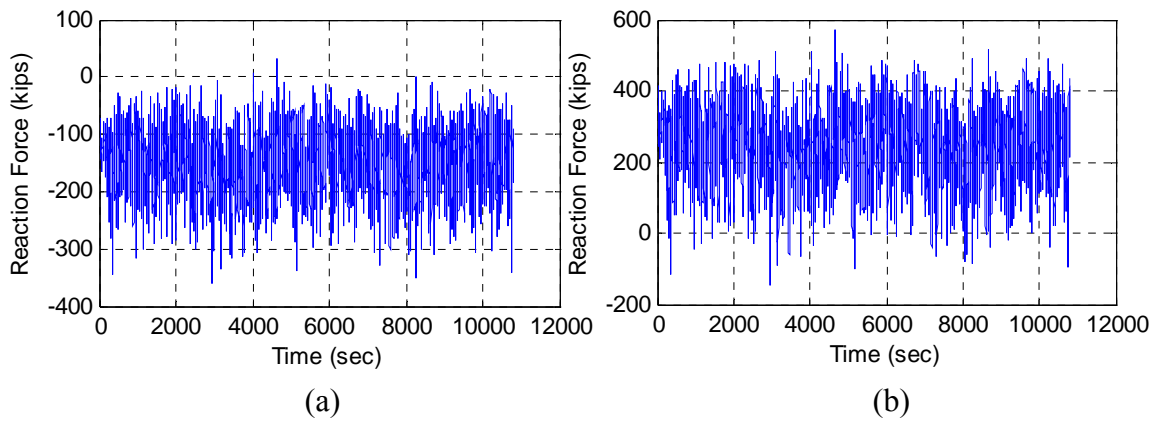


**Fig 7-14 (a) Surge Reaction (b) Heave Reaction on Footing 6 (90 Degrees)**

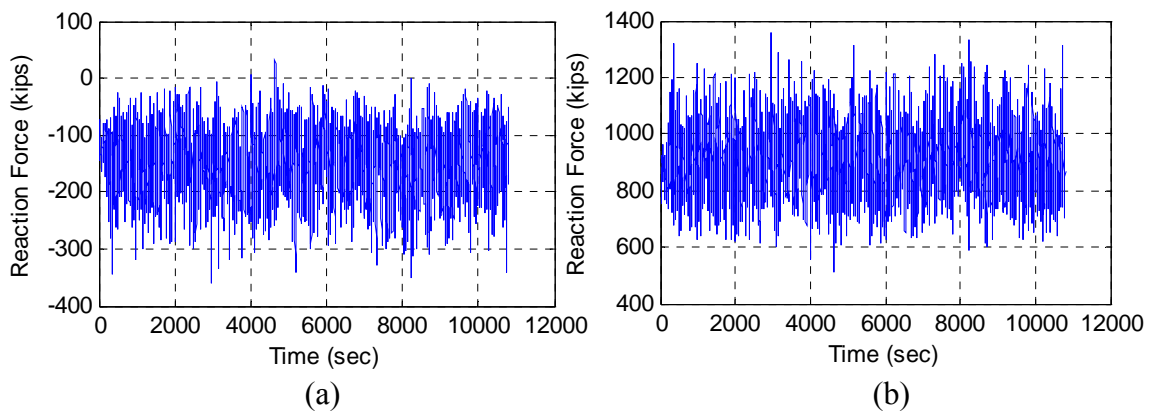


**Fig 7-15 (a) Surge Reaction (b) Heave Reaction on Footing 7 (90 Degrees)**

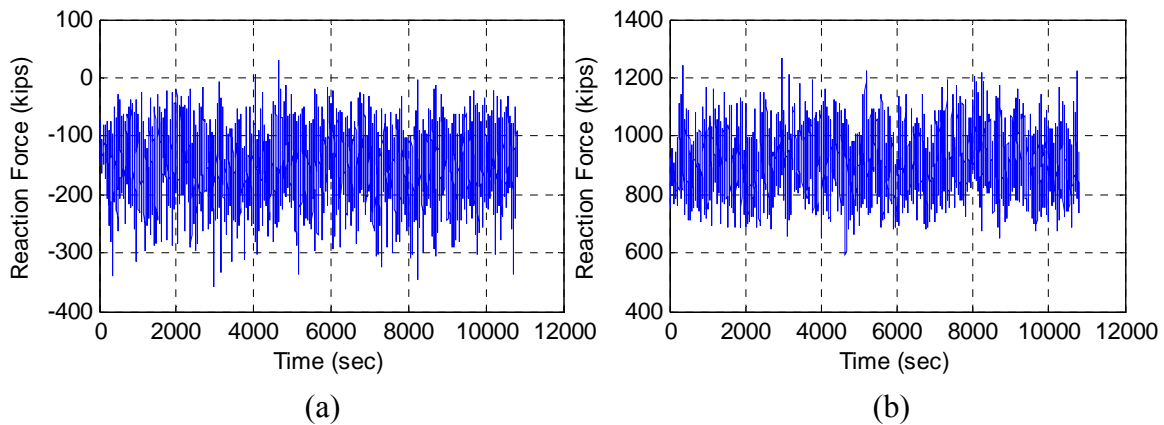


**Fig 7-16 (a) Surge Reaction (b) Heave Reaction on Footing 8 (90 Degrees)**

**Table 7-7 Skid Base Reaction Force Statistics (90 Degrees)**

Node	Reaction	X	Y	Z
5	MAX	4	29	663
	MIN	-6	-356	-249
	MEAN	0	-151	243

Node	Reaction	X	Y	Z
6	MAX	4	33	574
	MIN	-6	-359	-158
	MEAN	0	-151	244

Node	Reaction	X	Y	Z
7	MAX	5	33	1346
	MIN	-4	-359	513
	MEAN	0	-151	910

Node	Reaction	X	Y	Z
8	MAX	5	29	1255
	MIN	-4	-356	601
	MEAN	0	-151	909

### 7.7 200-year and 1000-year Hurricane Conditions

#### 7.7.1 200-year Hurricane Condition

Table 7-8 shows the force components of derrick and skid base footings for 200-year hurricane condition.

**Table 7-8 Force Statistics for (a) Derrick and (b) Derrick + Skid Base  
(90 Degrees, 200-year Hurricane Condition)**

<b>Inertia</b>	Surge	Sway	Heave
MAX	1	568	69
MIN	-1	-457	-52
MEAN	0	0	1

<b>Inertia</b>	Surge	Sway	Heave
MAX	1	726	91
MIN	-1	-585	-68
MEAN	0	0	1

<b>Wind</b>	Surge	Sway	Heave
MAX	2	848	113
MIN	-1	229	0
MEAN	0	457	39

<b>Wind</b>	Surge	Sway	Heave
MAX	2	908	121
MIN	-2	244	0
MEAN	0	488	42

<b>Gravity</b>	Surge	Sway	Heave
MAX	0	363	-1740
MIN	0	0	-1777
MEAN	0	148	-1770

<b>Gravity</b>	Surge	Sway	Heave
MAX	0	479	-2298
MIN	0	0	-2347
MEAN	0	196	-2338

<b>Total</b>	Surge	Sway	Heave
MAX	2	1317	-1603
MIN	-1	-21	-1779
MEAN	0	605	-1730

<b>Total</b>	Surge	Sway	Heave
MAX	2	1556	-2141
MIN	-2	-90	-2355
MEAN	0	684	-2295

(a)

(b)

The corresponding reaction force of each position is shown in Table 7-9.

**Table 7-9 Reaction Force Statistics (90 Degrees, 200-year Hurricane Condition)**

Node	Reaction	X	Y	Z
1	MAX	3	2	483
	MIN	-4	-326	-1524
	MEAN	0	-151	-448

Node	Reaction	X	Y	Z
2	MAX	3	8	434
	MIN	-4	-332	-1476
	MEAN	0	-151	-448

Node	Reaction	X	Y	Z
3	MAX	4	8	2334
	MIN	-3	-332	405
	MEAN	0	-151	1313

Node	Reaction	X	Y	Z
4	MAX	4	2	2283
	MIN	-3	-326	454
	MEAN	0	-151	1313

Node	Reaction	X	Y	Z
5	MAX	4	21	644
	MIN	-6	-387	-327
	MEAN	0	-171	195

Node	Reaction	X	Y	Z
6	MAX	4	24	552
	MIN	-6	-390	-239
	MEAN	0	-171	196

Node	Reaction	X	Y	Z
7	MAX	5	24	1409
	MIN	-5	-390	531
	MEAN	0	-171	952

Node	Reaction	X	Y	Z
8	MAX	5	21	1317
	MIN	-5	-387	623
	MEAN	0	-171	952

## 7.7.2 1000-year Hurricane Condition

Table 7-10 shows the force components of derrick and skid base footings for 1000-year hurricane condition.

**Table 7-10 Force Statistics for (a) Derrick and (b) Derrick + Skid Base (90 Degrees, 1000-year Hurricane Condition)**

<b>Inertia</b>	Surge	Sway	Heave
MAX	1	654	117
MIN	-1	-516	-87
MEAN	0	0	1

<b>Inertia</b>	Surge	Sway	Heave
MAX	1	837	155
MIN	-1	-660	-115
MEAN	0	0	2

<b>Wind</b>	Surge	Sway	Heave
MAX	2	1236	229
MIN	-2	319	0
MEAN	0	655	79

<b>Wind</b>	Surge	Sway	Heave
MAX	2	1326	245
MIN	-2	340	0
MEAN	0	700	84

<b>Gravity</b>	Surge	Sway	Heave
MAX	0	486	-1709
MIN	0	0	-1777
MEAN	0	209	-1764

<b>Gravity</b>	Surge	Sway	Heave
MAX	0	642	-2257
MIN	0	0	-2347
MEAN	0	275	-2329

<b>Total</b>	Surge	Sway	Heave
MAX	2	1694	-1450
MIN	-2	94	-1784
MEAN	0	863	-1683

<b>Total</b>	Surge	Sway	Heave
MAX	3	2014	-1960
MIN	-2	31	-2360
MEAN	0	975	-2243

(a)

(b)

The reaction force of each footing for 1000-year hurricane condition is shown in Table 7-11.

**Table 7-11 Reaction Force Statistics (90 Degrees, 1000-year Hurricane Condition)**

Node	Reaction	X	Y	Z
1	MAX	4	-27	313
	MIN	-5	-420	-2117
	MEAN	0	-216	-836

Node	Reaction	X	Y	Z
2	MAX	4	-20	260
	MIN	-5	-427	-2058
	MEAN	0	-216	-835

Node	Reaction	X	Y	Z
3	MAX	5	-20	2859
	MIN	-4	-427	570
	MEAN	0	-216	1678

Node	Reaction	X	Y	Z
4	MAX	5	-27	2808
	MIN	-4	-420	623
	MEAN	0	-216	1677

Node	Reaction	X	Y	Z
5	MAX	5	-10	573
	MIN	-7	-502	-622
	MEAN	0	-244	21

Node	Reaction	X	Y	Z
6	MAX	5	-6	473
	MIN	-7	-506	-513
	MEAN	0	-244	22

Node	Reaction	X	Y	Z
7	MAX	6	-6	1616
	MIN	-5	-506	596
	MEAN	0	-244	1101

Node	Reaction	X	Y	Z
8	MAX	6	-10	1523
	MIN	-5	-502	696
	MEAN	0	-244	1100

The mean reaction forces of each footing are compared in Figures 7-17 and 7-18.

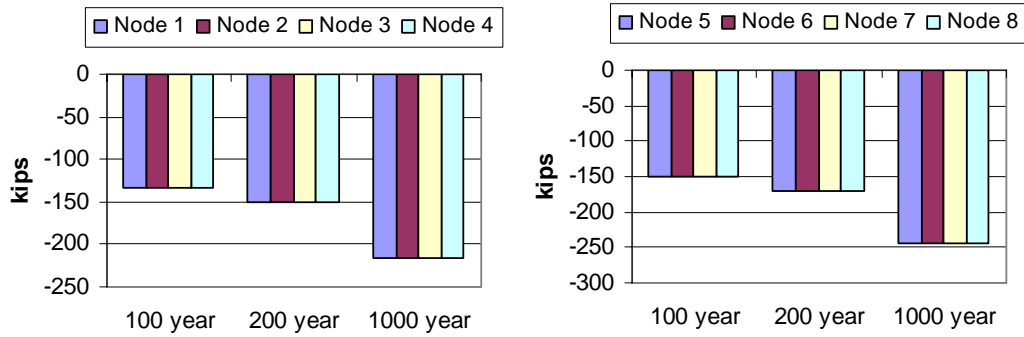


**Fig 7-17 SPAR Mean Sway Reaction Force (90 Degrees)**

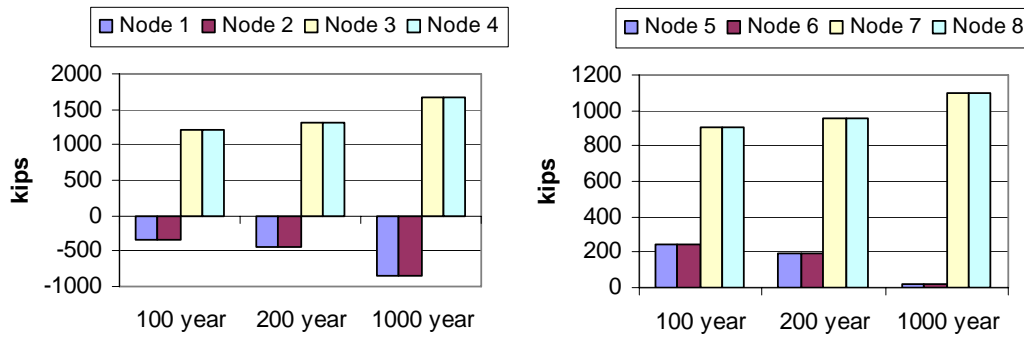


**Fig 7-18 SPAR Mean Heave Reaction Force (90 Degrees)**

## 8 SUMMARY

### 8.1 TLP vs SPAR Analysis

Due to the difference of motion characteristics between TLP and SPAR, resultant reaction force is also different. As we have already seen, total force exerted on the SPAR derrick and skid base is generally bigger than total force on TLP derrick. Figures 8-1 to 8-4 show the forces exerted on the derrick for both TLP and SPAR. A comparison of the reaction force is also presented for 0 degree case in 100-year hurricane condition.

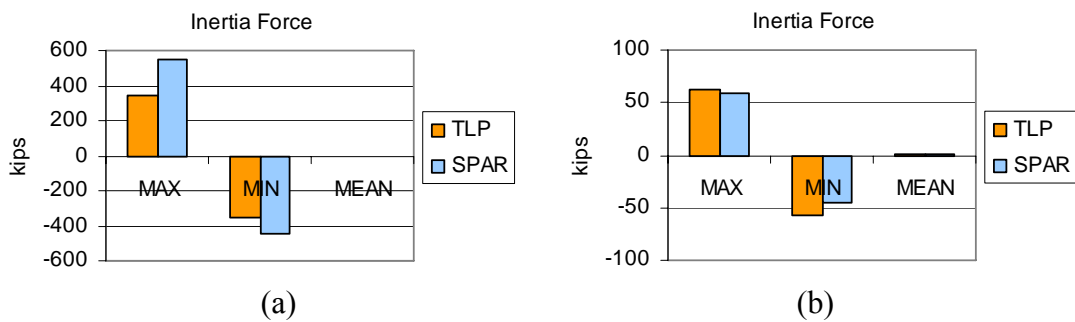


Fig 8-1 (a) Surge and (b) Heave Inertia Force

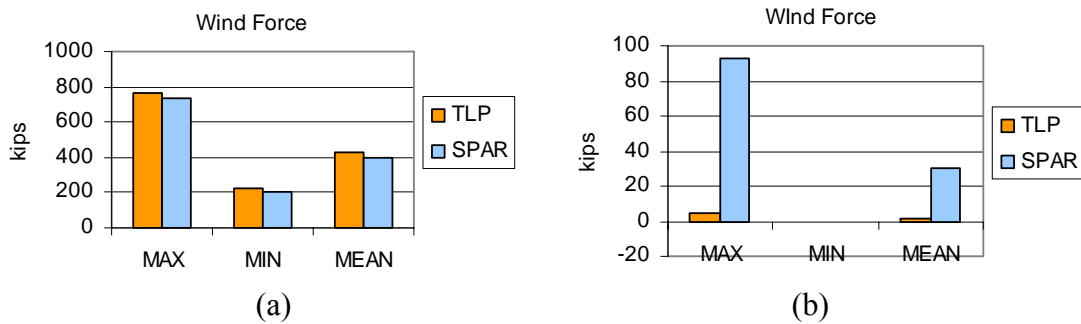
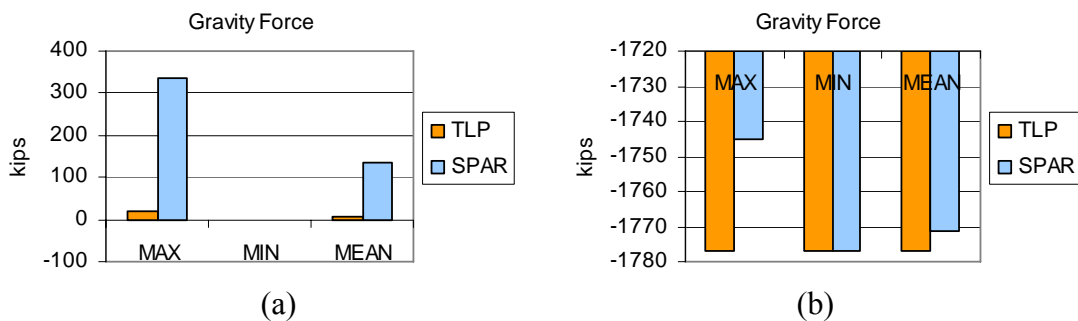
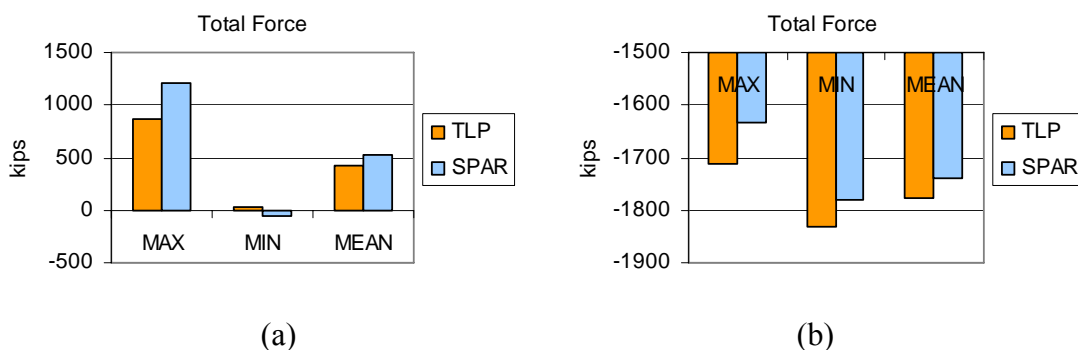


Fig 8-2 (a) Surge and (b) Heave Wind Force





**Fig 8-3 (a) Surge and (b) Heave Gravity Force**



**Fig 8-4 (a) Surge and (b) Heave Total Force**

Surge inertia force shows that maximum and minimum force of SPAR is bigger than TLP surge inertia force. That's because pitch acceleration of SPAR which contribute surge acceleration is much bigger than that of TLP. In general, hull acceleration of heave direction of TLP is greater, so the heave inertia of TLP could be bigger for 100 year case. However, once the environmental condition becomes severe, tilted hull of SPAR could generate more heave inertia force, so the heave inertia of SPAR could be greater than that of TLP.

Wind force for surge direction of TLP is stronger because the location of derrick of TLP is higher than location of SPAR derrick; however, the heave wind force of SPAR

is bigger due to large tilt angle that causes a bigger vertical component of wind force. For the same reason, surge gravity force of SPAR is bigger. Most of these differences come from the large pitch motion of SPAR and the trend of resultant reaction force of each footing is affected by these differences.

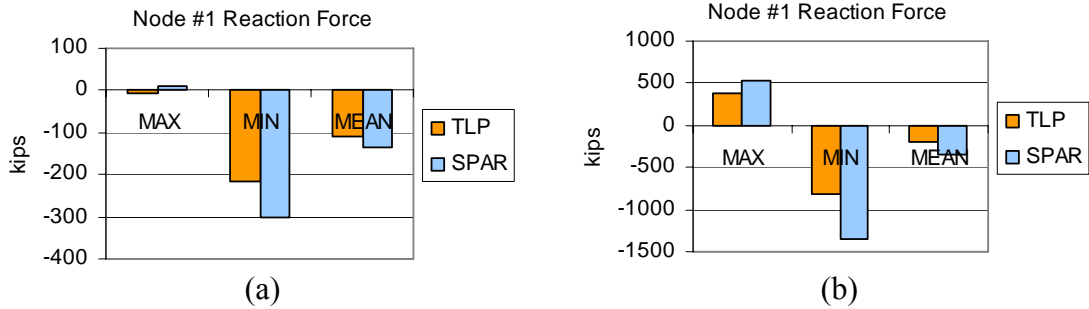


**Fig 8-5 (a) Surge and (b) Heave Reaction Force at Node 1**

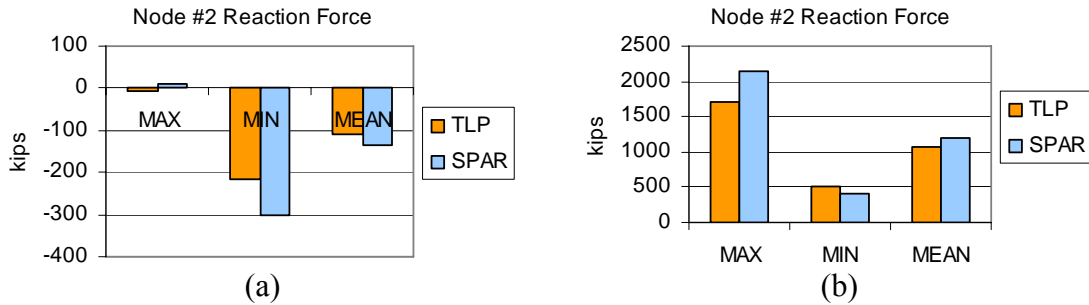


**Fig 8-6 (a) Surge and (b) Heave Reaction Force at Node 2**

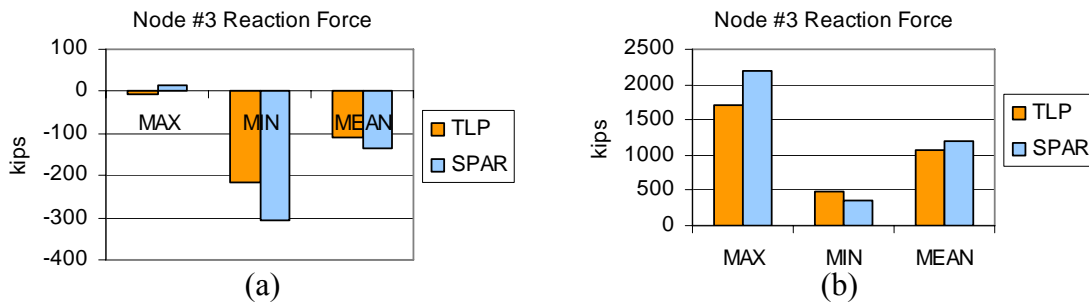


**Fig 8-7 (a) Surge and (b) Heave Reaction Force at Node 3**

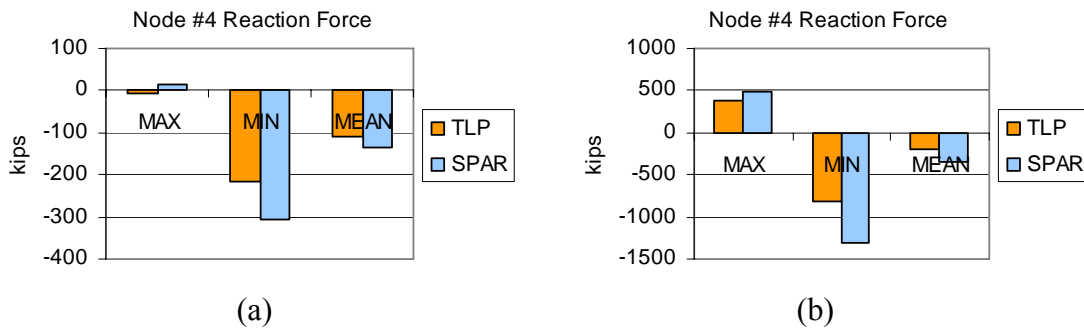


Fig 8-8 (a) Surge and (b) Heave Reaction Force at Node 4

For all footings, reaction force of SPAR is bigger than TLP reaction force when all other conditions are the same except for derrick height as shown in Figures 8-5 to 8-8. This means the design criteria of derrick footings of SPAR should be more severe than that of TLP.

### 8.2 Incident Angle Analysis

In this study, a total of 4 different incident angles have been selected, and for each incident heading, maximum uplift forces of SPAR are presented.

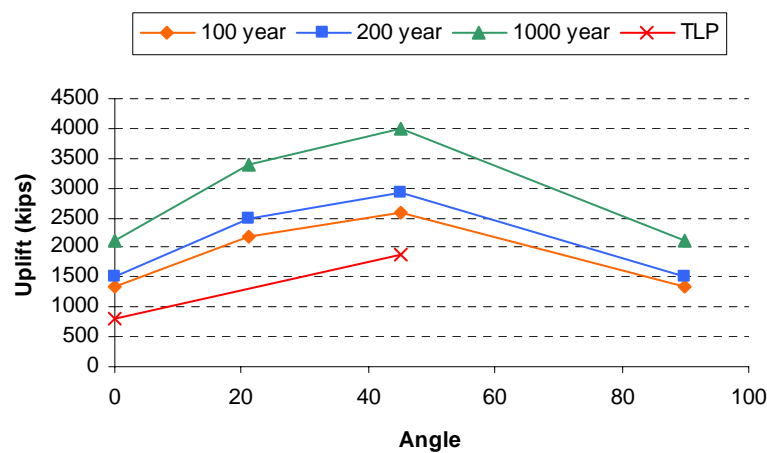
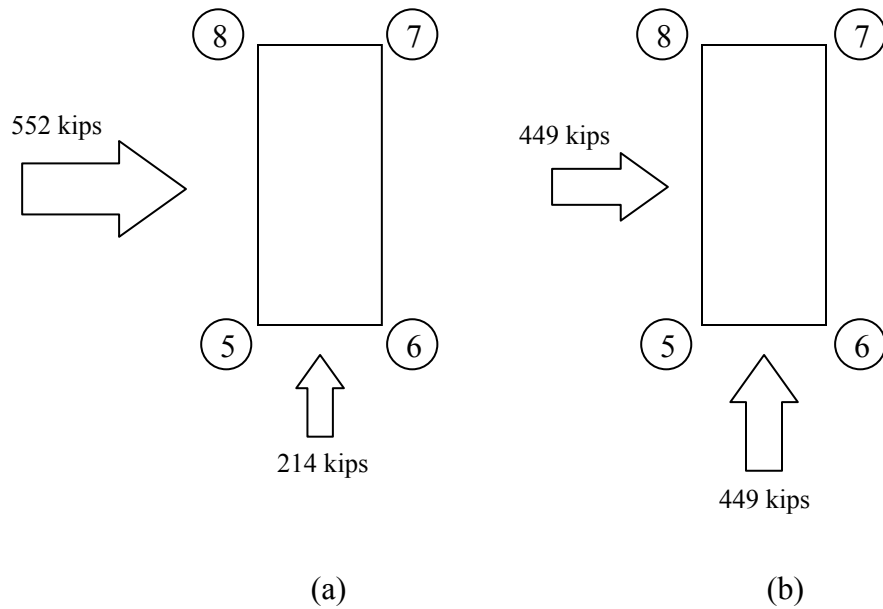


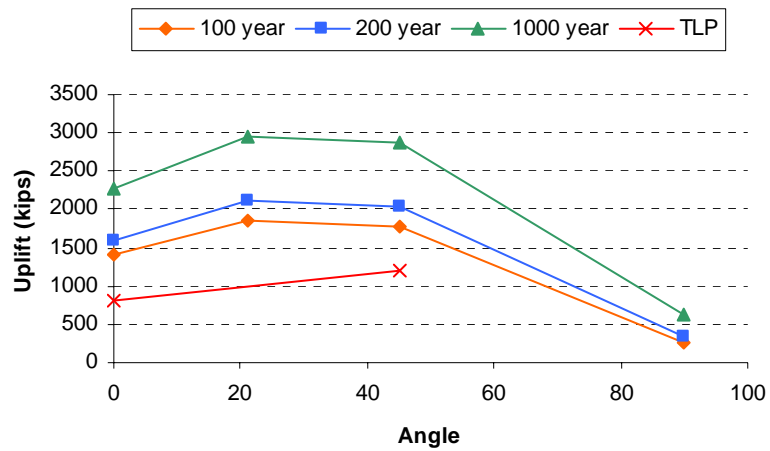
Fig 8-9 SPAR Derrick Uplift Force

Figure 8-9 shows that the maximum uplift force on the derrick occurs when external force is applied from 45 degrees. It is obvious that the squared shape derrick has its maximum wind projected area when it stands at a 45 degree angle. The maximum uplift of TLP case is also illustrated for the reference purpose.

The trend of uplift reaction forces of skid base footing seems different. In Figure 8-10 for 21.25 degree case, the total mean force on the derrick and skid base is 552 kips of surge direction and 214 kips of sway direction. Similarly, the total mean force of 45 degree case is 449 kips of surge and sway direction. Thus, the means force of 21.25 degree case is  $\sqrt{552^2 + 214^2} = 592$  kips, and that of 45 degree case is  $\sqrt{449^2 + 449^2} = 635$  kips. Admittedly, the mean total force of 45 degree case is still bigger because the total projected area of 45 degree case is also larger. However, the external force of surge component for 21.25 degree case is 552 kips and for 45 degree case is 449 kips. The uplift force of node 5 is decided by both surge and sway components of external forces, but the contribution of surge component of external force is more critical causing the uplift force of 21.25 degree case to be bigger than uplift force of 45 degree case.



**Fig 8-10 External Force Components of SPAR (a) 21.25 Degree and (b) 45 Degree**



**Fig 8-11 SPAR Skid Base Uplift Force**

Figure 8-11 shows that the maximum uplift force occurs when external force is applied from either 21.25 degree or 45 degree or any angle between them. It doesn't seem that the difference is noticeable, but the uplift force is slightly bigger for 21.25

degree case. This phenomenon is more clearly observed in the SPAR case compared to TLP case. The gravity force due to hull pitch motion of SPAR plays an additional role in increasing the surge component of total force.

The horizontal reaction forces related to slip failure are also checked. The slip failure of derrick is caused by sway reaction forces, while the slip failure of skid base is caused by surge reaction forces as shown in Figure 8-12. Figure 8-13 shows the reaction forces that may cause derrick footing slip of the SPAR with referenced TLP respectively.

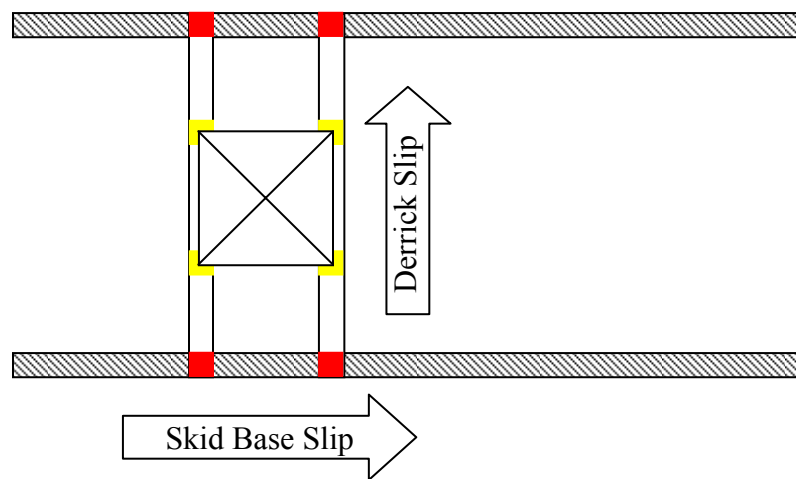


**Fig 8-12 Derrick and Skid Base Slip Conditions**

The maximum slip reaction of derrick occurs in 90 degree heading case. The reaction of 45 degree incident angle case is also comparable to that of 90 degree heading case because the maximum projected area of derrick of 45 degree case contributes a similar level of sway force with 90 degree case.

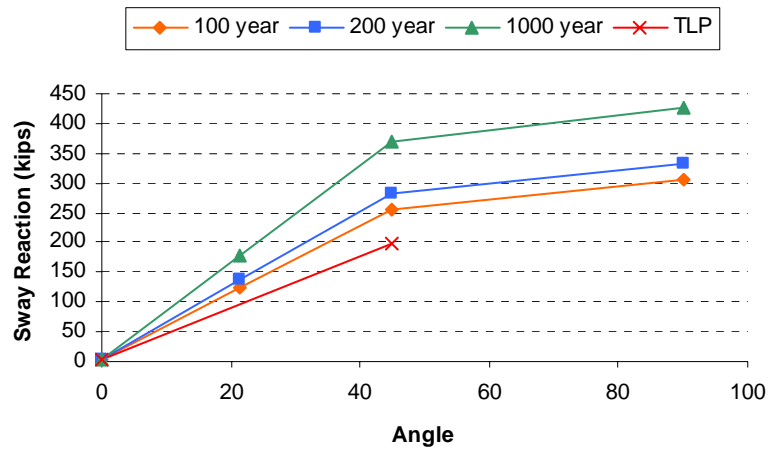


**Fig 8-13 SPAR Derrick Slip Reaction**

The maximum slip reaction of skid base shows different patterns with derrick case as shown in Figure 8-14. In this case, the maximum slip of skid base occurs when external forces are coming from 21.25 degree angle. The reason for this result can be explained by the same reason we discussed in the maximum uplift reaction force case.

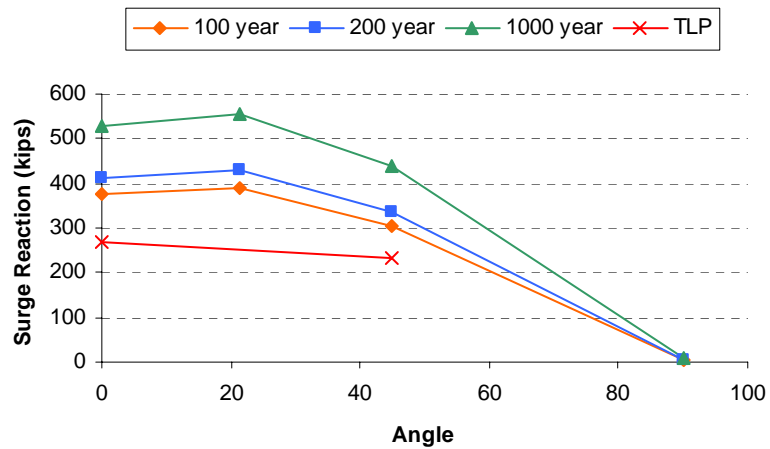


**Fig 8-14 SPAR Skid Base Slip Reaction**

### 8.3 External Force Contribution Analysis

The external forces applied on the derrick and skid base consist of three different components and the portions of these forces are different from TLP and SPAR. Figures 8-15 and 8-16 show the different contribution of external forces which cause the maximum surge reaction forces. Wind force is dominant in this case, and gravity force is nearly zero because TLP does not have serious roll and pitch motions.

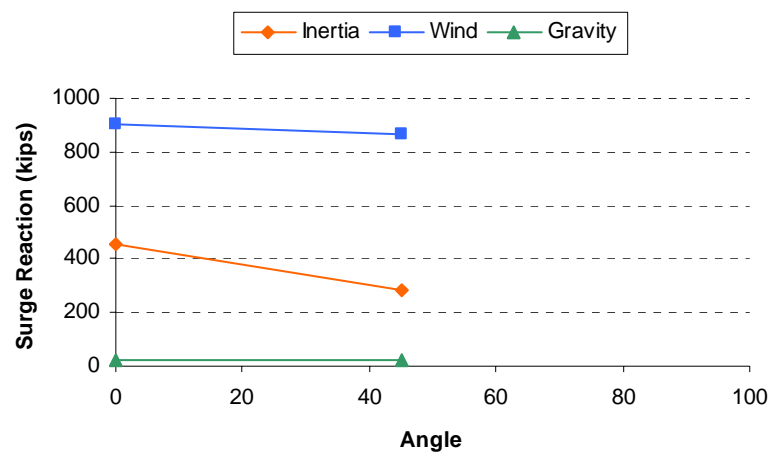


**Fig 8-15 TLP Skid Base Surge Reaction Component**

This pattern is different for SPAR case. The contribution of inertia and gravity forces are greatly increased compared to TLP case. The gravity force contribution for surge reaction force is comparable to the inertia force contribution of TLP.



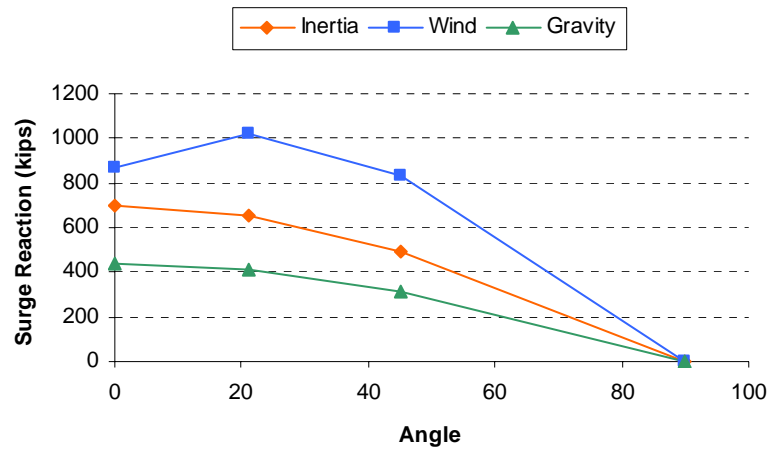


**Fig 8-16 SPAR Skid Base Surge Reaction Component**

The reason for these differences has already been discussed and a similar trend can be observed for the sway reaction force case as shown in Figures 8-17 and 8-18.

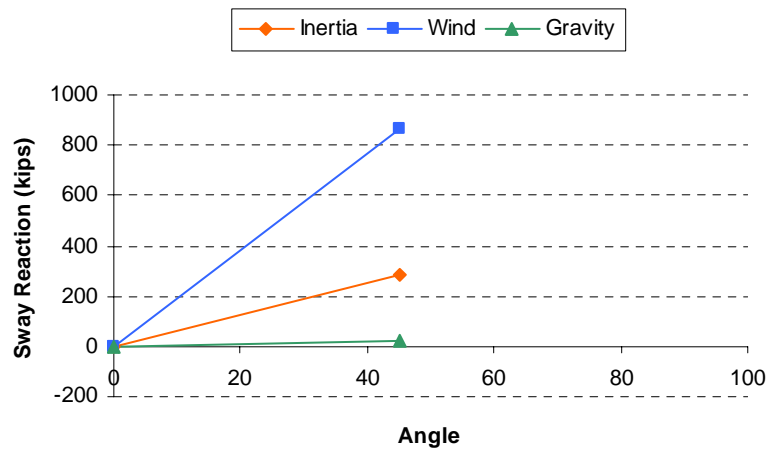


**Fig 8-17 TLP Skid Base Sway Reaction Component**

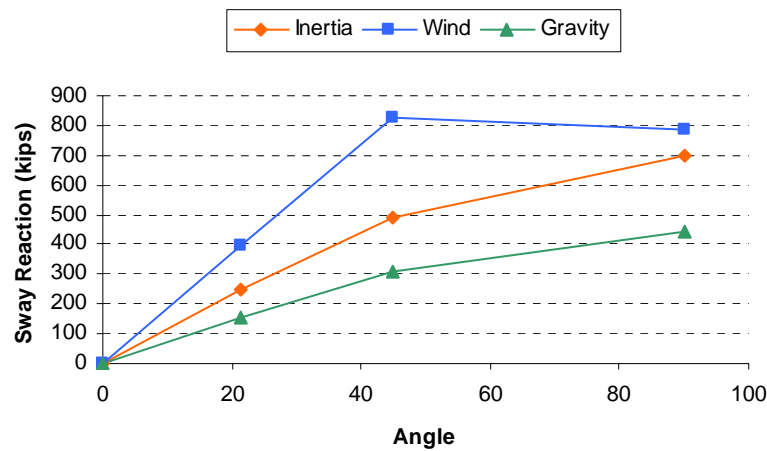


**Fig 8-18 SPAR Skid Base Sway Reaction Component**

Both cases show that the horizontal reaction force of derrick and skid base footings are mostly caused by the wind force, but inertia and gravity forces play an important role in the SPAR case as well.

#### 8.4 Reaction Force Contribution Analysis

The reaction forces of footings are caused by different external forces. The frequency domain analysis of reaction forces can show which part of the external forces affect the reaction forces.

In Figure 8-19, the time history of reaction force of horizontal direction and its spectral density are presented. The low frequency contribution of reaction force is mostly due to the wind force, and the other frequency region which is greater than 0.2 rad/sec is a surge inertia force contribution. Uplift reaction force of same footing shows a similar pattern as illustrated in Figure 8-20.

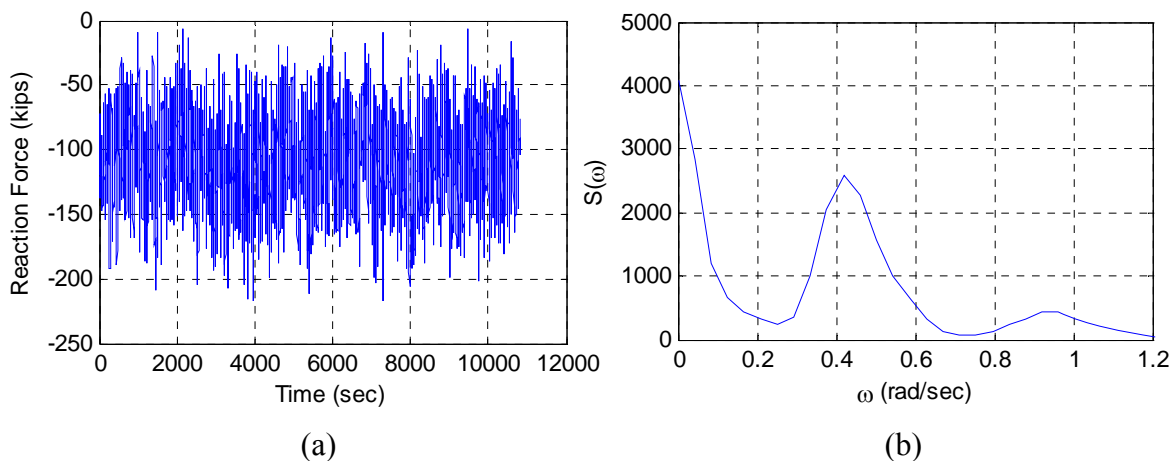


**Fig 8-19 (a) TLP Surge Reaction and (b) Spectral Density**

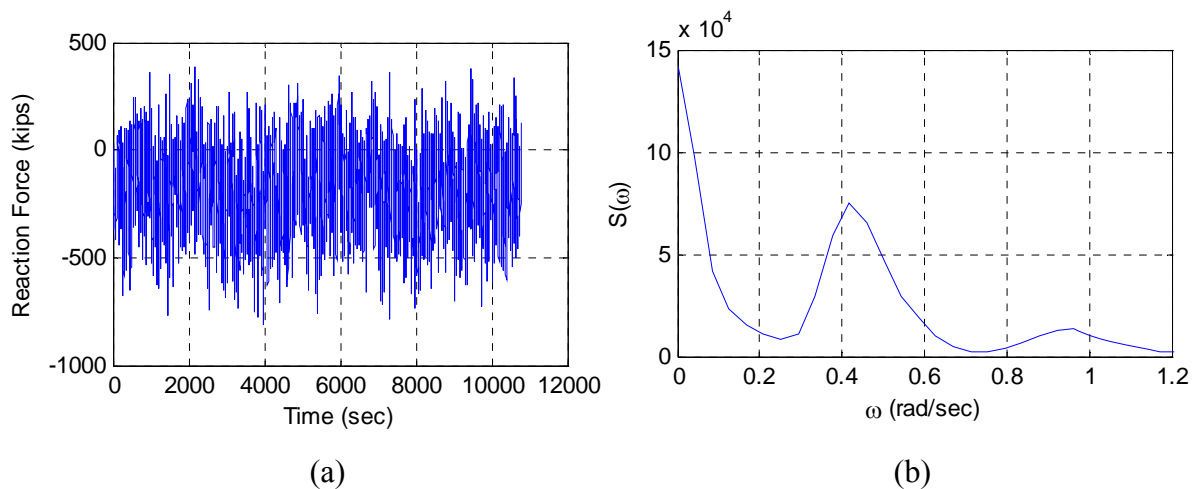


**Fig 8-20 (a) TLP Heave Reaction and (b) Spectral Density**

For SPAR case, the overall trend of reaction force in frequency domain is similar to that of TLP as shown in Figures 8-21 to 8-22, in that the reaction force of surge and heave components are affected by both wind force and inertia force. The differences are that the inertia force contribution that has frequency range from 0.2 rad/sec is considerable compared to inertia contribution of TLP case.

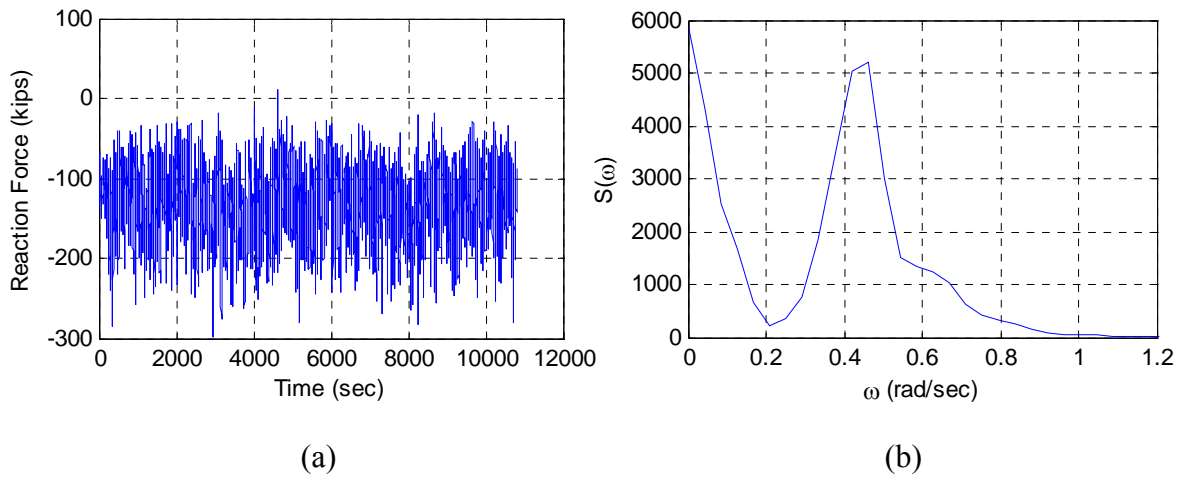


**Fig 8-21 (a) SPAR Surge Reaction and (b) Spectral Density**

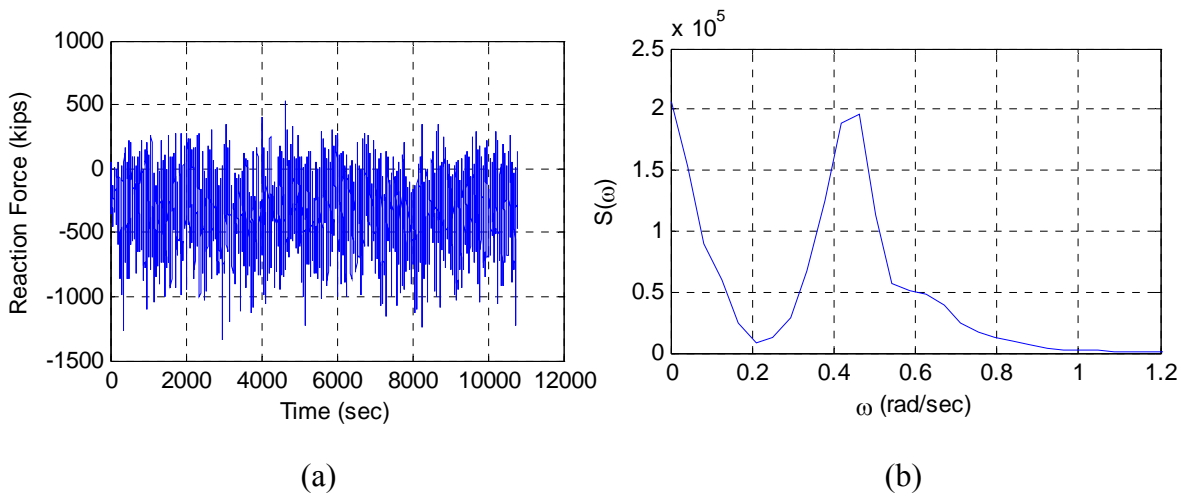


**Fig 8-22 (a) SPAR Heave Reaction and (b) Spectral Density**

Similarly, wind force contribution on derrick can be seen in low frequency range and inertia force effect also plays an important role on the derrick.

## 9 CONCLUSION

At this point, the reaction forces on derrick and skid base footing have been investigated for both TLP and SPAR in hurricane conditions. Under the same conditions, SPAR is expected to experience bigger tensile or shear forces at the footings compared to TLP because SPAR moves with bigger roll or pitch motions in the ocean. In addition, the direction of external force, especially for wind force, exerted on the derrick structure needs to be carefully considered in order to provide reliable strength of footings. Further investigations regarding directional dependence of maximum reaction forces are needed if the shape of the derrick or skid base in which we are interested is not an exact square.

The present study is applicable to the design of offshore structures to ensure safety during hurricane conditions. Detail of structural design specification such as bolt and clamp capacity can be determined using the output of this research. Tensile, shear, and slip failure of tie-down systems can also be checked in time domain once the configuration of the footing clamp is given.

## REFERENCES

- API Bulletin 2INT-MET, 2007. Interim Guidance on Hurricane Conditions in the Gulf of Mexico. American Petroleum Institute, Washington, DC.
- API Specification 4F 2<sup>nd</sup> Edition, 1995. Specification for Drilling and Well Servicing Structures. American Petroleum Institute, Washington, DC.
- API Specification 4F 3<sup>rd</sup> Edition, 2008. Specification for Drilling and Well Servicing Structures. American Petroleum Institute, Washington, DC.
- Donnes, J., 2007. Comparison between the Current API Specification 4F 2<sup>nd</sup> Edition and the Proposed API Specification 4F 3<sup>rd</sup> Edition. Masters Project Report, Louisiana State University, LA.
- Gebara, J. M. and Ghoneim, N., 2007. Assessment of the Performance of Tie-Down Clamps for a Drilling Rig on a Spar in Severe Hurricane Environments. MMS Project #551 Analysis Report Appendix A, New Orleans, LA.
- Kim, M.H., 1997. CHARM3D User's Manual. Ocean Engineering Program, Civil Engineering Department, Texas A&M University, College Station, TX.
- Kim, M.H., Tahar, A., Kim, Y.B., 2001. Variability of TLP Motion Analysis against Various Design Methodologies/Parameters. In: Proceedings of the 11th International Offshore and Polar Engineering Conference, ISOPE 3. Stavanger, Norway.
- Kim, M.H., Koo, B.J., Mercier, R.M., Ward, E.G., 2005. Vessel/Mooring/Riser Coupled Dynamic Analysis of a Turret-Moored FPSO Compared with OTRC Experiment. Ocean Engineering 32, 1780-1802.

- Kim, M.H. and Yang, C.K., 2006. Global Motion of Deep Star TLP and the Corresponding Load at the Connection of Derrick and Substructure in Extreme Survival Condition. Ocean Engineering Program, Civil Engineering Department, Texas A&M University, College Station, TX.
- Lee, C.H., 1995. WAMIT Theory Manual. Department of Ocean Engineering, Massachusetts Institute of Technology, Cambridge, MA.
- Ran, Z., and Kim, M.H., 1997. Nonlinear Coupled Responses of a Tethered Spar Platform in Waves. *International Journal of Offshore and Polar Engineering* 7, 111-118.
- Steen, M. Irani, M. and Kim, M.H., 2004. Prediction of Spar Responses: Model Test vs. Analysis. In: *Proceedings of the Offshore Technology Conference*, OTC 16583. Houston, TX.
- Ward, E.G. and Gebara, J. M., 2006a. Assessment of Drilling & Workover Rig Storm Sea Fastenings on Offshore Floating Platforms during Hurricane Ivan Phase I Data Collection Report. Offshore Technology Research Center, Texas A&M University, College Station, TX.
- Ward, E.G. and Gebara, J. M., 2006b. Assessment of Storm Sea Fastenings for Drilling and Workover Rigs on Floating Production Systems during Hurricane Ivan. In: *Proceedings of the Offshore Technology Conference*, OTC 18324. Houston, TX.
- Yang, C.K., 2009. Numerical Modeling of Nonlinear Coupling between Lines/Beams with Multiple Floating Bodies. Ph.D. Dissertation, Texas A&M University, College Station, TX

**APPENDIX****Simulation Data**

Structure : TLP  
Derrick : AA  
Condition : Normal



### Simulation Conditions

Structure	Return Period	Incident Angle	Derrick Type	Footing Location	Derrick Loading
TLP	100 Yr	0 degree	AA	Derrick	Normal

### Dynamic Loads

		X	Y	Z	MX	MY	MZ
<b>Inertia</b>	MAX	345	0	61	847	32991	222
	MIN	-356	0	-56	-723	-34148	-181
	MEAN	0	0	0	0	0	0
<b>Wind</b>	MAX	765	0	5	39	78760	0
	MIN	222	0	0	-4	22850	0
	MEAN	424	0	1	21	43693	0
<b>Gravity</b>	MAX	19	0	-1777	16	1772	0
	MIN	0	0	-1777	0	-5	0
	MEAN	6	0	-1777	12	583	0
<b>Total</b>	MAX	869	0	-1715	884	88163	222
	MIN	23	-1	-1833	-686	4052	-181
	MEAN	430	0	-1776	33	44277	0

### Reaction Forces on the Footings

Node	Reaction	X	Y	Z
<b>1</b>	MAX	-6	2	383
	MIN	-217	-1	-815
	MEAN	-108	0	-188

Node	Reaction	X	Y	Z
<b>2</b>	MAX	-6	1	1704
	MIN	-217	-2	499
	MEAN	-108	0	1077

Node	Reaction	X	Y	Z
<b>3</b>	MAX	-5	1	1712
	MIN	-218	-2	489
	MEAN	-108	0	1076

Node	Reaction	X	Y	Z
<b>4</b>	MAX	-5	2	373
	MIN	-218	-1	-807
	MEAN	-108	0	-189

### Simulation Conditions

Structure	Return Period	Incident Angle	Derrick Type	Footing Location	Derrick Loading
TLP	100 Yr	0 degree	AA	Skid Base	Normal

### Dynamic Loads

		X	Y	Z	MX	MY	MZ
<b>Inertia</b>	MAX	455	0	80	1599	37014	444
	MIN	-468	0	-74	-1348	-38310	-364
	MEAN	0	0	0	0	0	0
<b>Wind</b>	MAX	905	0	6	43	86846	0
	MIN	259	0	0	-5	24824	0
	MEAN	499	0	2	23	47874	0
<b>Gravity</b>	MAX	25	0	-2347	18	1988	0
	MIN	0	0	-2347	0	-6	0
	MEAN	8	0	-2347	14	654	0
<b>Total</b>	MAX	1070	0	-2265	1640	97510	444
	MIN	-10	-1	-2421	-1307	3632	-364
	MEAN	507	0	-2345	37	48529	0

### Reaction Forces on the Footings

Node	Reaction	X	Y	Z
<b>5</b>	MAX	2	1	527
	MIN	-267	-1	-804
	MEAN	-127	0	-107

Node	Reaction	X	Y	Z
<b>6</b>	MAX	2	1	1982
	MIN	-267	-1	631
	MEAN	-127	0	1280

Node	Reaction	X	Y	Z
<b>7</b>	MAX	3	1	1989
	MIN	-268	-1	624
	MEAN	-127	0	1279

Node	Reaction	X	Y	Z
<b>8</b>	MAX	3	1	520
	MIN	-268	-1	-797
	MEAN	-127	0	-107

### Simulation Conditions

Structure	Return Period	Incident Angle	Derrick Type	Footing Location	Derrick Loading
TLP	100 Yr	45 degree	AA	Derrick	Normal

### Dynamic Loads

		X	Y	Z	MX	MY	MZ
<b>Inertia</b>	MAX	220	220	53	23906	21600	4
	MIN	-243	-243	-52	-21620	-23902	-4
	MEAN	0	0	0	0	0	0
<b>Wind</b>	MAX	765	765	8	-22858	78787	0
	MIN	222	222	-1	-78786	22858	0
	MEAN	424	424	2	-43708	43708	0
<b>Gravity</b>	MAX	14	14	-1777	224	1354	0
	MIN	-2	-2	-1777	-1355	-222	0
	MEAN	4	4	-1777	-406	406	0
<b>Total</b>	MAX	794	794	-1721	-11708	81450	4
	MIN	105	105	-1828	-81450	11710	-4
	MEAN	429	429	-1775	-44114	44115	0

### Reaction Forces on the Footings

Node	Reaction	X	Y	Z
<b>1</b>	MAX	-26	-26	106
	MIN	-198	-198	-1881
	MEAN	-107	-107	-817

Node	Reaction	X	Y	Z
<b>2</b>	MAX	-26	-26	457
	MIN	-198	-198	430
	MEAN	-107	-107	444

Node	Reaction	X	Y	Z
<b>3</b>	MAX	-26	-26	2773
	MIN	-198	-198	775
	MEAN	-107	-107	1704

Node	Reaction	X	Y	Z
<b>4</b>	MAX	-26	-26	457
	MIN	-198	-198	430
	MEAN	-107	-107	444

### Simulation Conditions

Structure	Return Period	Incident Angle	Derrick Type	Footing Location	Derrick Loading
TLP	100 Yr	45 degree	AA	Skid Base	Normal

### Dynamic Loads

		X	Y	Z	MX	MY	MZ
<b>Inertia</b>	MAX	286	287	71	27148	24497	9
	MIN	-317	-317	-69	-24497	-27171	-9
	MEAN	0	0	0	0	0	0
<b>Wind</b>	MAX	864	864	9	-25046	87232	0
	MIN	248	248	-1	-87231	25046	0
	MEAN	477	477	2	-48178	48179	0
<b>Gravity</b>	MAX	19	19	-2347	251	1519	0
	MIN	-3	-3	-2347	-1520	-249	0
	MEAN	6	6	-2347	-456	455	0
<b>Total</b>	MAX	922	922	-2273	-12381	90231	9
	MIN	87	87	-2415	-90230	12375	-9
	MEAN	483	483	-2345	-48634	48635	0

### Reaction Forces on the Footings

Node	Reaction	X	Y	Z
<b>5</b>	MAX	-22	-22	337
	MIN	-231	-231	-1201
	MEAN	-121	-121	-379

Node	Reaction	X	Y	Z
<b>6</b>	MAX	-22	-22	1377
	MIN	-231	-231	687
	MEAN	-121	-121	1011

Node	Reaction	X	Y	Z
<b>7</b>	MAX	-22	-22	2380
	MIN	-231	-231	827
	MEAN	-121	-121	1551

Node	Reaction	X	Y	Z
<b>8</b>	MAX	-22	-22	474
	MIN	-231	-231	-198
	MEAN	-121	-121	162

## VITA

Yoon Hyeok Bae was born in Busan, Korea on April 27, 1976. He received his Bachelor of Science degree in naval architecture and ocean engineering from Seoul National University in 2000. He worked as an engineer in the shipbuilding industry in Korea for over 6 years. He entered the graduate program at Texas A&M University in September 2006 and received his Master of Science degree in ocean engineering in May 2009.

He may be reached at this email address: [yoonyheok.bae@gmail.com](mailto:yoonyheok.bae@gmail.com). His permanent address is:

Beach Apt. 213-606

Namcheon2-dong, Suyoung-gu

Busan, Korea 613-751